

ALMA MATER STUDIORUM
UNIVERSITY OF BOLOGNA

SCHOOL OF ENGINEERING AND ARCHITECTURE

MASTER COURSE IN CIVIL ENGINEERING

Department of Civil, Chemical, Environmental and Materials Engineering

GRADUATION THESIS
in

Context Sensitive Design in Transportation Infrastructures

***EXPERIMENTAL ANALYSIS ON THE USE OF CCC SYSTEMS
TO ANALYZE THE IN-SITU BEARING CAPACITY OF C&D
MATERIALS***

SUPERVISOR:

Dr. Cesare Sangiorgi

CANDIDATE:

Alessandro Ninfa

CO- SUPERVISOR:

Dr. Claudio Lantieri

Academic year 2012/2013
III session

DEDICATION

This thesis would be incomplete without a mention of the support given to me by my mother and father for whom this thesis is dedicated. I would like to thank also Adriana and Husman for their incredible support and helpful.



Keywords

*Continuous Compaction Control (CCC);
Road Pavement;
Load Bearing capacity;
C&D materials;
Quality Control / Quality Assurance (Qc/Qa).*

INDEX

Abstract	7
Chapter 1.Introduction	3
1.1. General	3
1.2. Fundamentals of Vibration Theory	5
1.3. Rollers	6
1.3.1. Static Rollers	6
1.3.2. Dynamic Rollers.....	7
1.3.3. Vibratory Roller	7
<i>1.3.3.1. Operation Modes of Vibratory Roller.....</i>	<i>8</i>
1.3.4. Oscillatory Roller	10
1.3.5. VARIO Roller	10
1.3.6. VARIO Control Roller.....	11
1.4. Continuous Compaction Control and Intelligent Compaction.....	13
1.4.1. Description of CCC/IC Technology	13
1.4.2. Definition of CCC and IC systems.....	13
1.4.3. Advantages and Drawbacks of CCC/IC technology	14
1.5. Principal Theories of Operation of CCC/IC Systems	15
1.5.1. Compaction Meter Value (CMV)	16
1.5.2. Compaction Control Value (CCV)	18
1.5.3. OMEGA	19
1.5.4. Stiffness (ks)	20
1.5.5. Vibratory Modulus (Evib) value.	24
1.5.6. Evaluation of Vibratory Measurement Values.....	27
1.6. Roller manufacturers	30
1.6.1. Bomag Soil IC System	31
1.6.2. Case/Ammann Soil IC System.....	32
1.6.3. Caterpillar Soil IC System	33
1.6.4. Dynapac Soil IC System	34
1.6.5. Sakai Soil IC System.....	35

Chapter 2. Current CCC/IC Construction Specifications.....	37
2.1. State of practice.....	37
2.2. Current CCC/IC Construction Specifications	39
2.2.1. Austrian/ISSMGE Specifications.....	40
2.2.1.1. Method 1: Acceptance Based on Calibration.....	41
2.2.1.2. Method 2: Acceptance Based on Percentage Change of MVs	43
2.2.2. German CCC Specifications	43
2.2.2.1. Calibration Approach (Method M2 in German specifications).	44
2.2.2.2. CCC to identify weak areas for spot testing.....	45
2.2.3. Swedish CCC Specifications	46
2.2.4. Minnesota DOT Pilot Specifications	48
2.2.5. 4th Draft on European CCC regulations.	50
2.2.5.1. Method 1: "FV-process" (fault-in-variables-method).....	53
2.2.5.2. Method 2: "KQ-method" (method of smallest squares).....	54
2.2.5.3. Weak spots analysis – "proof rolling"	56
2.2.5.4. Soil groups.....	57
2.3. Conclusions	58
Chapter 3. Quality Assurance of Pavement Earthwork Using Roller-Integrated CCC.....	60
3.1. Definitions.....	63
3.2. Notation	64
3.3. Important consideration.....	64
3.3.1 Applicable Soil Types	64
3.3.2 Measurement Depth	64
3.3.3 Evaluation Section	65
3.3.4 Verification of Roller MV Repeatability.	66
3.4. In-situ Strength-based test approaches that can be used for compaction QA/QC	67
3.4.1 Plate Load Test (PLT).....	67
3.4.2 Light Weight Deflectometer (LWD).....	69
3.4.3 Falling Weight Deflectometer (FWD)	70
3.5 QA Option 1: Spot Testing of Roller-Informed Weakest Area	71
3.5.1 QA Option 2: Limiting Percentage Change in Roller MV	72
3.5.2 Option 2a: Monitoring Percentage Change in Mean MV	73
3.6. Option 2b: Monitoring Spatial Percentage Change in Roller MVs	73

Chapter 4 Construction and demolition (C&D) materials	75
4.1. Premise.....	75
4.2. C&D wastes: definition and EU context.....	75
4.3. C&D waste: composition	76
4.4. Environment and sustainability issues	77
4.5. Research Steps	78
4.6. Physical and mechanical properties of the mixtures	79
4.6.1. Prequalification of the materials	80
4.6.2. The Atterberg limits	80
4.6.3. Particle size distribution through sieve	81
4.6.4. Tests for geometrical properties of aggregates	83
4.6.5. Shape Index (S.I.).....	85
4.6.6. Aggregate Flakiness Index.....	86
4.6.7. Particle Density Of Filler	88
4.6.8. (Apparent) Particle Density	89
4.6.9. Loose Bulk Density And Voids	89
4.6.10. Density	90
4.6.11. Resistance to fragmentation-Los Angeles (L.A.).....	90
4.6.12. Assessment of fines- Sand equivalent test (S.E.).....	92
4.7. Study of mixtures for embankment construction	93
4.7.1. qualification and study of the unbound mixtures.....	93
4.7.1.1. <i>Particle-size analysis of unbound mixtures</i>	94
4.7.1.2. <i>Proctor test for the densification of the mixtures</i>	95
4.7.1.3. <i>Pre and post compaction particle size</i>	96
4.7.1.4. <i>Californian Bearing Ratio (presaturation)</i>	98
4.7.1.5. <i>Californian Bearing Ratio (postsaturation)</i>	99
4.7.2. Qualification of the bound mixtures	101
4.7.2.1. <i>Grading curve analysis of the bound mixtures</i>	102
4.7.2.2. <i>CBR test for the bound mixtures</i>	102
4.7.2.3. <i>Compressive strength of hydraulically bound mixtures</i>	104
4.7.2.4. <i>Indirect tensile strength of hydraulically bound mixtures</i>	105

Chapter 5 Test Field & Data Analysis	108
5.1 Premises	108
5.2 The Test field	108
5.2.1 Constructing the Embankment.....	109
5.2.2. Subgrade.....	111
5.2.2. Layer 1 (Unbound materials)	112
5.2.3. Layer 2 (bounded materials)	113
5.2.4. The equipment used.	114
5.3 Factors that may have influenced the measured data.....	117
5.4. DataAnalysis	118
5.4.1. Analysis of passes	120
5.4.2 Data analysis of the 11-09: layer S	120
5.4.3. Layer L1 (mixtures M1 and M2)	123
5.4.4. Layer L2 (mixture M3 and M4).....	125
5.5 Mapping of Evib values	129
5.5.1. Layer L2	129
5.5.2. Layer L1	132
5.5.3. Subgrade S	134
5.6 Comparison between the layers.....	136
5.7 Depth of measurements.....	137
Chapter 6 Study of the compaction.....	140
6.1 State of Practice.....	140
6.2. Acceptance using specification option 2a	140
6.2.1 Analysis of the percentage change $\%??MV_i$	141
6.3. Acceptance using specification option 2b.....	148
6.3.1. Layer 2	149
6.3.2. Layer 1	152
CONCLUSIONS.....	154
REFERENCES	157

ABSTRACT

Compaction is one of the most important processes in roadway construction. It is needed to achieve high quality and uniformity of pavement materials, which in turn better ensure long lasting performance.

The substantial increase in recent decades in transport demand, both demographic and industrial, has led to an increase in construction of new communication ways.

Although the interventions on infrastructure works are currently more oriented to maintenance work, even deep, compared to new constructions, is still high the need to use large amounts of gravelly-sandy soil with high performance characteristics.

The depletion of existing quarries and the consequent limitations imposed by regulatory plans for mining activities in line with a gradual increase in sensitivity on environmental issues, has led to a lack of availability at moderate cost, the aggregates with suitable mechanical properties.

From these conditions, it was necessary to look for solutions that would enable the use of low cost materials and, possibly, available on-site, in such a way as to break down the load due to the economic and environmental transport without sacrificing the quality of the intervention.

To do this we use the Compaction: one of the most important processes in roadway construction. It is needed to achieve high quality and uniformity of pavement materials, which in turn better ensure long lasting performance. Pavement materials often possess optimum densities that ensure adequate support, stability, and strength.

Achieving the uniformity is a key for successful compaction.

Starting from these premises, the University of Bologna in collaboration with Bomag, world market leader in compaction technology for the compaction of soil, and CONCAVE srl, a mining and construction materials Company in Trebbo di Reno (Bologna), have developed an experimental test in order to characterize, with high-performance methods, C&D materials for subbase layers.

CI-CCC rollers and deflectometric pressure cells instruments has been used over the test field.

The goal of this thesis is to present the results from the aforementioned research project, providing a detailed description of the activities that were performed from the beginning

to the end of this project.

The following paper is composed of seven chapters:

- the first chapter provides a state of the art overview of vibration based measurement systems used on vibratory roller compactors to continuously measure soil properties during and after earthwork compaction.
- In the second chapter we deal in more detail with the concept of intelligent compaction reporting the reference standards and comparing the more important European regulations;
- The third chapter provides a detailed evaluation of several aspects of roller NCHRP acceptance criterions.
- The fourth chapter deals with Construction and demolition (C&D) waste, information about C&D waste management in Europe and shows physically, chemically and mechanically characterizations performed on the basecourse and the lifts composed by bound and unbound mixtures.
- The fifth chapter begins by briefly illustrating test field construction procedures to describe then the data analysis of the several mixtures placed in lifts.
- In the sixth chapter we make analysis of the recommended quality assurance (QA) specification options detailed in Chapter 3.
- Conclusions are summarized in the seventh and final chapter.

Chapter 1.

Introduction

Compaction is one of the most critical process in soil construction. Its job is to reduce the volume of pores in the soil to be compacted, which are filled with water and air. Compaction will give soil the desired properties: its resistance to stresses induced by traffic and climate will be improved by increasing its stability while simultaneously reducing its tendency to swell due to water absorption. The latter will additionally make the soil resistant to frost.

1.1. General

The quality of roads, highways, motorways, rail tracks, airfields, earth dams, waste disposal facilities, foundations of structures and buildings, etc. depends highly on the degree of compaction of filled layers consisting of different kinds of materials, e.g. soil, granular material, artificial powders, fly ashes and grain mixtures, unbound and bound material. Thus, both compaction method and compaction equipment have to be selected carefully taking into consideration the used material suitable for the prevailing purpose. Compaction process should be optimized in order to achieve sufficient compaction and uniform bearing and settlement conditions.

Traditionally, soil and rock fill materials are compacted with static or vibrating rollers (Figure 1.1).

Compaction of a certain area is carried out by parallel strips (edge to edge or with some overlapping) covering each strip with a fixed number of passes. Most rollers are vibrating rollers; their vibration frequency and amplitude is kept constant and the operator chooses the roller speed. A certain number of passes and a constant roller speed, vibration frequency and amplitude do not necessarily lead to a homogeneous compaction result on a layer due to variation in material properties, water content of the layer being compacted, and stiffness of the underlying layer. A constant number of passes and constant roller parameters will often leave a certain part of the area insufficiently compacted, another part over-compacted and the rest sufficiently compacted.

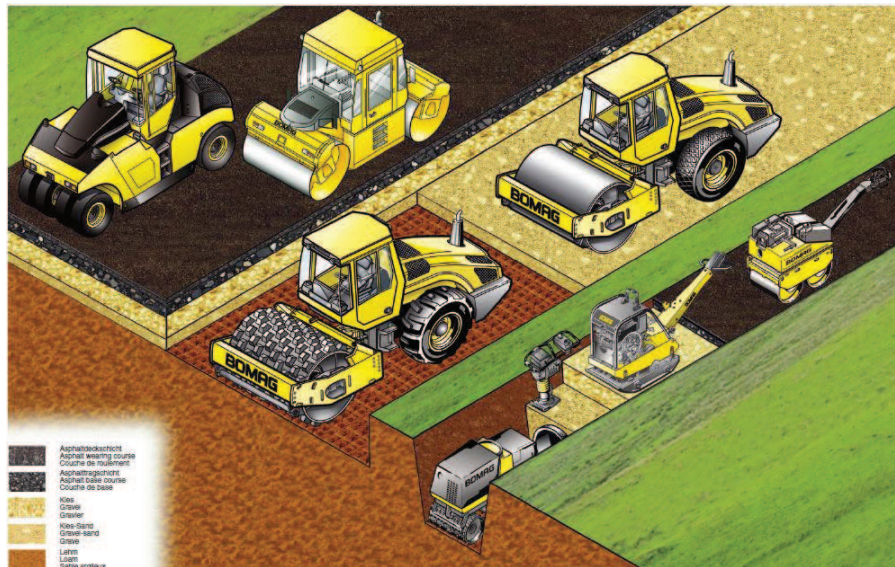


Figure 1.1 Soil and asphalt compaction equipment (from BOMAG Brochure)

If compaction control can be included in the compaction process, time can be saved and cost reduced. Furthermore, a high-leveled quality management requires continuous control all over the compacted area, which can only be achieved economically by roller-integrated methods. The roller-integrated continuous compaction control (CCC) provides relative values representing the developing of the material stiffness all over the compacted area. These values have to be calibrated in order to relate them to conventional values (deformation modulus of static load plate test) given in contractual provisions and standards.

CCC can be applied to virtually all materials that require compaction during construction:

- Type I – Granular, non-cohesive subgrade soils
- Type II – Fine-grained, cohesive subgrade soils
- Type III – Aggregate base material
- Type IV – Asphalt pavement material
- Type V – Stabilized subbase material

Coarse, widely grained material (gravel, sandy gravel) is best suited for CCC application (Figure 1.2, A). Single size fraction sands (Loess) tend to surface near re-loosening due to dynamic loads and achieve only a low maximum density compared to other soil types. In widely grained soil (clayey, silty and sandy gravel) containing a high amount of fines (ca. 30–50%) the water content influences the compaction behavior

noticeably. The higher the moisture content the more water is trapped in the voids of the low permeable material. Consequently, pore water pressures reduce the compactibility more and more (Figure 1.2, B) and thus, influence CCC values. Fine grained soil and artificial material (e.g. fly ash) can hardly be compacted due to the low water and air permeability. Pore water and air produce excessive pore pressure during the compaction process. Sufficient compaction can only be gained by kneading the material to relieve the pore pressures (Figure 1.2, C).

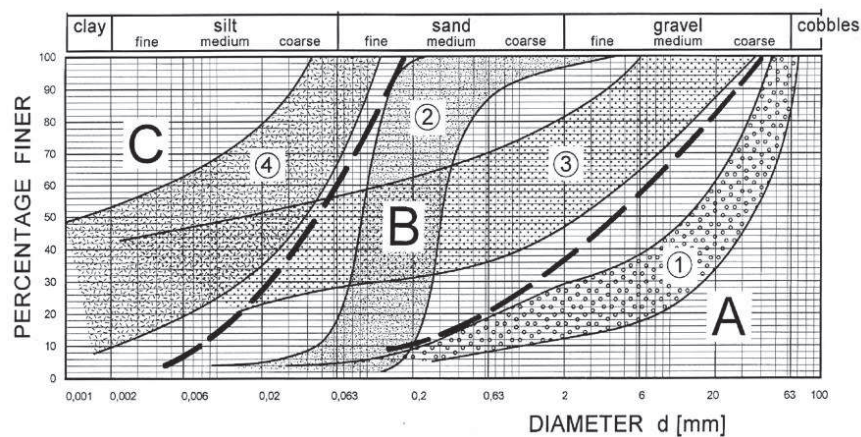


Figure 1.2 Application of CCC to different materials: A – excellent, B – good, C – moderate.

1.2. Fundamentals of Vibration Theory

Before proceeding to the main portion of this literature review, it is timely to define some basic concepts in vibration theory. This will make future discussion of vibratory soil compaction processes clearer.

Frequency (f , Hz) is the number of occurrences of a repeating event per unit time.

Angular frequency (ω , rad/s) is defined as the rate of change in the orientation angle during rotation (Equation 1):

$$\omega = 2\pi f \quad (1.1)$$

Period (T , s) is the duration of one cycle of a repeating event. The period is the reciprocal of the frequency.

Phase (ϕ , radians) of an oscillation or wave is the fraction of a complete cycle corresponding to an offset in the displacement from a specified reference point at time $t = 0$.

The **Harmonic** of a wave is a component frequency of the signal that is an integer multiple of the fundamental frequency. For example, if the fundamental frequency is f , the harmonics have frequencies $f, 2f, 3f, 4f$, etc. The harmonics have the property that they are all periodic at the fundamental frequency, therefore the sum of harmonics is also periodic at that frequency. Harmonic frequencies are equally spaced by the width of the fundamental frequency and can be found by repeatedly adding that frequency. For instance, if the fundamental frequency is 25 Hz, the frequencies of the harmonics are: 25 Hz, 50 Hz, 75 Hz, 100 Hz, etc.

Subharmonic frequencies are frequencies below the fundamental frequency of an oscillation at a ratio of $1/x$. For example, if the fundamental frequency of an oscillator is 440 Hz, sub-harmonics include 220 Hz (1/2) and 110 Hz (1/4).

Amplitude (mm) is the magnitude of change in the oscillating variable, with each oscillation, within an oscillating system.

1.3. Rollers

Rollers are widely used for compacting soil, fill, and asphalt. Rollers are selected depending on the thickness of the layer to be compacted, and the properties of the material to be compacted. The machine parameters include the roller weight (total and drum), the compaction type (static or vibratory), and the diameter and surface of the drum (sheepfoot or smooth). The material properties include grain size distribution, grain shape, maximum grain size, water content, water and air permeability.

1.3.1. Static Rollers

Rollers with static drums (Figure 1.3) use the effective dead weight of the machine to apply pressure on the surface. Thus, soil particles are pressed together and the void content is reduced. Adequate compaction with static rollers is normally achieved only in the upper layers of the material because the effective depth of static compaction is limited.

Cohesive fine grained soil can be compacted sufficiently with static sheep foot roller.

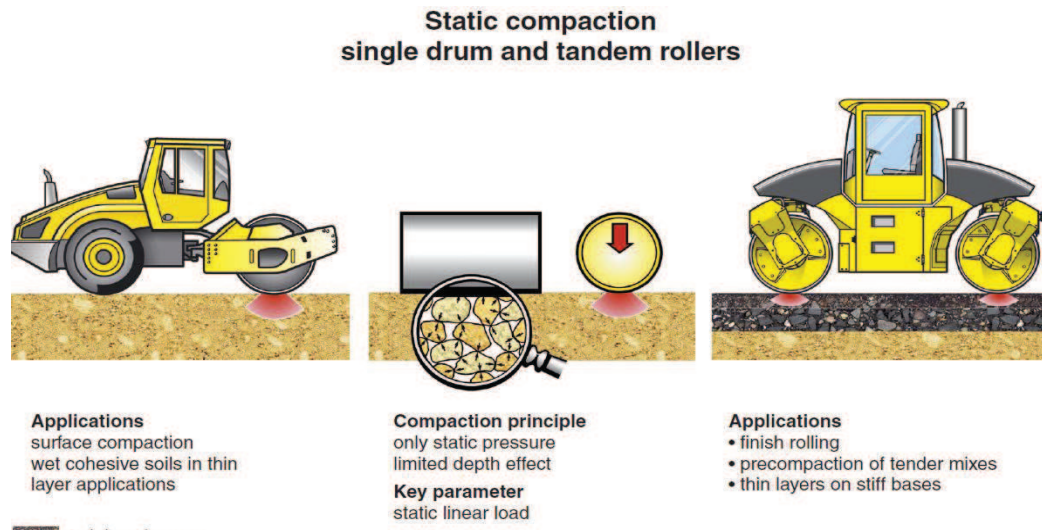


Figure 1.3 Static Roller (from BOMAG Brochure)

The low permeability of fine grained soils leads to pore water pressures when applying (dynamic) compressive stress. Pore water pressures reduce the compaction effect significantly or prevent compaction all together. However, a statically passing sheep-foot drum “kneads” the soil near the surface resulting in a reduction of pore pressures and void ratio respectively. Nevertheless, only thin layers can be compacted at time.

1.3.2. Dynamic Rollers

As reported by Adam and Kopf (2000), dynamic rollers make use of a vibrating or oscillating mechanism, which consists of one or more rotating eccentric weights.

During dynamic compaction, a combination of dynamic and static load is used. The dynamically excited drum delivers a rapid succession of impacts to the underlying surface where the particles are set in motion by the transmission of compressive and shear waves. These vibrations eliminate periodically the internal friction between particles and facilitate, in combination with the static load, the rearrangement of the particles into positions that result in a lower void ratio and a higher density. Furthermore, the increase in the number of contact points and planes between the grains leads to higher stability, stiffness, and lower long-term settlement behavior.

1.3.3. Vibratory Roller

The drum of a vibratory roller is excited by a rotating mass which is connected to the shaft of the drum axis (Figure 1.4) The rotating mass sets the drum in motion and the

direction of the resultant force is tied to the position of the eccentric mass. Compaction is achieved mainly by the series of compression waves penetrating the soil or the asphalt in combination with the effective static weight of the drum. The resulting compaction force is almost vertical.

The behaviour of a vibratory roller drum (amplitude, frequency) changes depending on the soil response. Numerous investigations have revealed that the drum of a vibratory roller operates under different conditions depending on roller and soil parameters.

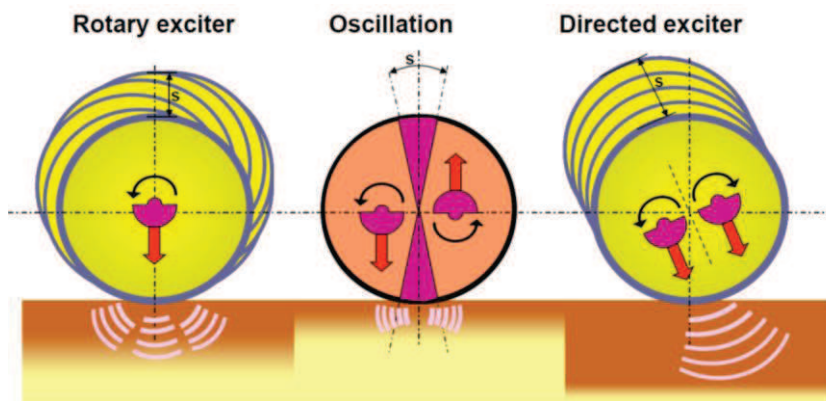


Figure 1.4 Vibratory roller drum (Compaction by cyclic compression) and oscillatory roller drum (Compaction by cyclic shearing) (Adam and Kopf, 2000).

1.3.3.1. Operation Modes of Vibratory Roller

When a given vibratory roller is compacting, five modes of operation may occur, which can influence the dynamic compaction values distinctively (Table 1.1) (Anderegg and Kaufmann 2004).

table 1.1. Operating condition of a vibratory roller drum.

drum motion	Interaction drum-soil	operating condition	soil contact force	application of CCC	soil stiffness	roller speed
periodic	continuous contact	CONT. CONTACT		yes	low	fast
	periodic loss of contact	PARTIAL UPLIFT		yes	↓	↑
		DOUBLE JUMP		yes		
		ROCKING MOTION		no		
chaotic	non-periodic loss of contact	CHAOTIC MOTION		no	high	slow

Generally, soil stiffness influences the operating condition of the drum, but roller parameters also contribute (Brandl and Adam 2004).

Continuous contact only occurs when the soil stiffness is very low; this is the case of uncompacted or soft layers with fines.

Partial uplift and *double jump* are the most frequent operating conditions. The distinction between these two conditions is that the double jump mode contains more excitation cycles (Adam 1997).

Figure 1.5 shows the vertical movement of the soil at different depth under the drum of a vibrating roller in the double jump condition.

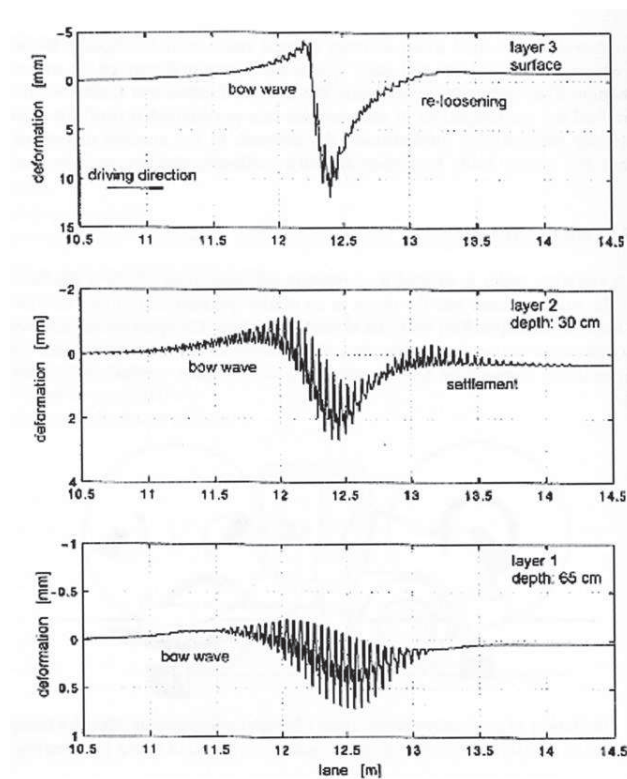


Figure 1.5 Soil deformation at three depths below the impacts of a vibratory roller drum operating in the double jump condition (Adam and Kopf, 2000)

Rocking motion is the other mode that occurs when the stiffness of the soil increases. As the roller runs into this mode, the drum axis is no longer vertical and the drum starts rocking (Adam 1997, Brandl and Adam 2004). Bouncing (double jump) and rocking are not desirable modes since they tend to have a loosening effect on the top layer of the soil and the roller loses its maneuverability. The only difference between bouncing and rocking is a phase shift of 180° that occurs between the subharmonic vibrations of the right and left edges of the drum. The theory predicts rocking if the natural frequency of

the rocking motion is lower than that of the vertical vibration; otherwise, bouncing will occur (Anderegg and Kaufmann 2004).

Chaotic motion is the last one, which occurs on soils with a very high stiffness (Adam 1997). At this point, the roller is not manoeuvrable any more (Brandl and Adam 2004). The chaotic behavior of the vibratory roller originates from the nonlinearity and occurrence of subharmonics during compaction. In a chaotic mode of vibration, the dynamic behavior of the roller may be unstable and erratic. To prevent this condition, one solution can be to reduce the power of excitation by increasing the static moment mere (Anderegg and Kaufmann 2004).

In summary, as the soil stiffness increases, the drum goes into the later modes of vibration (rocking and chaotic), which make the continuous compaction control process inaccurate and unreliable (Adam 1997). Among the previously discussed modes of operation, continuous contact, partial uplift, and double jump can be described theoretically by a one-degree-of-freedom interaction system while the rocking motion and chaotic motion require a more sophisticated multi-degree-of freedom system (Brandl and Adam 2004).

1.3.4. *Oscillatory Roller*

The drum of an oscillatory roller oscillates torsionally. The torsional motion is caused by two opposite rotating excentered masses, which shafts are arranged eccentrically to the axis of the drum. Thus, the soil is shaken horizontally in addition to the vertical dead load of the drum and the roller frame. These cyclic horizontal forces result in soil shear deformation. In this case, compaction is achieved mainly by transmitted shear waves through the material. Oscillatory rollers are used mainly for asphalt compaction and for cohesive soils. Furthermore, oscillatory rollers are used in the vicinity of sensitive structures, because the emitted vibrations are typically lower in amplitude and in zone of influence than the vibratory rollers.

1.3.5. *VARIO Roller*

The VARIO roller is a development of the BOMAG Company. In a VARIO roller two counter-rotating exciting masses cause a directed vibration. These masses are concentrically placed on the shaft of the drum. The direction of vibration can be adjusted by turning the complete exciter unit in order to optimize the compaction effect

for a given soil type (Figure 1.6). If the exciter direction is vertical or inclined, the compaction effect of a VARIO roller can be compared with that of a vibratory roller. However, if the exciter direction is horizontal, the VARIO roller compacts the soil much like an oscillatory roller. There is some difference between a Vario roller and an oscillatory roller because the shear deformation of the soil is caused by a horizontal translation in the VARIO roller, whereas the drum of an oscillatory roller is working torsionally. Nevertheless, a VARIO roller can be used both for dynamic compression compaction, for dynamic shear compaction, and for a combination of these two conditions. Consequently, VARIO rollers are applicable to more soil types and the optimum direction of vibration can be found by a site investigation for each project.

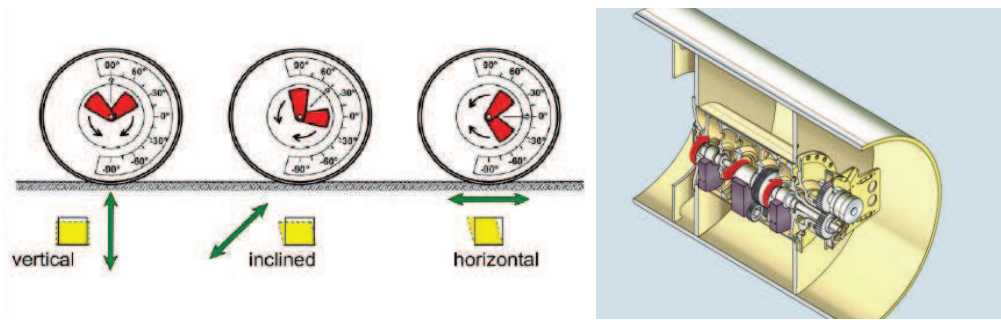


Figure 1.6 Adjustable excitation direction of a VARIO roller drum and compaction effect (Adam and Kopf, 2000)

1.3.6. VARIO Control Roller

Based on the findings related to the operation of different dynamic rollers, BOMAG developed the first automatically controlled roller: the VARIO CONTROL roller (Figure 1.7).

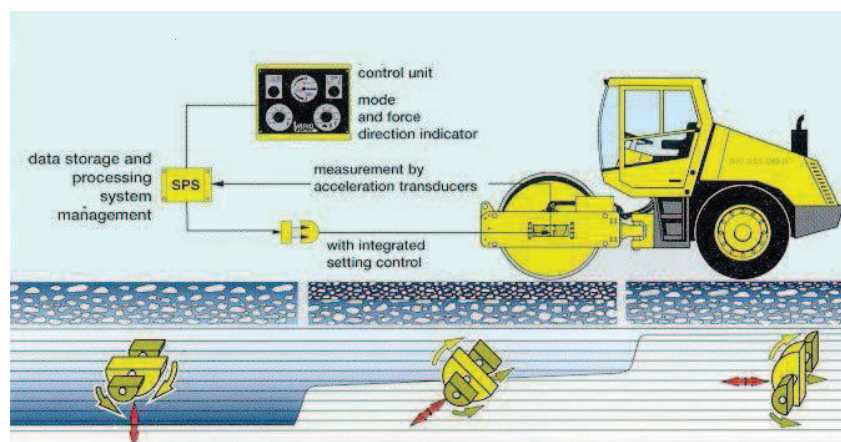


Figure 1.7

Figure 1.8 VARIOCONTROL Single Drum Rollers (from CCC control MnROAD demonstration)

In this roller, the direction of vibration can be varied automatically from vertical to horizontal by using defined control criteria (Figure 1.8), which allow an optimized compaction process (intelligent compaction) and consequently, a highly uniform compaction. These criteria are:

- Operating criterion: If the drum passes to the operating condition called “double dump,” the excitation direction is immediately changed, so that the drum goes back to the operating condition of partial uplift.
- Force criterion: If the specified maximum compaction force is reached, the excitation direction is changed by the automatic control system, so that the applied force does not exceed the maximum force.

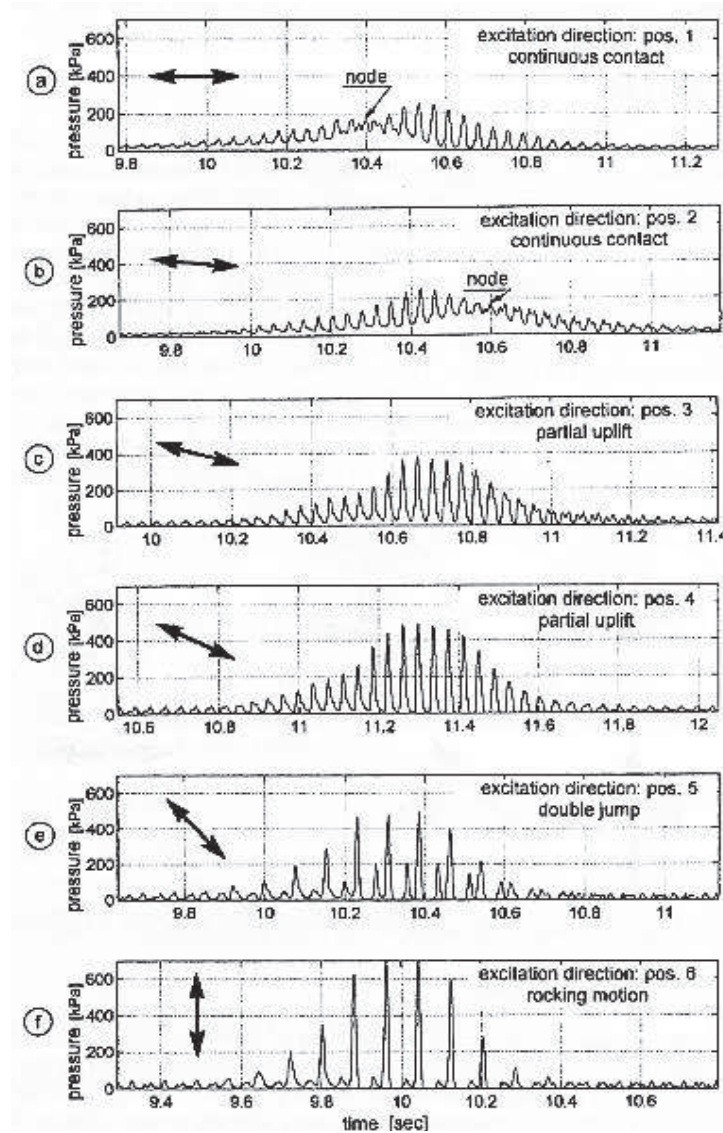


Figure 1.9 Soil pressure and operating condition depending on the VARIO exciter direction (Adams and Kopf, 2000).

Two accelerometers, which are mounted on the bearings of the drum, record the drum acceleration continuously. The soil contact force, the energy delivered to the soil, and the displacements are calculated in a process unit taking into consideration the roller parameters such as masses, exciter force and frequency. The data are transmitted to an integrated system, which manages the parameters automatically.

1.4. Continuous Compaction Control and Intelligent Compaction

Continuous compaction control systems (CCC) and intelligent compaction (IC) were introduced to the compaction industry in an attempt to address the limitations of commonly used in situ quality assurance and quality control (QA/QC). In this portion of the literature review, explanation of CCC and IC systems is presented followed by a detailed description of different systems used in the new technology as well as the theoretical background of different CCC/IC systems.

1.4.1. Description of CCC/IC Technology

The primary purpose of continuous compaction control and intelligent compaction systems is to enhance the final quality of the compacted material. Quality in compaction of unbound soil layers means achievement of both uniform compaction and sufficient bearing capacity. Efficient compaction requires compaction to be concentrated in areas where further compaction is useful (where there is the potential to further increase the bearing capacity). Efficient compaction reduces the overall compaction time for a given lift of soil, while effectively avoiding under-compaction (which causes a higher risk of settlement problems) as well as overcompaction (which wastes time and has the tendency to crush aggregates) (Turner 1993). “Ideal” compaction on a given project can be characterized by the following factors (Brandl and Adam 2004):

- Compaction optimization
- Compaction documentation, which is essential not only for site acceptance but also for quality control and long-term risk assessment.
- Compaction control

1.4.2. Definition of CCC and IC systems

Continuous Compaction Control (CCC) systems are data acquisition systems installed

on compaction equipment that continuously collect real-time information about the operation and performance of the compactor (Turner and Sandström 1980, Adam 1997, Adam and Brandl 2003). For vibratory compactors (see Sections 1.3.3 to 1.3.6), the data that is often collected includes the vibratory frequency, the amplitude of the roller drum, and the speed of the roller (Adam 1997).

For machine drive power based systems, the engine gross power of the compacting roller is typically recorded, in addition to other properties such as roller speed, roller acceleration, and the slope angle (White et al. 2005).

Intelligent Compaction (IC) is a machine-driven process whereby CCC data is interpreted and used in real-time to adjust the operation of the compactor in an attempt to optimize the compaction process and to achieve more uniform soil compaction (Adam and Brandl 2003, Anderegg et al. 2006). As an example of this process, on a typical granular-soil compaction project, IC optimization begins by compacting the soil using high amplitude and low frequency vibratory energy for the initial compactor passes, which encourages effective compaction of the layer to deeper depths. As the compaction progresses, in order to avoid crushing soil aggregates and to encourage compaction of more surficial soil layers, the IC system raises the excitation frequency and decreases the amplitude automatically using a machine feed back loop in conjunction with the CCC system (Anderegg and Kaufmann 2004).

1.4.3. Advantages and Drawbacks of CCC/IC technology

After conducting several projects in Europe, a comparison between projects that utilized CCC equipped compactors and the those which utilized conventional compaction equipment and traditional in-situ tests showed that by using new technology provides substantial quality and cost benefits. Among these are:

1. Higher efficiency and maximized productivity by automatic control of amplitude, frequency, and speed
2. Minimized Number of Passes
3. Higher adaptability (thin/thick layers, soft/stiff subbase)
4. Wider application range
5. Optimal Compaction Results, better quality
6. More uniform compaction

7. Less aggregate crushing
8. Better flatness
9. Complete coverage of compaction surface evaluation
10. Dynamic measurement of soil stiffness
11. No Danger of Overcompaction
12. Compaction Control on the Job
13. Easy to operate
14. Extended life of the roller by minimizing the double jump situation.

Continuous compaction control and intelligent compaction have also been criticized in some cases. The most commonly referenced drawbacks are as follows (Petersen et al. 2006):

1. It requires sophisticated equipment in a rugged environment
2. It requires some operator training
3. It is more expensive than conventional compaction
4. Need RTK GPS for precise compactor location

These drawbacks are of little relevance compared to the benefits. In fact the added quality of the final product is likely to represent significant savings associated with less disputes with the clients. Intelligent compaction develops in Europe in large part because of the evolution of contracts and procurements.

1.5. Principal Theories of Operation of CCC/IC Systems

There are various recording systems that have been introduced into the CCC/IC industry over the years. In this section, these recording systems are discussed in more detail. In the first few sections, vibratory-based systems are reviewed.

All of the following vibratory-based systems that are discussed consist of a sensor set containing one or two accelerometers attached to the bearing of the vibratory roller drum, a processor unit, and a display to visualize the measured values.

The sensor continuously records the acceleration of the drum. The time history of the acceleration signal is analyzed in the processor unit in order to determine dynamic compaction values with respect to specific roller parameters (Brandl and Adam 2004).

1.5.1. Compaction Meter Value (CMV)

The drum of a vibratory roller exposes the soil to repeated blows – one per cycle of the vibration. These blows can be considered analogous to a repeated dynamic plate load test of the soil. It can be shown that the force amplitude F of the blows is proportional to the first harmonic of the vertical acceleration. The vertical displacement z_d during the blow can be approximated by the amplitude of the double integral of the fundamental acceleration component (Sandström 1993, Adam 1996, Thurner and Sandström 2000). Therefore, it is relevant to express the “cylinder deformation modulus” E_c as the ratio of the applied force and the corresponding displacement:

$$E_c = C_1 \frac{F}{z_d} = C_2 \omega^2 \frac{\hat{a}(2\omega_0)}{\hat{a}(\omega_0)} \quad (1.2)$$

where, C_1 and C_2 are constants, ω = fundamental angular frequency of the vibration, $\hat{a}(2\omega_0)$ = Amplitude of the first harmonic of the acceleration response signal, and $\hat{a}(\omega_0)$ = Amplitude of the exciting frequency (Thurner and Sandström 2000).

Using the general framework of Equation 1.2, engineers at Geodynamik (Thurner and Sandström 1980) developed a roller measurement value called Compaction Meter Value (CMV). CMV is calculated by dividing the amplitude of the first harmonic of the acceleration signal by the amplitude of the exciting frequency (Equation 1.3).

$$CMV = C \cdot \frac{\hat{a}(2\omega_0)}{\hat{a}(\omega_0)} \quad (1.3)$$

where, $C = A$ constant value chosen to empirically scale the output CMV values to an easier-to-interpret range. Using $C = 300$ has become a commonly accepted and standardized approach for calculating CMV values from measured vibratory roller data (Sandström and Pettersson 2004).

Thurner and Sandström tested the CMV equation shown above on compacted soils at a range of different densities and stiffnesses. It was observed that if the drum of the roller moves on a very soft zone, then there was no first harmonic.

In this case, CMV was approximately zero. When the drum moves over a loose, coarse-grained material (beginning of compaction) the amplitude of the first harmonic will be low and consequently CMV will remain at a low value. As compaction progresses, the amplitude of the first harmonics becomes relatively high and the corresponding CMV

values increase.

The ratio of $\hat{a}(2\omega_0)/\hat{a}(\omega_0)$ is a measure of nonlinearity. In a truly linear roller-soil system, a roller with an excitation frequency of 30 Hz (a reasonable value) would produce a 30 Hz drum acceleration response and $\hat{a}(2\omega_0)/\hat{a}(\omega_0)$ would equal to zero. However, because the roller-soil system is nonlinear, the drum acceleration response is distorted and is not purely sinusoidal. (The response of soil to vibratory compaction is actually nonlinear elastic-plastic, and because a partial loss of contact occurs, the contact surface varies nonlinearly during each cycle of loading). Fourier analysis can reproduce a distorted waveform by summing multiples of the excitation frequency. Therefore, the ratio $\hat{a}(2\omega_0)/\hat{a}(\omega_0)$ is a measure of the degree of distortion or nonlinearity (Mooney and Adam 2007).

From an analytical stand point, the value of CMV is determined by performing spectral analysis of the measured vertical drum accelerations over two cycles of vibration (Figure. 1.9). The reported CMV values are the average of a number of two-cycle calculations. Geodynamik typically averages the values over 0.5 sec; however, this can be modified as needed. CMV precision is governed by a 1% distortion resolution of the accelerometer. By using Equation 1.3 with $C = 300$, a 1% acceleration distortion equates to a $CMV = 3$ or ± 1.5 . However, Geodynamik reports less reliability for CMV when recorded values are below 8-10 (Mooney and Adam 2007).

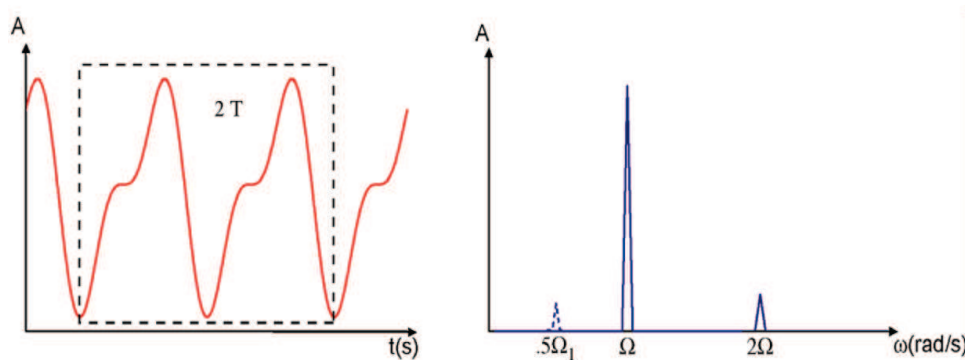


Figure 1.10 Method to determine CMV involves spectral analysis (right) of two cycles of vertical drum acceleration time history data (left) (modified from Mooney and Adam 2007)

Another control value that is commonly used in Compactometer systems is the Resonant Meter Value (RMV), which is proportional to the quotient of the amplitude of the half frequency of the acceleration signal divided by the amplitude of the exciting frequency (Equation 1.4). A non-zero RMV indicates that the drum is not in the mode

of continuous contact (Adam 1997).

$$RMV \sim \frac{\hat{a}(0.5 \omega_0)}{\hat{a}(\omega_0)} \quad (1.4)$$

where $\hat{a}(0.5 \omega_0)$ = Amplitude of subharmonic acceleration caused by jumping, i.e., the drum skips every other cycle, and $\hat{a}(\omega_0)$ = Amplitude of the exciting frequency.

Currently, Dynapac, Caterpillar and Ingersoll Rand (via Geodynamik equipment) are utilizing a Compactometer system for CCC roller monitoring (Mooney and Adam 2007).

A compaction meter for oscillatory rollers has also been developed that is based on a measurement of the horizontal acceleration of the center axis of the drum.

When the drum is operating at frequencies above the resonance frequency, and there is no slip, the amplitude of this signal is a function of soil stiffness as well as the roller parameters. This stiffness value, called the Oscillometer Value (OMV), is not sensitive to moderate variations in the excitation frequency. When there is slip between the drum and soil, the signal processor of the oscillometer uses a special algorithm to calculate the OMV. This calculation is based solely on the time intervals during which the soil and the drum move together without slipping (Turner and Sandström 2000, Sandström and Pettersson 2004).

1.5.2. *Compaction Control Value (CCV)*

In an attempt to improve upon the Compaction Meter value, the Japanese company Sakai has introduced a continuous compaction value (CCV), which considers the first subharmonic ($0.5\omega_0$) and higher-order harmonics in addition to the fundamental and first harmonic (Mooney and Adam 2007).

$$CCV = \left[\frac{a(0.5 \omega_0) + a(1.5 \omega_0) + a(2.5 \omega_0) + a(3 \omega_0)}{a(2.5 \omega_0) + a(3 \omega_0)} \right] \cdot 100 \quad (1.5)$$

Research conducted by Sakai (Scherocman et al. 2007) found that as the ground stiffness increases and the roller drum starts to enter into a “jumping” motion, vibration accelerations at various frequency components are developed as illustrated in Figure 3.

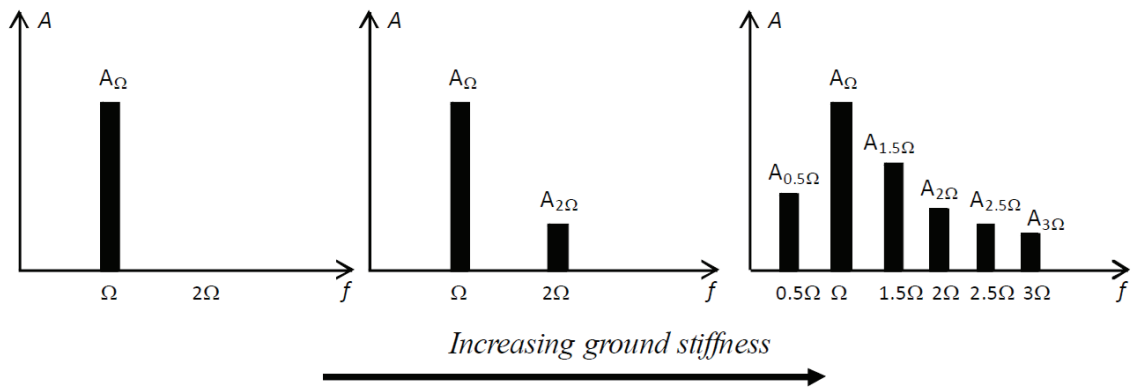


Figure 1.11 Changes in amplitude spectrum with increasing ground stiffness (modified from Scherocman et al. 2007)

1.5.3. OMEGA

In 1988, Kröber from the American-German company Bomag, developed the OMEGA value and incorporated it into the Terrameter system (Mooney and Adam 2007). The OMEGA value provides a measure of the energy transmitted to the soil.

The concept is illustrated by the schematic of the roller compactor and the forces acting on the drum in Figure 1.11. Here, F_s is the force transmitted to the soil, which is determined by summing the static force (roller weight), drum inertia and eccentric force $m_0 e_0 \omega^2$ while ignoring the effect of frame inertia (Adam 1997).

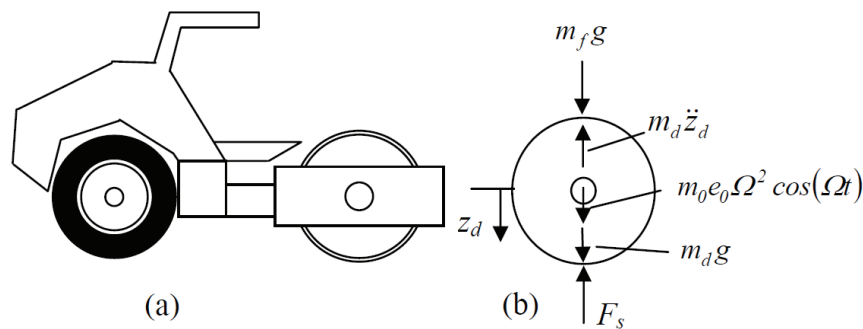


Figure 1.12 One-degree-of-freedom lumped parameter model representation of vibratory compactor (modified from Mooney and Adam 2007)

The drum acceleration \ddot{z}_d is measured in two perpendicular directions. An accelerometer provides the time history of the drum acceleration. The OMEGA value is determined by integrating the transmitted force F_s and drum displacement z_d time history over two consecutive cycles of vibration to consider the operating condition of double jump (Adam 1997):

$$OMEGA \sim W_{eff} \oint_{2T} [-(m_d)\ddot{z}_d + (m_d + m_f)g + m_0 e_0 \omega^2] \dot{z}_d \cdot dt \quad (1.6)$$

where, \ddot{z}_d = Drum vertical velocity (m/s²), m_d = Drum mass (kg), m_f = Frame mass (kg), m_0 = Mass of the rotating eccentric (kg), e_0 = Eccentricity (m), ω = Circular frequency (rad/s), g = Gravitational acceleration (9.81 m/s²), and W_{eff} = Absorbed energy by soil (N·m).

Like CMV, OMEGA values increase as drum behavior transitions from continuous contact to double jump. Consequently, under similar operating conditions, OMEGA values increase with increasing soil stiffness. Upon entering the double jump mode, a sudden drop in OMEGA values occurs, followed by a continued increase with increasing soil stiffness within the double jump mode (Adam 1997).

OMEGA values correlate well to soil stiffness, provided that a linear transformation between dynamic compaction values is performed. However, this conformity is valid only for values within a particular mode of drum vibrational behavior. The correlation between CMV and OMEGA is approximately linear within the operating conditions of continuous contact and partial uplift (Brandl and Adam 1997).

1.5.4. Stiffness (k_s)

In the late 1990s, Ammann introduced a roller-determined soil stiffness parameter k_s (Anderegg 2000). Using this approach, the roller free body shown in Figure 1.12 is treated as a lumped parameter model to represent the vertical kinematics of the soil-drum-frame system. Within this framework, the soil behavior is modeled using a Kelvin-Voigt spring-viscous dashpot model (Mooney and Adam 2007). As shown in figure, the roller can be subdivided into two separate pieces, the frame and the drum, where the frame is supported using an elastic suspension element whose behavior is modelled using stiffness k_t and damping c_t . The subgrade behavior can then be modelled as a spring with stiffness k_s and a viscous damper connected in parallel, having a damping constant c_s . In conjunction with the drum, this creates the spring-mass-dashpot vibration system, which describes the characteristics of a dynamic compactor (Anderegg and Kaufmann 2004). This model is valid provided that the excitation frequency is well above the resonance frequency for the frame-suspension elements (Anderegg et al. 2006).

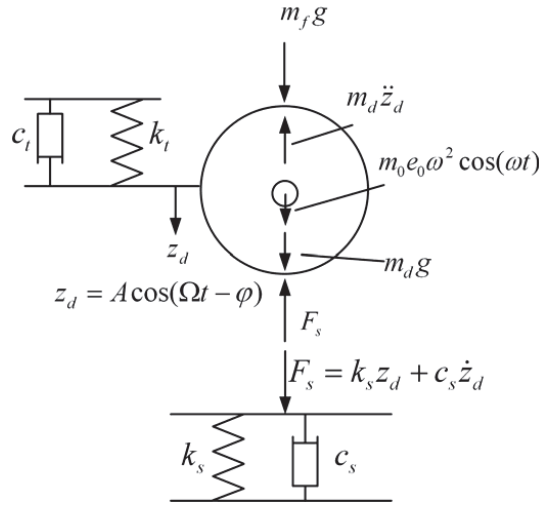


Figure 1.13 Lumped parameter two-degree-of-freedom spring dashpot model representing vibratory compactor and soil behavior (reproduced from Yoo and Selig 1980)

As the compaction progresses, the stiffness increases and the damping decreases. Assuming constant machine parameters, the vibration behavior of the system varies accordingly and this can be used as a measurement indicator value in a continuous compaction control system. The steady-state dynamic behavior of the soilmachine system is described by the following equations (Anderegg and Kaufmann 2004):

$$F_s = -m_d \ddot{z}_d + m_0 r_0 \omega^2 \cos(\omega t) + k_t(z_d + z_f) + C_t(\dot{z}_d - \dot{z}_f) + m_d g \quad (1.7)$$

$$0 = -m_f \ddot{z}_f + k_t(z_f + z_d) + C_t(\dot{z}_f - \dot{z}_d) + m_f g \quad (1.8)$$

where, F_s is soil-drum interaction force,

$$F_s = k_s z_d + c_s \dot{z}_d \quad \text{if } F_s \geq 0 \quad (1.9)$$

$$F_s = 0 \quad \text{)else} \quad (1.10)$$

where, f = Frequency of excitation (Hz), $m_0 r_0$ = Eccentric moment of unbalanced mass (kgm), k_s = Soil stiffness (MN/m), c_s = Soil damping (MNs/m), k_t = Suspension stiffness (MN/m), c_t = Suspension damping (MNs/m), t = Time (s). The other parameters used in Equations 1.7 through 1.10 have been defined previously (for Equation 1.6). In the equations above, the subscripts d and f denote drum and frame, respectively.

The nonlinearity caused by drum lift-off can be recognized by the occurrence of additional frequency overtones that correspond to integral multiples of the excitation

frequency. As an example, subharmonic vibrations may occur at harmonic frequency multiples of 1/2, 1/4, 1/8. etc. of the excitation frequency (Anderegg and Kaufmann 2004). As shown in Figure 1.13, this characterization makes use of the time progression of the soil reaction force F_s or the frequency analysis of the drum motion z_d :

$$z_d = \sum_i A_i \cos(i\Omega t - \phi_i) \tag{1.11}$$

where, A_i is the amplitude at frequency if and ϕ_i is the phase lag between the generated dynamic force and the part of the drum displacement with frequency if (Anderegg and Kaufmann 2004). Depending on the operational status, the vibration displacement has one or more frequencies: Permanent drum-ground contact, linear: $i = 1$; Periodic loss of contact, nonlinear: $i = 1, 2, 3$; Bouncing or rocking: $i = 1/2, 1, 3/2, 2, 5/2, 3$

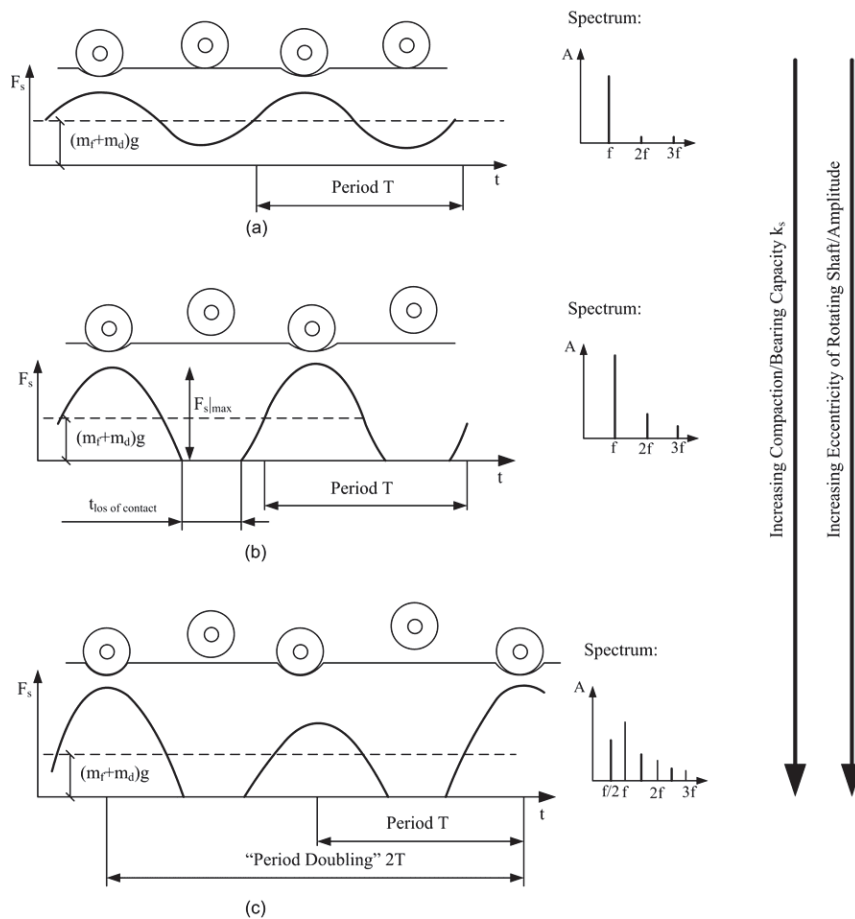


Figure 1.14 Three basic types of behavior of vibrating drum: (a) contact (every time) (b) periodic loss of contact (c) bouncing or rocking (modified after Anderegg and Kaufmann 2004)

By summing Equations 1.7 and 1.8, while considering only the static frame mass and

neglecting the dynamic forces imposed by the elastic frame, Equation 1.11 can be obtained (Andregg and Kaufmann 2004):

$$F_s = (m_d + m_f)g + m_0 r_0 \omega^2 \cos(\omega t) - m_d \ddot{z}_d \quad (1.11)$$

The resulting F_s vs. z_d response is graphically illustrated in Figure 1.14 for continuous contact and partial uplift behavior (after Mooney and Adam 2007). The Ammann k_s is the ratio of F_s to z_d and is computed when the drum is at the bottom of its trajectory and z_d is at its maximum (see Fig. 1.14). This k_s represents a composite static stiffness (spring constant) for the soil and is only valid to the degree which the Kelvin-Voigt model is a reasonable approximation for the soil behavior. The springdashpot model has been shown to be effective in representing roller-soil system behavior (e.g., Yoo and Selig 1979, Adam 1996, Mooney and Rinehart 2007).

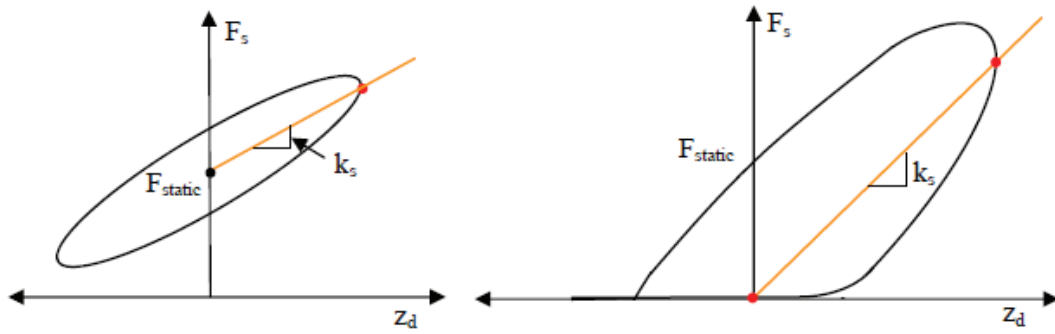


Figure 1.15 Illustration of k_s during contact (left) and partial loss of contact behavior (right) (modified after Mooney and Adam 2007)

Assuming linear elastic soil behavior and nonlinear vibration of the roller, the measured vibration amplitude “ A ”, and the measured phase angle “ ϕ ” can be used to determine the corresponding value of k_s (Andregg Kaufmann 2004):

$$k_s = \frac{F_s|_{\dot{z}_d=0} - (m_d + m_f)g}{A} \quad (1.11)$$

where, $A = |z_d|$ if $\ddot{z}_d = 0$, and if $\ddot{z}_d < 0$ no bouncing or rocking ($A_{1/2}=0$).

In the case of linear vibration without a loss of contact between the drum and soil, k_s can be calculated using the following equation:

$$k_s = 4 \cdot \pi^2 \cdot f^2 \left[m_d + \frac{m_0 \cdot r_0 \cdot \cos(\phi)}{A} \right] \quad (1.12)$$

Subject to the condition of:

$$F_s|_{max} \leq 2(m_d + m_f)g \quad (1.13)$$

Where,

$$F_s|_{max} = (m_d + m_f) \cdot g \cdot \pi \cdot \frac{1 \cos(\frac{t_{l.o.c.}}{T} \cdot \pi)}{(1 - \frac{t_{l.o.c.}}{T}) \cdot \pi \cdot \cos(\frac{t_{l.o.c.}}{T} \cdot \pi) + \sin(\frac{t_{l.o.c.}}{T} \cdot \pi)} \quad (1.14)$$

$F_s|_{max}$ is the maximum of the soil-drum interaction force during one period T , and $t_{l.o.c.}$ is the time where there is a loss of contact between the drum and soil during one period T (Anderegg and Kaufmann 2004)

1.5.5. Vibratory Modulus (E_{vib}) value.

Using stiffness (k_s) as an indicator for compaction improvement has some disadvantages. The stiffness k_s increases with the drum width and the drum diameter.

Furthermore, it depends on the vibrating mass, the mass of the frame structure and the installed unbalanced mass. Generally, it can be observed that, in contrast to the formerly common indirect characteristic quantities (e.g. OMEGA value), the stiffness (k_s) is a physically verifiable characteristic magnitude; unfortunately however, its measured values cannot be directly transferred from one type of roller to another.

Consequently, a variety of approaches that use modulus have been developed to address this limitation (Kröber et al. 2001). Bomag has more recently utilized a lumped parameter vibration model developed using elastic half-space theory to calculate an additional compaction control value called vibratory modulus (E_{vib}) (Kröber et al., 2001). The same assumptions and definitions used for calculating the stiffness value are used in this derivation (see Figure 1.15).

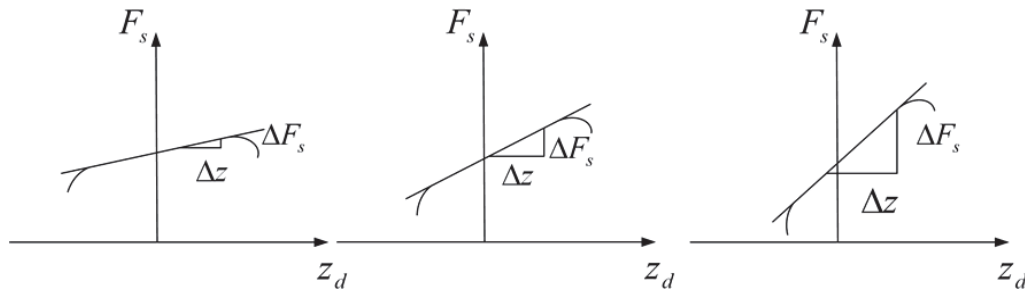


Figure 1.16 Increasing stiffness values in a higher gradient of the force-path characteristic curve

(modified after Kröber et al. 2001)

The stiffness is extracted from the loading portion of the drum-force deflection curves (Fig. 1.16) to come up with a vibration modulus value (E_{vib}) (Mooney and Adam, 2007). The ratio of ΔF_s to Δz_d represents a characteristics quantity for the evaluation of the soil stiffness (Kröber et al. 2001):

$$k = \frac{\Delta F_s}{\Delta z_d} \quad (1.16)$$

A similar but more simple mechanistic load-response process takes place during a field plate load test (PLT). In a PLT, a circular plate is gradually loaded and unloaded to determine the deformation modulus, as follows:

$$k = \frac{\Delta F_s}{\Delta z_d} = \frac{4 G r}{1-\nu} \quad (1.17)$$

where, G = Shearing modulus, r = Radius of plate, and ν = Poisson ratio.

Equation 1.17 is derived using a closed-form solution for the linear, elastic, isotropic half volume and can be interpreted using the following approach: Based on a measured force-displacement interrelationship (ΔF , Δz_d) and in the presence of a certain geometry (r), the following equations can be applied (Kröber et al., 2001):

$$G = \frac{E}{2(1+\nu)} \quad (1.18)$$

$$k = \Delta \sigma \cdot \pi \cdot r^2 \quad (1.19)$$

Combining equation 2.15 to 2.17, we have:

$$E = \frac{\pi \cdot (1+\nu^2)}{2} \cdot r \cdot \frac{\Delta \sigma}{\Delta z} \quad (1.20)$$

As noted previously, true soil behavior cannot be captured using a linear, elastic, and isotropic material model. If it would fulfill these conditions, the deformation modulus would be the same as the E-modulus. In contrast to a PLT, where the loaded area is defined by the precisely circular load plate, the shape of the contact area for a vibratory roller can be modeled as a cylinder that is lying on its side.

The contact width (b), which controls the overall area of roller contact and the corresponding applied static and dynamic pressures, can be determined from the depth of the depression that the drum makes in the soil using Lundberg's formulas (Kröber et al. 2001):

$$b = \sqrt{\frac{16}{\pi} \cdot \frac{R(1-\nu^2)}{E} \cdot \frac{F_B}{L}} \quad (1.21)$$

$$z_d = \frac{1-\nu^2}{E} \cdot \frac{F_B}{L} \cdot \frac{2}{\pi} \cdot \left(1.8864 \ln \frac{L}{b}\right) \quad (1.22)$$

where, b = Contact width, R = Radius of drum, ν = Poisson's ratio, E = Modulus, F_s = Ground contact force, L = Width of drum, and z_d = Depth of depression. These formulas are derived based on a parabolic load area acting across the contact width, where the contact width is always smaller than the width of the drum and the cylindrical roller body is supposed to have a slightly spherical shape (Kröber et al. 2001).

During the PLT, the load curve is used for evaluation. As an analogy to this, the compression part of the indicator diagram is used for calculating the soil modulus, which is called E_{vib} . The relationship between k_s and E_{vib} is shown in Figure 1.16 (Mooney and Adam 2007).

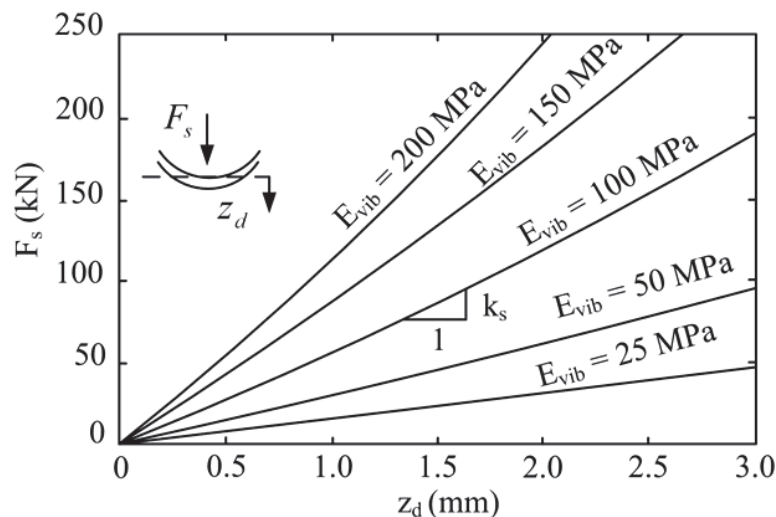


Figure 1.17 Relationship between contact force and drum displacement for a cylinder on an elastic half-space (modified after Mooney and Adam 2007)

By treating the roller like the plate in a PLT, and the underlying soil as the elastic half space, a similar relationship can be derived between the measured stiffness (k_s) and the

vibratory modulus (E_{vib}) of the compacted material based on Lundberg's theory (Anderegg and Kaufmann 2004):

$$k_s = \frac{E_{vib} \cdot L \cdot \pi}{2 \cdot (1 - \nu^2) \cdot \left\{ 2.14 + \frac{1}{2} \cdot \ln \left[\frac{\pi \cdot L^3 \cdot E_{vib}}{(1 - \nu^2) \cdot 16 \cdot (m_f + m_d) \cdot R \cdot g} \right] \right\}} \quad [\text{MN/m}] \quad (1.23)$$

As a result of these calculations, a compaction indicator value can be derived which is not dimensionless, and which can be transferred to different machines using a special calibration process. This allows the vibration modulus of the ground to be determined with different machines and machine types. Although this approach has been developed for vertical vibration, it is also promising for oscillatory rollers, provided that the direction of oscillation deviates more than 12-15 degrees from the horizontal plane (Kröber et al. 2001). In summary, the benefits of the compaction indicator value E_{vib} are as follows:

- It allows direct determination of soil stiffness in the form of the vibration modulus E_{vib} , which has units of MPa (tsf) during the compaction process
- E_{vib} is directly related to E_{v1} and E_{v2} , which are the first and second loading modulus values obtained from two cycle plate load tests.
- E_{vib} is relatively independent from the amplitude, frequency, and working speed of the roller.

1.5.6. Evaluation of Vibratory Measurement Values

A number of independent studies have been performed to investigate dynamic roller measurement values. Adam and Kopf (2004) numerically simulated roller-soil behavior using finite element analysis of a roller vibrating on an elastic half-space to explore the influence of the soil's Young's modulus (E-modulus in Figure 1.17) on the roller measurement values. The y-axis in Figure 1.17 depicts the relative drum vibration amplitude, i.e., the ratio of z_d to the theoretical maximum $z_{d(max)}$ given by Equation 1.23. The theoretical maximum drum displacement $z_{d(max)}$ is determined by measuring the drum vibration in air (e.g. frame propped up on jack stands); $z_{d(max)}$ is a term often cited in the soil compaction community (Mooney and Adam 2007).

$$z_{d(max)} = \frac{m_0 e_0}{m_d} \cdot \quad (1.23)$$

Figure 1.16 shows the relative location of various contact modes, their presence as a

function of relative drum displacement, amplitude, and soil modulus, and how they are influenced by relative amplitude and soil modulus. Since double jump, rocking, and chaos are now typically avoided via feedback control of the roller, it is most interesting to focus on the behavior of the system during continuous contact and partial uplift modes. As illustrated in Figure 1.18, values of CMV are very low and constant when the drum is operating in a continuous contact mode, regardless of the soil modulus. Given that the soil is modelled here as linear elastic, only the curved drum/soil interaction nonlinearity is contributing to the CMV during the continuous contact mode.

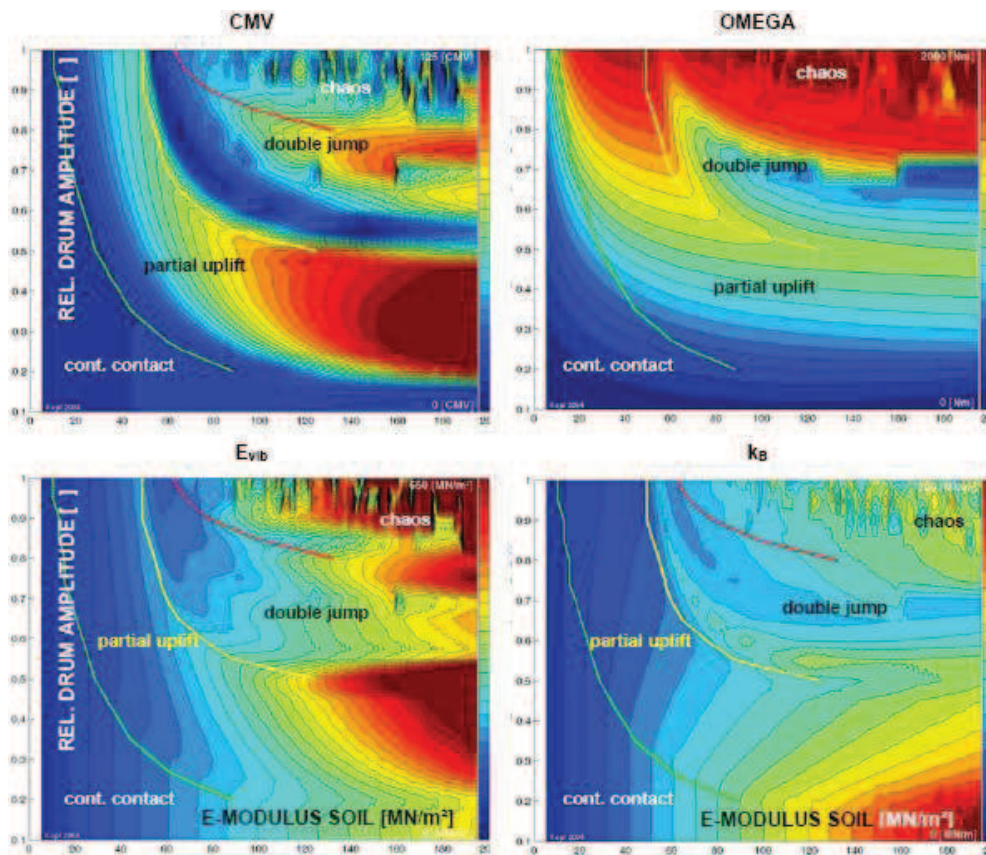


Figure 1.18 Variation of roller measurement value with soil modulus and relative drum vibration amplitude - results of numerical simulations; a) CMV , b) E_{vib} , c) $OMEGA$, and d) k_b (modified after Mooney and Adam 2007)

This figure also illustrates how CMV values respond to soil stiffness during partial uplift; CMV increases as the soil modulus E increases. However, CMV at a constant soil modulus is amplitude dependent; therefore, a higher eccentric force will yield a greater CMV for the same soil. The amplitude dependency of CMV is more pronounced for softer soils than for stiffer soils (Mooney and Adam 2007).

E_{vib} is sensitive to changes in soil modulus during continuous contact and partial uplift

modes; an increase in soil modulus leads to an increase in E_{vib} .

E_{vib} exhibits little or no amplitude dependency in continuous contact mode but increases with increasing amplitude during partial uplift. This amplitude dependency is more pronounced for stiffer soil. Similar to E_{vib} , k_s increases with soil modulus and is amplitude dependent during partial uplift. However, k_s decreases with increasing amplitude during partial uplift, particularly for stiffer soil. The amplitude-dependency of soil stiffness was also demonstrated in field testing by Mooney and Rinehart (2007). Finally, the OMEGA value was found to be much less sensitive to underlying soil stiffness for constant amplitudes of input vibration. CMV , E_{vib} , and k_s each exhibit amplitude dependency at a constant soil modulus. Ideally, one would like the measurement value to be independent of eccentric force and amplitude, particularly for variable amplitude control compaction (Mooney and Adam 2007).

Figure 1.19 presents the numerically derived measurement values as a function of soil modulus for a given relative amplitude. OMEGA, E_{vib} and k_s are linearly dependent on soil modulus during continuous contact mode and CMV is fairly constant. During partial uplift, CMV is the most sensitive and OMEGA is the least sensitive to changes in soil modulus. Again, the performance of each measurement value during double jump is not so relevant given today's roller technologies (Mooney and Adam 2007).

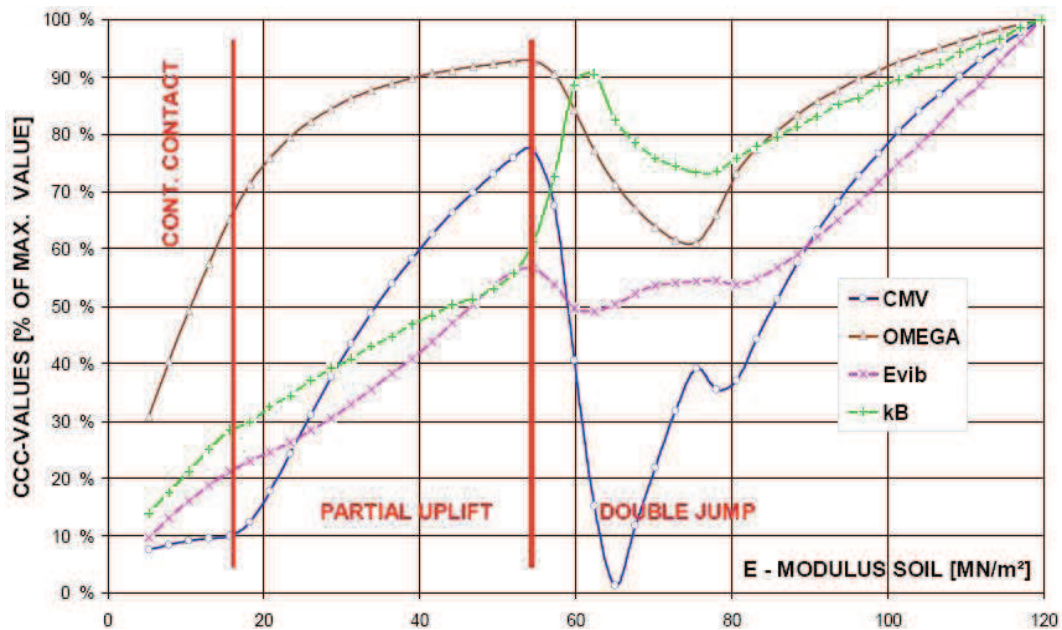


Figure 1.19 Relative roller measurement values (CCC values) as a function of soil modulus as determined from numerical simulations (modified after Adam and Kopf 2004, Mooney and Adam 2007)

A summary of commonly used CCC values, their descriptions, and the associated compaction equipment manufacturers are presented in Table 1.2.

table 1.2. Established CCC systems, CCC values, and the associated equipment manufacturers

CCC System	CCC Value	Definition of CCC Value	Manufacturer
Compactometer	CMV (unitless)	acceleration amplitude ratio (first harmonic div. by excitation frequency amplitude) - frequency domain	Geodynamik, Sweden
Terrameter	OMEGA (N.m)	energy transferred to soil (considering soil contact force displacement relationship of 2 excitation cycles) - time domain	Bomag, Germany
Continuous Compaction Value	CCV (unitless)	acceleration amplitude ratio - frequency domain	Sakai, Japan
Terrameter	Evib (MPa)	dynamic elasticity modulus of soil beneath drum (inclination of soil contact force displacement relationship during loading) - time domain	Bomag, Germany
ACE	ka (MN/m)	spring stiffness of soil beneath drum (derived from soil contact force displacement relationship at maximum drum deflection) - time domain	Ammann, Switzerland
Machine Drive Power	MDP (kW)	net power to propel the roller	Caterpillar, USA

1.6. Roller manufacturers

Rollers vary in weight from 5 tons to 25 tons. They operate at frequencies around 30 Hz. The contact force can reach 40 tons and the displacement under the roller varies from 30 mm (first pass) down to a fraction of a millimeter (last pass). The modulus measured after compaction can range from 30 MPa to 200 MPa.



Figure 1.20 single-drum IC roller manufacturers

There are at least 5 vendors around the world have been developing single-drum IC rollers. Currently, there are two various types of soils/subbase IC rollers available in the EU that meet the above IC roller requirements: Bomag , Case/Ammann, Caterpillar, Dynapac, Sakai and Volvo (figure 1.19). Most of the above single-drum IC roller manufacturers offer smooth drum and padfoot models.

1.6.1. Bomag Soil IC System

The Bomag IC system is called VarioControl IC system(BVC). The Bomag IC roller is equipped with two acceleration transducers, processor/control unit, distance measurement, GPS radio/antenna, Bomag Operation Panel (BOP), and onboard BCM 05 documentation system (Figure 1.21).

The direction of vibration is adjustable from horizontal to vertical. The BVC allows the use of much larger amplitudes than is possible with conventional vibration systems. The vertical direction vibration gives the maximum energy available from the roller and the horizontal direction gives the minimum energy from the roller. This flexibility improves compaction close to the surface and reduces loosening.

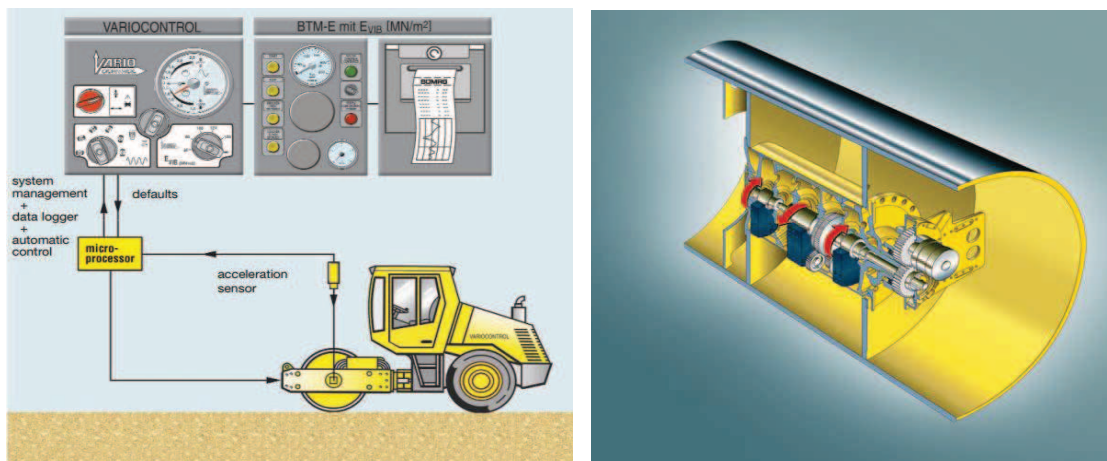


Figure 1.21 BTM-E and BVC (from BOMAG Brochure)

The Bomag IC measurement value is called E_{vib} [MN/m²] or vibration modulus (more strictly, stiffness). The E_{vib} values are computed based on the compression paths of contact forces vs. drum displacement curves (figure 1.22) . The E_{vib} values increase with increasing pass number. E_{vib} also responds to changes of material density and asphalt mixture temperature (with dropping compaction temperature, E_{vib} of asphalt mixtures becomes greater).

The operator can pre-select 6 minimum values ($E_{vib} = 45, 80, 100, 120, 150 \text{ MN/m}^2$ and maximum). During the compaction, the dynamic modulus and speed are continuously measured, recorded and displayed. When the pre-set minimum value is reached or at maximum compaction the VARIOCONTROL system reduces compaction forces and a green light on the Evib display indicates the end of compaction.

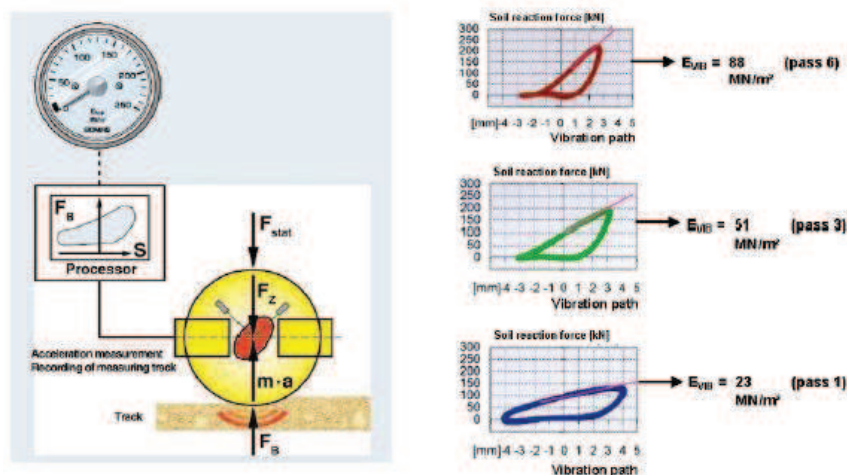


Figure 1.22 Principle of the Evib measurement system - BTM-E (from Kloubert's presentation at TRB-2004, BOMAG)

The Bomag Evib values correlate well with load bearing capacities (E_{v1}/E_{v2}) from the plate loading tests. The feedback control in the Bomag IC system is called VarioControl that enables the automatic adaption of the amplitude during the compaction process.

1.6.2. Case/Ammann Soil IC System

The Case/Ammann IC system is called the ACE and feedback drum system. The ACEplus system was formed by combining the former Ammann Compaction Expert (ACE) measurement and control system with continuous compaction control (CCC).

The roller-integrated stiffness (k_s) measurement system on the Case/Ammann IC rollers was introduced by Ammann during late 1990's considering a lumped parameter two-degree-of-freedom spring-mass-dashpot system. The spring-mass-dashpot model has been found effective in representing the drum-ground interaction behavior. (figure 1.23) The drum inertia force and eccentric force time histories are determined from drum acceleration and eccentric position (neglecting frame inertia). The IC soil stiffness, k_s , can be determined when there is no loss of contact between drum and soil. It is closely related to the plate loading test results.

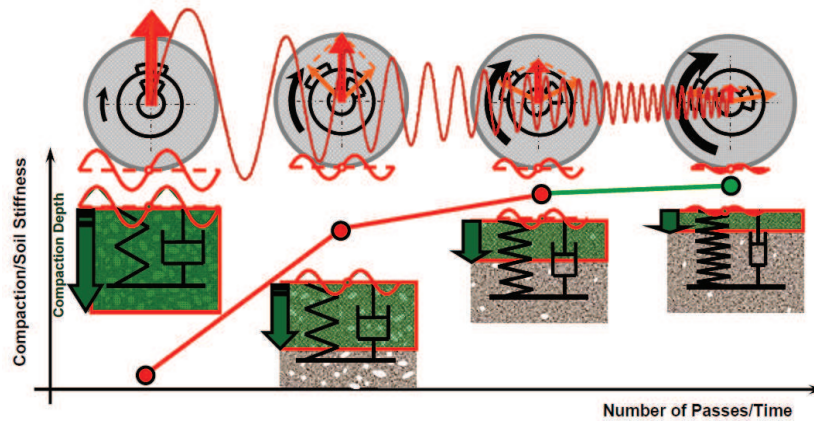


Figure 1.23 Principle of the ACE measurement system.

ACE is an electronic measuring and controlling system for vibrating rollers. It is an automatic close-loop control automatically adjusts roller vibratory amplitudes and frequencies to suit the characteristic of the compacted ground condition. The Case/Ammann ACE auto feedback system can adjust the roller vibratory frequency and amplitude at each roller pass – depending on the condition of the compacted ground condition – thus, optimize the compaction with least desirable number of passes.

1.6.3. Caterpillar Soil IC System

The Caterpillar IC system include an accelerometer, slope sensor, controllers, communication data radio, Real-time Kinematic (RTK) GPS receiver, an off-board GPS base station, and onboard report system. The slope (angle) sensor measures the left/right tilt of the drum to a range of $\pm 45^\circ$. Collectively, the above components are integrated into so-called Caterpillar AccuGrade system to provide accurate IC measurements during compaction.

The Caterpillar IC measurement values for indication of levels of compaction include compaction meter values (CMV), resonance meter values (RMV), and machine drive power (MDP).

The CMV was developed by Geodynamic in 1970's. CMV is defined as a scaled ratio of the second harmonic vs. the first harmonic of the drum vertical acceleration amplitudes based on a spectral analysis. The scaling is made so that CMV values could cover a range of 150 (figure 1.23).

The CMV is reported as average values within two cycles of vibration or typically 0.5 seconds. The resulting CMV is a dimensionless, relative value requiring constant roller

parameters such as drum diameter, linear load, frequency, amplitude, speed, and etc.

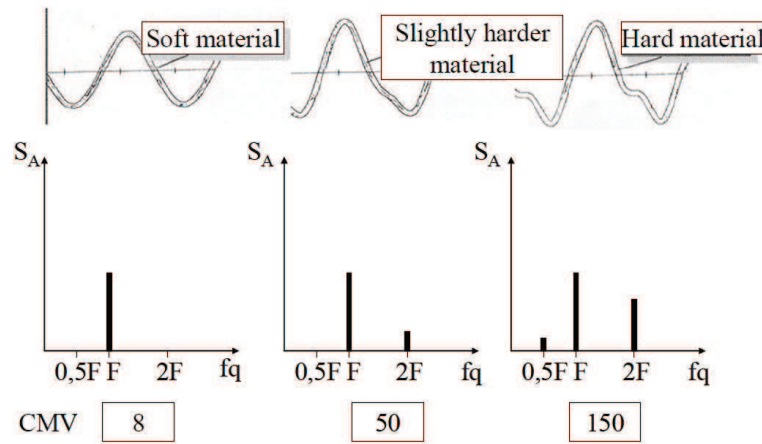


Figure 1.24 Principle of the Caterpillar measurement system (CMV),

Since the CMV is an integral with contribution from large depths (0,9 to 1,8 m for Caterpillar IC rollers) with the highest weighting of the layers closest to the surface, caution should be taken when comparing CMV to the top layer compaction level (often measured by other in-situ devices such as nuclear gauges or LWD) only.

1.6.4. Dynapac Soil IC System

The DCA system measures CMV as an indicator of compaction quality. The CMV technology uses accelerometers to measure drum accelerations in response to soil behaviour during compaction operations (Figure 1.25).

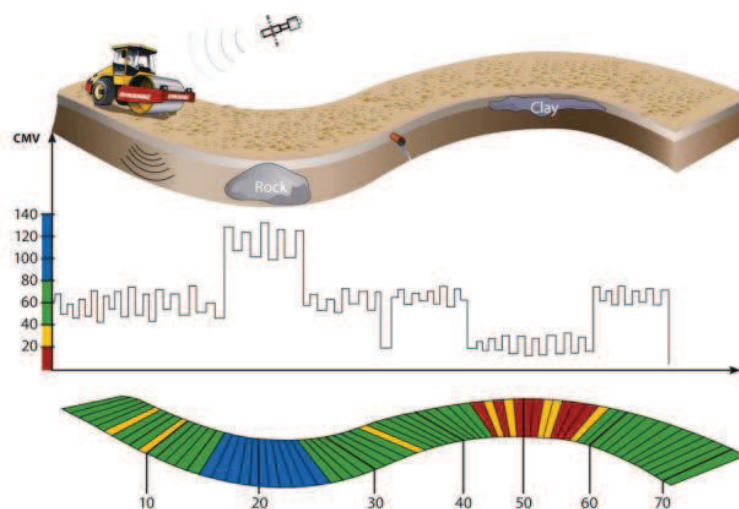


Figure 1.25 Principle of the Dynapac Soil IC System

The ratio between the amplitude of the first harmonic and the amplitude of the fundamental frequency provides an indication of the soil compaction level. An increase in CMV value indicates increasing compaction.

CMV is a dimensionless parameter that depends on roller dimensions (i.e., drum diameter, weight) and roller operation parameters (i.e., frequency, amplitude, and speed). The machine reports a measurement value approximately every 0.5 m at the drum center along the direction of travel.

The machine also reports a bouncing value (BV) which provides an indication of the drum behavior (e.g., continuous contact, partial uplift, double jump, rocking motion, and chaotic motion) and is calculated using Equation 3. When the machine is operated in AFC mode, reportedly the amplitude is reduced when BV approaches 14 to prevent drum jumping.

1.6.5. Sakai Soil IC System

The basis of the Sakai IC system is the IC roller and a GPS with radio base station.

The Sakai Compaction control value (CCV) is a unitless vibratory-based technology which makes use of an accelerometer mounted to the roller drum to create a record of machine-ground interaction.

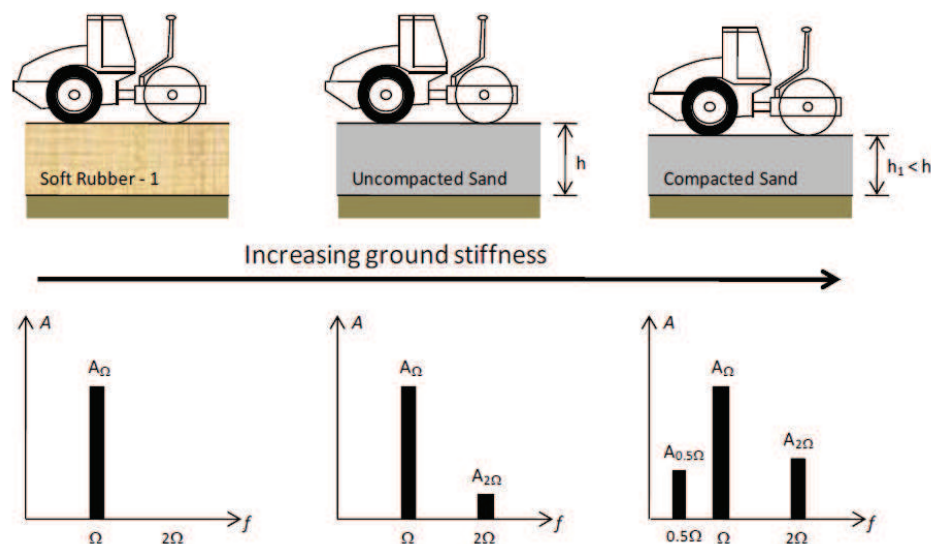


Figure 1.26 Illustration of changes in drum harmonics with increasing ground stiffness (modified from Thurner and Sandström 1980)

Its value represents the stiffness of the compacted pavement layers underneath. The

concept behind the CCV is that as the ground stiffness increases, the roller drum starts to enter into a “jumping” motion which results in vibration accelerations at various frequency components. The current Sakai IC system does not yet consist of auto-feedback.

Chapter 2.

Current CCC/IC Construction Specifications

2.1. State of practice

The first attempts to measure, record, and monitor vibration-integrated measurements during compaction were performed with vibratory plates in the 1930s (Mooney and Adam, 2007). The initial research development of roller integrated measurement dates to 1974 when Dr. Heinz Thurner of the Swedish Highway Administration performed field studies with a 5-ton tractor-drawn Dynapac vibratory roller instrumented with an accelerometer.

The tests indicated that the ratio between the amplitude of the first harmonic and the amplitude of the excitation frequency could be correlated to the compaction effect and the stiffness of the soil as measured by the static plate load test.

In 1975, Dr. Thurner partnered with Åke Sandström and founded Geodynamik to continue research and development on CCC/IC. In 1976, Compactometer™ Compaction Meter Value (CMV) measurement was developed by Geodynamik in cooperation with the Dynapac Research Department. In 1980, five technical articles were presented on the CMV measurement technology and its applications (Thurner 1980, Thurner and Sandström 1980, Forssblad 1980, Hansbo and Pramborg 1980, and Machet 1980) at the First International Conference on Compaction held in Paris.

In 1983, Geodynamik introduced the Oscillometer Value (OMV) for oscillatory rollers which is a dimensionless value obtained from the amplitude of the horizontal acceleration of the drum.

HAMM AG adopted the OMV measurement technology (Thurner and Sandström 2000) for use on their smooth drum oscillatory rollers, but virtually no published information is available in the English literature on OMV relationships with soil properties.

In the early 1980s, BOMAG developed the Terrameter® system measuring the Omega value (BTM 1983). The Omega value provides a measure of the compaction energy transmitted to the soil using accelerometer data. Hoover (1985) published a research

report from a field study evaluating the Omega value on three different types of granular soils which showed encouraging results. Later in 2000, BOMAG replaced the Omega value by introducing the Vibratory Modulus (EVIB) value which uses acceleration data to determine drum displacement, an estimated applied force, and a dynamic roller-soil model (Kröber et al. 2001).

In the 1990s, vibratory roller technology became much more sophisticated. In the 1990s Bomag introduced the Variocontrol® roller with counter-rotating eccentric masses and servo-hydraulic control of the vertical centrifugal force.

Likewise, Ammann introduced the ACE® roller with servo-hydraulic two-piece eccentric mass and frequency control (see Fig. 2.1) and it introduced the roller-integrated stiffness (k_s) measurement value, which provides a measure of quasi-static stiffness using the measured drum displacement, estimated applied force, and a spring-dashpot model representing roller-soil interaction (Anderegg and Kauffmann 2004).

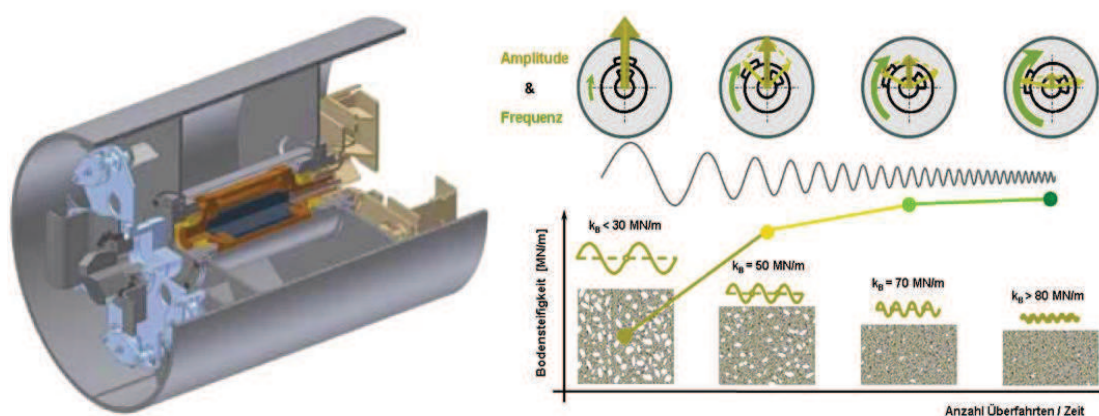


Figure 2.1. . Ammann two-piece eccentric mass assembly and variable control of eccentric force amplitude and frequency

Currently, Dynapac, Trimble, and Caterpillar use the CMV measurement technology as part of their CCC/IC systems by linking CMV data with GPS measurements for on-board real time display. Trimble offers a retrofit CCC system for smooth drum vibratory rollers (see White and Vennapusa 2009). In 2004, Sakai introduced Compaction Control Value (CCV) which is also a dimensionless parameter similar to CMV (Scherocman et al. 2007).

In 2003, a research collaboration project between the Iowa Department of Transportation, Federal highway Administration ((FHWA), and Caterpillar was initiated

to evaluate Caterpillar's Machine Drive Power (MDP) system for use on granular and cohesive soils. The MDP system is based on the principal of rolling resistance due to drum sinkage, and the approach works in both the vibratory and static modes. The measurement system has been investigated in field trials since 2003 (Tehrani and Meehan 2009, White et al. 2004, 2005, White and Thompson 2008, Thompson and White 2008) and has recently been recently used on a full-scale earthwork compaction project in Minnesota (White et al. 2009a, b).

Currently, BOMAG, Ammann, and Dynapac offer AFC/IC systems, wherein the vibration amplitude, and/or frequency are automatically adjusted when drum jumping is determined or when a preset threshold roller measurement value is reached.

2.2. Current CCC/IC Construction Specifications

Some agencies (Swedish Road Administration in 1990, Federal Ministry of Transport of the Federal Republic of Germany and The Austrian Federal Road Administration, International Society for Soil Mechanics and Geotechnical Engineering in 1994, and Mn/DOT in 2007) have developed specifications to facilitate implementation of CCC/IC into earthwork construction practices.

The specifications typically require performing either PLT or LWD on calibration strips to determine average target values (typically based on 3 to 5 measurements) and use the same for quality assurance later in production areas.

The German specification suggests performing at least three PLTs in locations of low, medium, and high degree of compaction during calibration process. Further, it is specified that linear regression relationships between roller measurement values and plate load test results should achieve a regression coefficient, $R \geq 0.7$.

White and Vennapusa (2009) documented the following as the key attributes required in CCC/IC specifications and noted that the largest dissimilarities exist in the current specifications with the attribute item number 10.

1. Descriptions of the rollers and configurations,
2. Guidelines for roller operations (speed, vibration frequency, vibration amplitude, and track overlap),
3. Records to be reported (time of measurement, roller operations/mode, soil type,

moisture content, layer thickness, etc.),

4. Repeatability and reproducibility measurements for IC measurement values (IC-MVs),
5. Ground conditions (smoothness, levelness, isolated soft/wet spots)
6. Calibration procedures for rollers and selection of calibration areas,
7. Regression analysis between IC-MVs and point measurements,
8. Number and location of quality control (QC) and quality assurance (QA) tests,
9. Operator training, and
10. Acceptance procedures/corrective actions based on achievement of minimum MV-TVs (MV target values) and associated variability.

2.2.1. *Austrian/ISSMGE Specifications*

Austria first introduced roller-integrated CCC specifications in 1990 with revisions in 1993 and 1999. Further revisions are not currently being considered. The ISSMGE recently developed recommended CCC specifications (ISSMGE 2005), largely based on Austrian standards (Adam 2007).

The Austrian/ISSMGE specifications allow two different approaches for roller-integrated CCC. The first approach involves acceptance testing using a regression-based correlation developed during on-site calibration. An alternative approach, recommended for small sites or where calibration cannot be performed, involves compaction with roller-integrated measurement until the mean roller MV increases by no more than 5%. Acceptance is then based on static PLT or LWD (dynamic PLT) modulus at the weakest area. In the Austrian/ISSMGE specifications, roller MVs must be dynamic (i.e., based in part on measurement of drum acceleration). The specification is applicable to all subgrade, subbase, and base materials and recycled materials that can be compacted dynamically and statically. For soils compacted dynamically, measurement occurs during compaction. For soils compacted statically, dynamic measurement occurs after static compaction. If the fine-grained portion [< 0.06 mm (0.002 in)] exceeds 15%, moisture content must be given special attention; however, moisture content criteria are not specified.

2.2.1.1. Method 1: Acceptance Based on Calibration

The more recently developed Austrian/ISSMGE roller-integrated CCC method involves the development of a relationship between roller MV and the initial PLT modulus E_{V1} or E_{LWD} . Density spot testing is allowed as an alternative, although it is not recommended. Calibration is required over the entire width of the construction site and for a length of at least 100 m (328 ft) for each material (subgrade, subbase, and base). Roller-integrated measurement must be carried out with constant roller parameters (frequency, amplitude, and forward velocity) throughout calibration. Roller MV data are captured during each measurement run, and subsequent PLT or LWD testing is performed at values of low, medium, and high roller MV (see Figure 2.2). PLT is required at a minimum of nine locations. If LWD testing is used, the average of four E_{LWD} values at a minimum of nine locations is reported (hence 36 LWD tests are required). The engineer of record is given the authority to design the rolling and measurement pattern used during calibration.

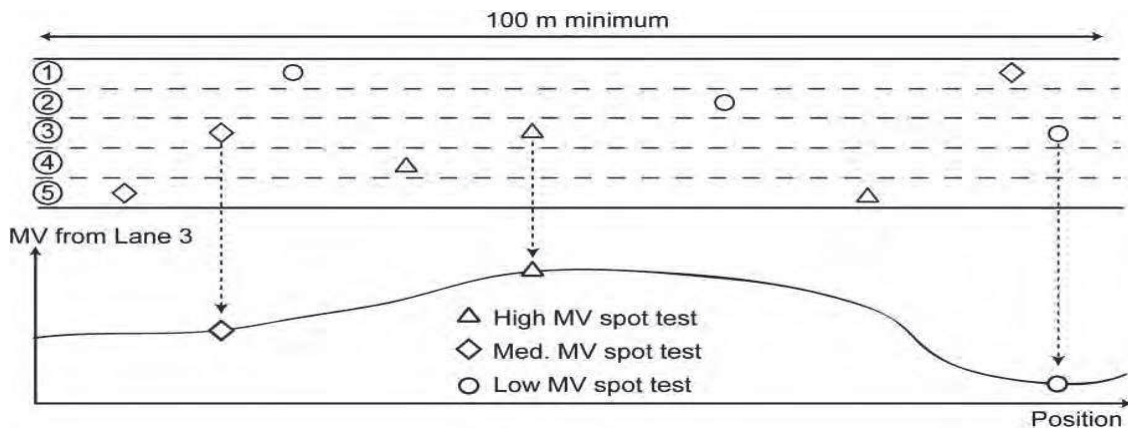


Figure 2.2. . Illustration of calibration approach for Austrian/ISSMGE specifications.)

Linear regression analysis is performed on the resulting roller MV versus E_{V1} or E_{LWD} values (see Figure 2.3). The regression coefficient R^2 must be ≥ 0.5 ; additional PLT or LWD tests may be performed to achieve $R^2 \geq 0.5$. The engineer of record may remove outliers if good cause exists. This approach may not be carried forward to production QA if $R^2 < 0.5$. Using the regression equation and a specified E_{V1} or E_{LWD} (see Table 2.3 for Austrian values) leads to determination of a minimum roller MV (MIN) and a mean roller MV (ME).

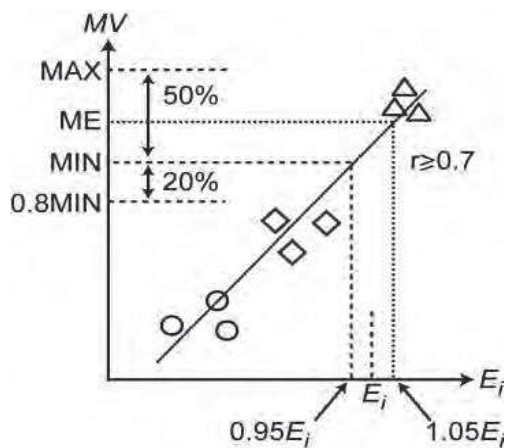


Figure 2.3. Roller MV vs. E_{V1}/E_{LWD} regression and key parameters in Austrian/ISSMGE specifications.

As illustrated in Figure 2.24, the MIN corresponds to $0.95 E_{V1}$ or E_{LWD} , and the ME corresponds to $1.05 E_{V1}$ or E_{LWD} . The MAX value is defined to be 1.5 MIN . The Austrian/ISSMGE acceptance criteria are summarized as follows:

- The mean roller MV must be $\geq \text{ME}$;
- 100% of roller MVs must be $\geq 0.8 \text{ MIN}$;
- 90% of roller MVs must be $\geq \text{MIN}$.

table 2.1. Table 2.3. E_{V1} and E_{LWD} values required (Austria).

Level	E_{V1} (MN/m ²)
1 m below subgrade ^a	15 (cohesive); 20 (cohesionless)
Top of subgrade	25 (cohesive); 35 (cohesionless)
Top of subbase	60 (rounded); 72 (angular)
Top of base	75 (rounded); 90 (angular)

Level	E_{LWD} (MN/m ²)
1 m below subgrade ^a	18 (cohesive); 24 (cohesionless)
Top of subgrade	30 (cohesive); 38 (cohesionless)
Top of subbase	58 (rounded); 68 (angular)
Top of base	70 (rounded); 82 (angular)

^aIf fill section is to be constructed.

In addition to these requirements, compaction must be continued until the mean roller MV is less than 5% greater than the mean value from the previous pass. The Austrian/ISSMGE specification also requires the following uniformity criteria:

- If 100% of roller MVs $\geq \text{MIN}$, then the roller MV coefficient of variation (COV)

for the entire area must be $\leq 20\%$.

- If $0.8 \text{ MIN} \leq \text{minimum roller MV} \leq \text{MIN}$, then 100% of roller MVs must be $\leq \text{MAX} = 1.5 \text{ MIN}$.

The recommended control area over which acceptance should be performed has traditionally been 100 m long by the width of the roadway. However, recent experience with 200- to 500-m-long control areas has shown effective results (D. Adam, personal communication, 2008). These ISSMGE/Austrian correlations and acceptance criteria are valid for roller/soil contact and partial loss of contact roller operation. The Austrian/ISSMGE specifications permit measurement during double jump mode; however, a separate calibration is required for such operation.

2.2.1.2. Method 2: Acceptance Based on Percentage Change of MVs

For small construction sites and areas where calibration cannot be reasonably performed, the Austrian/ISSMGE recommends the following method. Compaction should be continued until the mean roller MV is less than 5% greater than the mean roller MV from the previous pass. Subsequently, PLT or LWD testing is conducted at the weakest area as determined by the roller MV output. The E_{V1} or E_{LWD} must be greater than or equal to the required value (e.g., Table 2.1 for Austria). A minimum of three PLT or nine LWD tests must be performed in the weakest area.

2.2.2. German CCC Specifications

German specifications for earthwork QC/QA using CCC were introduced in 1994 and updated in 1997. Further revisions are expected in 2009. Referred to as ZTVE-StB, the German CCC specifications apply to subgrade and embankment soils. The lack of CCC specifications for base and subbase layers is predicated on the belief that roller MVs measure much deeper than the 20- to 30-cm-thick base course layers used in Germany. There are two ways in which CCC can be specified in Germany. First, CCC can be implemented through initial calibration of roller MVs to PLT modulus or density and subsequent use of the correlation during QA. A second approach uses CCC to identify weak areas for spot testing via PLT, LWD, or density methods. The key elements of each approach are described here, as are the proposed 2009 revisions..

2.2.2.1. Calibration Approach (Method M2 in German specifications)

This CCC approach involves two principal steps:

- Onsite initial calibration to develop the correlations between the roller MV to be used and soil density or PLT modulus (E_{V2});
- Identification of roller MV target value (MV-TV) consistent with required density or E_{V2} ; and:
- Acceptance testing by comparing roller MV data against the MV-TV.

Calibration is performed on an area equal to three 20-m-long (minimum) test strips (see Figure 2.4).

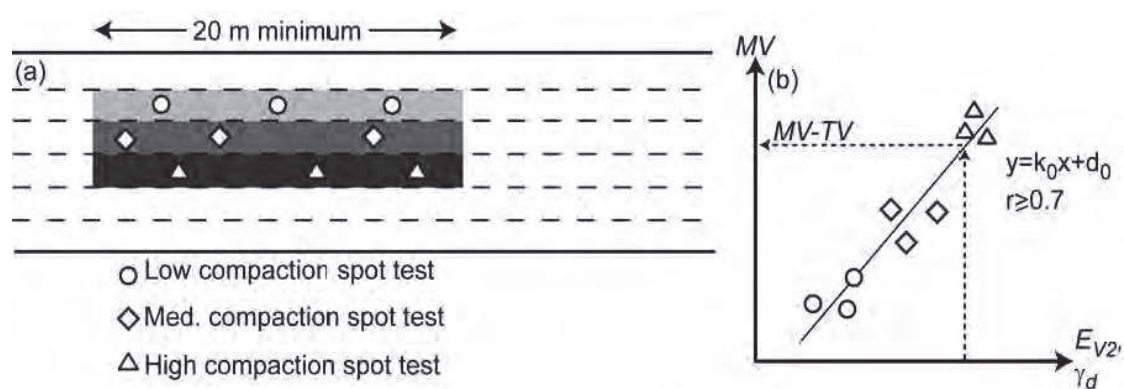


Figure 2.4. Illustration of calibration approach for German specifications.

Roller MV data are collected during roller operation on a low degree of compaction test strip (e.g., after one compaction pass), a medium degree of compaction test strip (e.g., three to five compaction passes), and a high degree of compaction test strip (multiple passes until no further compaction observed).

Three to five static PLTs or density tests are performed on each test strip. Regression analysis is performed on the roller MV versus spot-test data (see Figure above). When using the PLT, the German procedure uses the unload-reload secant modulus (M_{E2} or E_{V2}). The correlation coefficient r must be ≥ 0.7 ($R^2 \geq 0.5$). Additional spot tests may be performed to achieve $R^2 \geq 0.5$. If $R^2 \geq 0.5$ cannot be achieved, CCC is not permitted via Method M2.

The regression equation and required minimum values for E_{V2} or density lead to determination of an MV-TV. In Germany, minimum E_{V2} values must be achieved for the top of subgrade. Specifically, E_{V2} must be 45 MPa for clay or silty soils and 80 to 100 for granular materials. Density requirements (typically 98% standard Proctor) exist

for all layers below the top of subgrade. There are no moisture requirements.

During acceptance testing, 90% of all roller MVs in an evaluation area must exceed the MV-TV value. There are currently no additional criteria for acceptance using this method.

The German specification does not permit variable frequency and amplitude control or jump-mode during calibration or acceptance testing. The project site must be homogeneous in soil type and in underlying stratigraphy; otherwise CCCbased QA is not recommended.

The German group overseeing the CCC specifications is planning some moderate updates (G. Bräu, 2008). The LWD or dynamic PLT may be used in place of the static PLT. Target values of LWD modulus (E_{LWD}) will be published but were not available at press time. In addition, the issue of uniformity criteria was addressed. The German specifications will require that the 10% of MVs that fall below MV-TV be reasonably distributed around the evaluation area. Acceptance of this issue will be subjective and left to the on-site engineer. The German specifications will include language permitting the use of automatic feedback control intelligent compaction rollers during compaction but will prohibit their use during calibration and acceptance testing.

table 2.2. *Further recommendations for compaction of soil layers (from Kloubert's presentation at TRB-2004, BOMAG)*

Laying and compaction specification for road construction in Germany

Soil layers	Density (Standard Proctor)	Bearing capacity (load bearing test, EV2)	Eveness (4 m straight edge)
Subbase	100 - 103 % *	100 - 150 MN/m ² *	20 mm
Capping layer	100 - 103 % *	100 - 120 MN/m ² *	40 mm
Formation	97 - 100 % *	45 - 80 MN/m ² *	60 mm

* depending on road classification and road design

2.2.2.2. CCC to identify weak areas for spot testing

In this approach, CCC is used to map the compacted area. The weakest spots are identified from the roller-generated maps for spot testing (density methods or PLT). A minimum number of spot tests are specified (e.g., four per 5,000 m²).

To meet acceptance, each density or E_{V2} value must be greater than or equal to the

desired value. If acceptance is not achieved, the soil must be reworked until the criterion is met.

Assuming roller operating parameters are held constant and the soil, moisture, and subsurface have not changed, then by inference all other areas of the map meet acceptance. There is no initial calibration required for this approach. This approach is the more common of the two approaches used in Germany (G. Bräu, personal communication, 2008).

2.2.3. *Swedish CCC Specifications*

Specifications for the use of CCC on unbound materials in Sweden were first introduced in 1994; current use of roller-integrated CCC is governed by 2005 specifications (ATB Vag 2005). The QA of unbound material is mandated at two surface levels:

- 1) top of the base course and
- 2) a layer 300 to 750 mm below the top of the base layer.

Typically, Swedish construction includes a 300- to 700-mm-thick base layer and a 300- to 500-mm subbase or frost protection layer. Therefore, QA is typically performed on the surface of the base and subbase layers. QA is not required for the subgrade due primarily to the considerable thickness of base and subbase layers used. The maximum percentage of particles less than 0.06 mm permitted in base and subbase layers is 7%; therefore, by default CCC is only performed on material with predominantly cohesionless soil.

Swedish specifications permit the use of roller-integrated CCC to identify weak spots for PLT. First, it is useful to explain the general QA specification. In Sweden, conventional QA of base and subbase layers is based solely on PLTs performed at a minimum of eight randomly selected locations within each 5,000 m² control area. Density and moisture QA are not prescribed. The number of tests can be reduced to five if no previous control area has failed or if the standard deviation σ is small. The unload-reload PLT deformation modulus E_{V2} and the ratio E_{V1}/E_{V2} are used. All measured E_{V2} values must exceed a layer-dependent minimum value for acceptance (see Table 1.3). The average E_{V2} should also meet the criteria summarized in Table 1.3. If criterion 2 is violated, an alternative can be used for the top 500 mm only.

table 2.3. Unbound material acceptance criteria (per 5.000 m2 control area)

Depth Below Base Course Surface (mm)	N	Asphalt Pavement			Concrete Pavement		
		(1) $E_{V2(min)}$ (MPa)	(2) $E_{V2(ave)}$ (MPa)	(3) E_{V2}/E_{V1} Alternative if (2) not met	(1) $E_{V2(min)}$ (MPa)	(2) $E_{V2(ave)}$ (MPa)	(3) E_{V2}/E_{V1} Alternative if (2) not met
0-250	8	125	$\geq 140 + 0.96\sigma$	≤ 2.8	105	$\geq 120 + 0.96\sigma$	≤ 2.8
0-250	5	125	$\geq 140 + 0.83\sigma$	$1 + 0.013 E_{V2}$	105	$\geq 120 + 0.83\sigma$	$1 + 0.015 E_{V2}$
251-500	8	32	$\geq 40 + 0.96\sigma$	≤ 3.5	45	$\geq 55 + 0.96\sigma$	≤ 3.5
251-500	5	32	$\geq 40 + 0.83\sigma$	$\leq 1 + 0.063 E_{V2}$	45	$\geq 55 + 0.83\sigma$	$\leq + 0.046 E_{V2}$
500-550	8	32	$\geq 40 + 0.96\sigma$	NA	45	$\geq 55 + 0.96\sigma$	NA
500-550	5	32	$\geq 40 + 0.83\sigma$	NA	45	$\geq 55 + 0.83\sigma$	NA
551-650	8	20	$\geq 30 + 0.96\sigma$	NA	30	$\geq 35 + 0.96\sigma$	NA
551-650	5	20	$\geq 30 + 0.83\sigma$	NA	30	$\geq 35 + 0.83\sigma$	NA
651-750	8	15	$\geq 20 + 0.96\sigma$	NA	20	$\geq 25 + 0.96\sigma$	NA
651-750	5	15	$\geq 20 + 0.83\sigma$	NA	20	$\geq 25 + 0.83\sigma$	NA

NA= not applicable

When using roller-integrated CCC, the number of PLTs can be reduced to two. The PLTs are conducted at the two weakest areas as indicated by the roller MV data map. The number of PLTs can be reduced from two to one if no control area has failed the test or the previous control areas show small variations.

The criteria for acceptance are summarized in Table 1.4. The E_{V2} value in these points must not be lower than the threshold value, which is different for different levels below the top of the base layer and for flexible and rigid pavements. For granular base materials an additional criterion based on the E_{V2}/E_{V1} ratio must also be fulfilled.

table 2.4. Unbound material acceptance criteria when CCC used [per 5,000-m2 (1,993-yd2) control area].

Depth Below Base Course Surface (mm)	N	Asphalt Pavement		Concrete Pavement	
		(1) $E_{V2(min)}$ (MPa)	(2) E_{V2}/E_{V1} Alternative if (2) not met	(1) $E_{V2(min)}$ (MPa)	(2) E_{V2}/E_{V1} Alternative if (2) not met
0-250	1-2	125	$\leq 1 + 0.0136 E_{V2}$	105	$\leq 1 + 0.0162 E_{V2}$
251-500	1-2	32	$\leq 1 + 0.078 E_{V2}$	45	$\leq 1 + 0.056 E_{V2}$
500-550	1-2	32	NA	45	NA
551-650	1-2	20	NA	30	NA
651-750	1-2	15	NA	20	NA

LWD testing cannot currently be used in place of static PLT for QA of base and subbase materials. Sweden does recommend QC/QA during subgrade compaction via either PLT or LWD testing. LWD testing can be used instead of PLT “if similar results can be shown.” The Swedish specifications provide recommended E_{V2} and E_{LWD} for depths of 800 mm (2.6 ft) or greater (see Table 1.5). A note within the specifications states that the average of five LWD tests can be used over a 2,500-m2 (997-yd2) area.

table 2.5. Recommended PLT and LWD QA values at depth.

Depth Below Base Course Surface (mm)	Construction with Only Base and Subbase Material Above Crushed Rock		Construction with Only Base and Subbase Material Above Sand Subgrade	
	E_{v2} (MPa)	E_{LWD} (MPa)	E_{v2} (MPa)	E_{LWD} (MPa)
800	12	10–15	16	12–18
900	9	8–12	11	10–14
1,000	6	5–8	8	7–11
1,100	4	4–5	5	5–8
1,200	3	3	4	3–5
1,300	2	2	3	3

2.2.4. Minnesota DOT Pilot Specifications

In 2007 the Minnesota Department of Transportation (Mn/DOT) developed pilot specifications for QC/QA of granular and nongranular embankment soil compaction using CCC and/or LWD. At the time of this writing, Mn/ DOT was in the process of revising these specifications; the most recent version is available online at <http://www.dot.state.mn.us/materials/gbintellc.html>. The 2007 specification required QC by the contractor and QA by the engineer on designated proof layers to ensure compliance with controlstrip-determined roller-integrated measurement target values and LWD target values. Proof layers are designated at the finished subgrade level (directly beneath the base) and at certain additional levels depending on the height of the constructed embankment. Additional proof layers are required for every 600 mm (2 ft) of placed granular soil thickness and every 300 mm (1 ft) of placed nongranular soil thickness. The engineer has the authority to modify proof layer designations.

The Mn/DOT specification requires construction of control strips to determine the intelligent compaction target value (IC-TV) for each type and/or source of soil. Note that Mn/DOT' s use of the term “intelligent compaction” is equivalent to CCC as defined in this study in that automatic feedback control of roller operating parameters is not permitted during measurement. Additional control strips are required if variations in material properties that affect the IC-TV are observed by the engineer. Each control strip must be at least 100 m long and at least 10 m wide, or as determined by the engineer. Lift thickness must be equal to planned thickness during production. To determine the moisture sensitivity correction for the IC-TV, a control strip is constructed at or near each extreme of 65% and 95% of standard Proctor optimum moisture—the moisture content limits specified in Mn/DOT earthwork construction. The resulting data are utilized to produce a moisture correction trend line showing a linear

relationship of the IC-TV with moisture content. The control strip construction procedure is as follows:

- The bottom of the excavation is mapped with the roller to create a base map. This map is reviewed by the engineer to ensure that the control strip subsurface is uniform and to identify areas that must be corrected prior to fill placement.
- The embankment soil is placed in lifts; each lift is compacted with repeated passes and with roller compaction measurement. The optimum value is reached when additional roller passes do not result in a significant increase in the roller MV as determined by the engineer.
- Moisture content testing is required at a minimum of 1 per 3,000 m³ of earthwork; the moisture must be maintained within 65% to 95% of standard Proctor optimum.
- Lift placement and CCC is repeated for additional lifts until the level-of-proof layer has been reached.
- The control strip IC-TV is defined to be the optimum MV obtained from the roller measurements during construction of the control strip. The optimum value is reached when additional passes do not result in a significant increase in MV, as determined by the engineer of record. The IC-TV is defined such that 90% of the MVs are greater than 90% of the IC-TV.

The IC-TV values for control strips at moistures near 65% and 95% of optimum are used to create a moisture correction trend line. It should be noted that the Mn/DOT pilot specifications also require LWD testing (three per proof layer) and the establishment of LWD target value (LWD-TV) for each proof layer. The LWD-TV is corrected for moisture in a way similar to that for IC-TV.

During QA the engineer observes the final compaction recording pass of the roller on each proof layer. For acceptance at each proof layer during general production operations, all segments shall be compacted so that at least 90% of the MVs are at least 90% of the moisture-corrected IC-TV prior to placing the next lift. All of the MVs must be at least 80% of the moisture-corrected IC-TV. The contractor must recompact (and dry or add moisture as needed) until all areas meet these acceptance criteria.

If a significant portion of the grade is more than 20% in excess of the selected corrected IC-TV, the engineer shall reevaluate the selection of the applicable control-strip-

corrected IC-TV. If an applicable corrected IC-TV is not available, the contractor shall construct an additional control strip to reflect the potential changes in compaction characteristics. Control section size criteria are currently under development.

The engineer will also perform an LWD test and a moisture content test at the minimum rate of one LWD test measurement per proof layer, per 300 m for the entire width of embankment being constructed during each operation. The engineer may perform additional LWD tests and moisture content tests in areas that visually appear to be noncompliant or as determined by the engineer.

Each LWD test measurement taken shall be at least 90% but not more than 120% of the moisture-corrected LWD-TV obtained on the applicable control strip prior to placing the next lift. The contractor shall recompact (and dry or add moisture as needed) to all areas that do not meet these requirements.

2.2.5. 4th Draft on European CCC regulations.

This standard provides guidance and recommendations on the use of CCC as a quality control method in earthworks on unbound and stabilised materials.

For the new European specification validity of the calibration is only ensured if the essential parameters used for preparing the calibration field correspond with those of the test lot. These are in detail:

- Soil type,
- water content for mixed and fine soils,
- thickness of the installed layer to be tested (deviations not in excess of $\pm 15\%$ from a thickness of 0.5 m),
- load bearing capacity (CCC-value) of the subsoil under the layer,
- measuring roller with machine dependent settings (vibration frequency, amplitude and operation related settings e.g. travel speed and travel direction, etc)
- measuring system to determine the CCC-values,
- settling time after compaction.

When using CCC for compaction control the test area does not need to meet any special requirements. When used for acceptance testing, the test area should be as uniform as

possible, or it should be limited in size, as appropriate.

In combination with the documentation of measuring values CCC (without positioning systems) is particularly well applicable for almost rectangular areas of 50 m to 100 m strip length. In case of long strip lengths (e.g. longer than 70m) intermediate markings must be made, because the slippage of drive wheels may result in errors when trying to determine distances for the localization of faults. Test area inclinations of less than 5% do not have any effect on the creation of measuring values.

Each measuring field for calibration should contain at least three sections with different compaction:

- light compaction (1 pass with measuring roller)
- medium compaction (approx. 2 passes with compacting roller, followed by 1 pass with measuring roller)
- heavy compaction (with as many compacting passes as required to achieve a state where no increase in measuring value can be detected, followed by 1 pass with the measuring roller)

The calibration test field should be selected with respect to layer thickness, soil type and stiffness of the subsoil. It may be beneficial to run calibrations for 3 different subsoil stiffness values. However, this triples the calibration effort.

The procedure of calibration can be sub-divided into 6 steps:

- 1). Execution of a calibration for the corresponding soil and construction site conditions.
- 2). Determination of the 10 % minimum quantile TM (see Fig A1) for the CCC measuring values. The requirements according to several European national earthworks regulations state that the fall-below ratio (fall-below area ratio) must not exceed 10 %
- 3). Testing the compacted layer using CCC (full test, number of measuring values N).
- 4). Calculation of the mean value μ and the standard deviation σ of all CCC measuring values of the test area and calculation of the test statistic z (CCC):

$$z = \mu - 1.28 \cdot \sigma \quad (1)$$

with

μ average of CCC measuring values within the test lot

σ root-mean-square deviation of CCC measuring values within the test lot.

5). Mapping of all measuring values in an area plot.

6). A test lot is accepted when the test statistic z is greater than or equal to the minimum quantile TM , i.e. $z \geq TM$ (decision rule) (figure 2.5). The test plot is additionally to be used to check whether the spots, where the minimum quantile is not achieved, are uniformly distributed over the tested area. Where the tested area contains larger continuous areas in which the CCC measuring values are below the specified minimum quantile TM , these spots must be mutually assessed by client and contractor. If the test statistic z falls below the minimum quantile TM , the test lot is rejected and must be corrected to a condition that meets the specification.

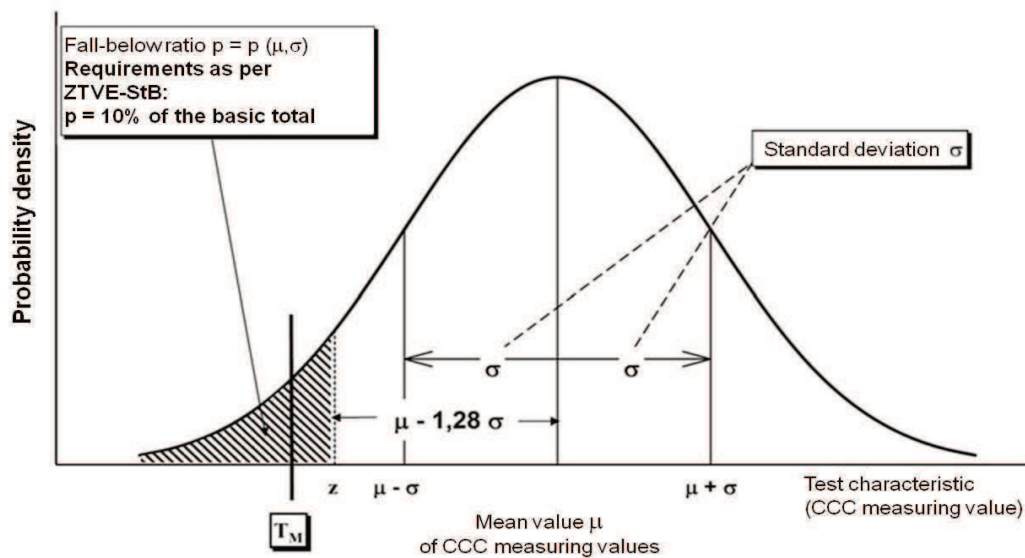


Figure 2.5. Distribution of CCC measuring values of the population and fall-below ratio (fall-below area ratio): Test lot is accepted, because $\mu - 1,28 \cdot \sigma > TM$

It is assumed that there is a linear connection between the independent variables x and the dependent variables y in the form of

$$y(x) = a_{y(x)} + b_{y(x)} \cdot x \tag{2}$$

If the correlation coefficient $|r| \geq 0.7$, the calibration cannot be used for the

determination of a required value for CCC. For $|r| \geq 0.7$ the calibration needs to be enhanced by further comparative measurements or it must be repeated. However, if this does not lead to any success, the test method is not suitable for this type of soil.

The empirical correlation coefficient r can result from two different method: the KQ-method or the FV-process.

The creation of the calibration curve requires at least three value pairs (x_i, y_i) for the KQ-method or four value triplets for the FV-method, so that the regression analysis for three fields can be made with at least nine value pairs in the KQ-method or 12 value pairs in the FV-method.

Since the FV-method, in contrast to the KQ-method, is based on only one regression function, irrespective of the direction of conclusion, this method should preferably be used in order to avoid application errors.

2.2.5.1. Method 1: FV-process" (fault-in-variables-method)

The evaluation method ("fault-in-variables-method", abbreviated "FV-method") described hereafter is used to determine the calibration straight between two test characteristics.

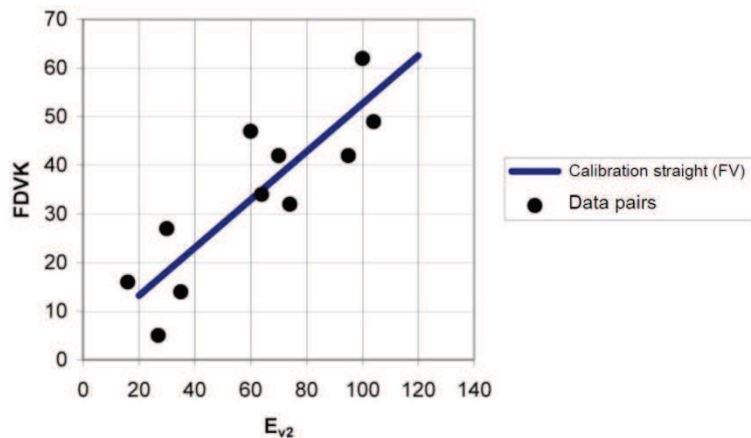


Figure 2.6. Example of a calibration curve of the modulus of deformation $E_{v2}(x)$ with the CCC-measuring value (y)

Since the test results for both the test characteristics x and y depend on the number z of passes, one refers to z as a co-variable for both test characteristics x and y (figure 2.6).

From the determined measuring value triplets (numerical triplets) $(x_i, y_i, z_i), i = 1, \dots, n$, one must first of all calculate the statistic characteristics: mean values variances and co-variances.

The variances and the co-variances can be used to determine the empiric calibration straight $x(z) = a_{x(z)} + b_{x(z)} z$ and $y(z) = a_{y(z)} + b_{y(z)} z$ between the number of compacting passes and the test characteristic x or y using the "Smallest-Square-Method":

$$b_{x(z)} = \frac{s_{xz}}{s_z^2} ; a_{x(z)} = \bar{x} - b_{x(z)} \bar{z} . \quad b_{y(z)} = \frac{s_{yz}}{s_z^2} ; a_{y(z)} = \bar{y} - b_{y(z)} \bar{z} . \quad (3)$$

The coefficient of determination B is calculated using the co-variance between the two test characteristics and the variances of both test characteristics .

$$B_{xy} = \frac{s_{xy}^2}{s_x^2 \cdot s_y^2} \quad B_{zx} = \frac{s_{zx}^2}{s_z^2 \cdot s_x^2} \quad B_{zy} = \frac{s_{zy}^2}{s_z^2 \cdot s_y^2} \quad (4)$$

The following generally applies for the coefficient of determination B :

- B is non-dimensional.
- $0 \leq B \leq 1$.
- (3) $B = 1$ exactly when all numerical pairs are exactly on a straight line.

The lesser B deviates from the value 1,

- the closer the monitored numerical pairs are to the associated calibration straight
- the higher the adaptation quality of the calibration straight to the monitored measuring value pairs
- the more reliable are the readings taken on the monitored calibration straight
- the more reliable are the conversions from one to the other test characteristic made with the calibration straight.

If the case $B_{xy} < 0.49$ occurs during a calibration test, the calibration straight determined on this basis must not be used for converting from one to the other test characteristic.

The coefficients of determination B_{zx} and B_{zy} allow further conclusions.

2.2.5.2. Method 2: "KQ-method" (method of smallest squares)

For calculation using the KQ-method the deformation modulus or the degree of compaction (x_i), $i = 1, 2, 3 \dots n$, and the CCC measuring value that has to be assigned to the area unit, is measured at various locations in the calibration field.

mean values of the measuring values must be determined using the numerical pairs (x_i , y_i),

The parameter a acc. to the equation $y(x) = a + b \cdot x$ then results from

$$a = \bar{y} - b \cdot \bar{x} \quad 5)$$

With $v_x = x_i - \bar{x}$ and $v_y = y_i - \bar{y}$ one finds the parameter b

$$b = \frac{\sum v_x \cdot v_y}{\sum v_x^2} \quad (6)$$

A calibration for the purpose of case [2] from chapter 4.3.1 requires the calculation of the function $x(y) = c + d \cdot y$ by replacing the independent and dependent variables in formulas (21) and (22):

$$c = \bar{x} - d \cdot \bar{y} \quad (7)$$

$$d = \frac{\sum v_x \cdot v_y}{\sum v_y^2} \quad (8)$$

In Fig. 22 the regression straight $x(y)$ is represented as a dotted straight line "Case [2]" and enables e.g. the transfer of CCC-values to Ev2-values. Both regression straights intersect in point

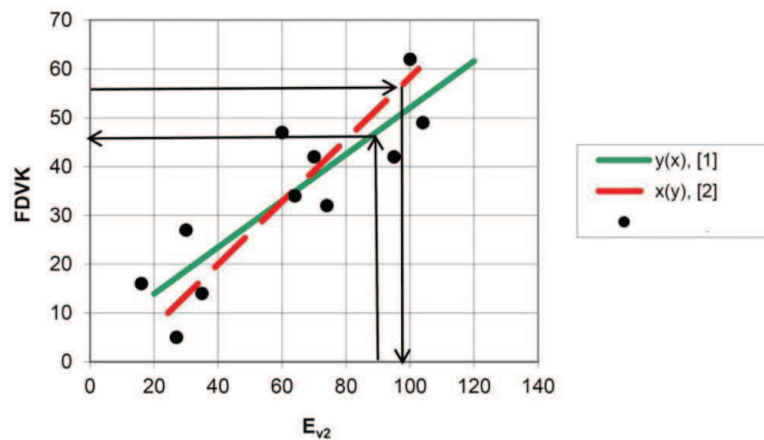


Figure 2.7. : Example of calibration straights between the deformation modulus E_{v2} and the CCC measuring value (KQ.-method)

The empirical correlation coefficient r is a dimension value for the strength of the linear correlation of both characteristics x and y and results from

$$r = b \cdot \frac{s_x}{s_y} \quad (9)$$

The aperture angle between the calibration straights descriptively represents the quality of calibration. The smaller the aperture angle, the better the allocation.

2.2.5.3. Weak spots analysis – “proof rolling”

Before a test lot can be accepted one must first examine the uniform two-dimensional distribution of fall-below spots in the test lot. This can take place by visual examination of a two-dimensional printout see figure 2.8.

In the past if sufficient compaction was found by using selective tests in the apparently weak selected locations, it could be assumed that the complete test lot was adequately compacted.

Continuous areas with high and low CCC measuring values can be detected and, based on this information, the test points for selective tests can be selected. Calibration of CCC is in this case not required. If selective tests reveal that the areas with particularly low CCC measuring values are sufficiently compacted, the rest of the area, which showed higher CCC measuring values, can be assumed to be properly compacted.

The Fig. Below shows a two-dimensional printout, which allows the application of selective individual conventional compaction tests (i.e PLT) in the areas with low CCC measuring values. Here the areas spreading over several tracks in width should preferably be used.

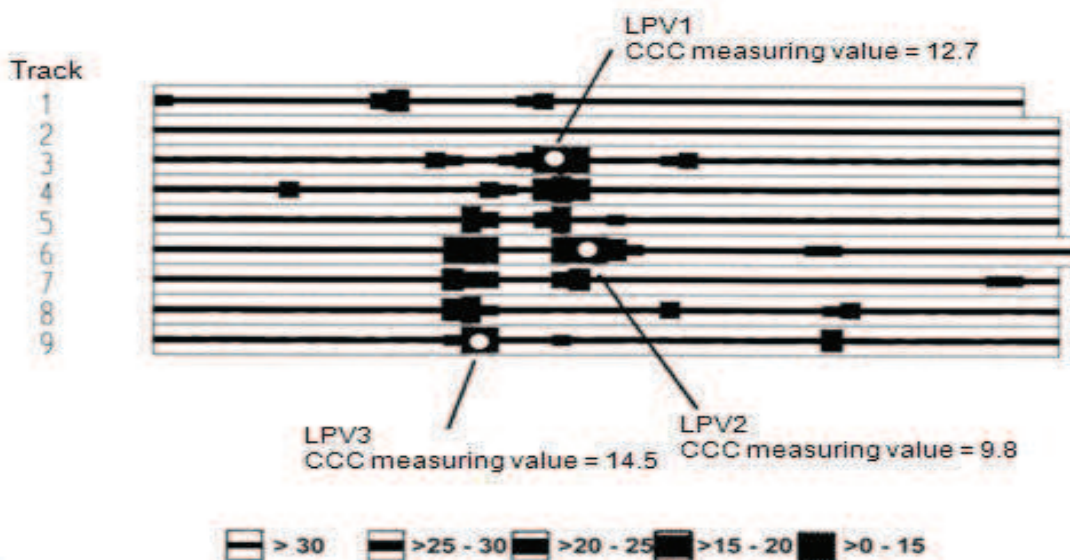


Figure 2.8. Two-dimensional printout for localizing areas with low measuring values, in which selective tests, e.g. plate load tests (LPV) will be carried out

With the "Nearest-Neighbour"-analysis (NNA) one can estimate the fall-below spots in the area on basis of just one test statistic. Furthermore, the uniform two-dimensional distribution of fall-below spots in the test lot can be estimated with the help of

variograms, using area moments of the fall-below spots or by means of digital image processing.

To assess the uniformity of the two-dimensional distribution of fall-below spots in the test lot using CCC the method of the "Nearest-Neighbour"-analysis can be used

This method provides the possibility to characterize the two-dimensional accumulation of appearances in form of just one value [...]. To be able to compare the results of this method a uniform size of the points is required

A differentiation is made in accordance with the following distribution patterns in Figure:

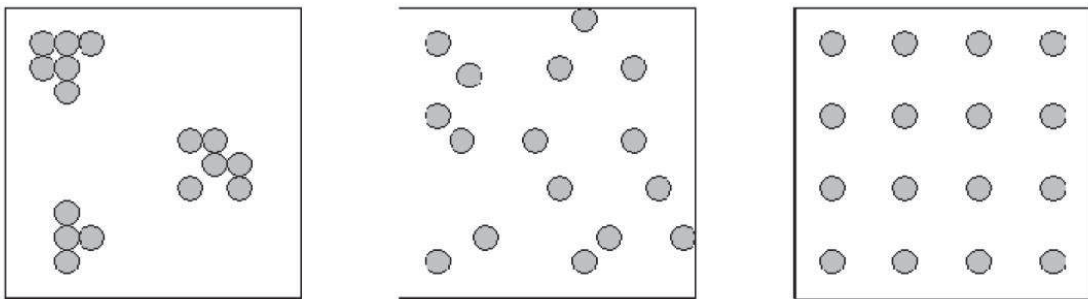


Figure 2.9. Different distribution patterns: sample C1, C2, C3

In reality the distributions will also appear in any intermediate form of the three listed samples. In order to be able to make a classification, the distances between paired data points must be measured.

2.2.5.4. Soil groups

- For **coarse soil** (fine proportion < 5 %) the influence of the water is in most cases negligibly low, when the degree of compaction DPr is higher than 95%. For coarse soils a relatively high correlation coefficient r ($r > 0.7$) between the static or dynamic deformation modulus or the degree of compaction and the CCC measuring value is normally determined during calibration .
- For **mixed soils** (fine proportion between 5 % and 15 %) calibration with a sufficiently high correlation coefficient as with coarse soils is possible, if the water contents are lower than the optimal water content wPr . With water contents above the optimum water content the influence of the water content on the CCC-value becomes significant so that any link to the deformation modulus or the degree of compaction is no longer clear.

- For **mixed soils** (15-40% fine) the influence of the water content is already so significant at water contents only slightly below the optimal water content w_{Pr} , that the link between the CCC measuring value and the deformation modulus is no longer clear.

With these soil groups information concerning the uniformity of compaction can already be obtained without calibration and inhomogeneities in the soil composition as well as deformed soil areas with high water contents can be localized.

- With **fine soils** good reproducibility of the measuring values and a sufficient correlation between the CCC measuring value and the deformation modulus only exists considerably below the optimal water content.

If these soils are used, e.g. for sealing, and the decisive parameters (e.g. soil type, water content) are maintained at a constant level by systematic treatment (e.g. in a central mixing plant), calibration to the degree of compaction or the deformation modulus is possible , even with water contents higher than optimum. Compliance with the requirements concerning the air void ratio must be examined.

- The assessment of the compaction achieved on improved or **stabilized soils** is only possible with integrated use of CCC or during a measuring pass immediately after the completion of compaction. The temporal sequence of installation, compaction and measurement in this case plays a decisive role for the CCC measuring value.
- **Rockfills** are normally not subject to testing using conventional methods because an accurate assessment would require the examination of considerable areas or volumes.

2.3. Conclusions

A variety of specification methodologies have been proposed for integrating Continuous Compaction Control (CCC) measurements into existing quality assurance and quality control (QA/QC) protocols.

The chapter has explored the use of alternative compaction specification approaches for performing QA/QC of compacted soils for embankment construction where CCC equipment is used. Table 3 provides a summary of key elements of the current CCC/IC specifications.

	GERMAN	AUSTRIAN	SWEDEN	AMERICAN	EUROPEAN
Reference	— ZTVE SB/TP BFSB (1994)	ISSMGE (2005)	ROAD 94 (1994)	Mn/DOT (2007a, b)	CEN / TC 396 (2012) 4th Draft
Equipment	Self-propelled rollers with rubber tire drive are preferred; towed vibratory rollers with towing vehicle are suitable.	Roller chosen by experience	Vibratory or oscillating single-drum roller. Min. linear load 15–30 kN. Roller-mounted compaction meter optional.	Smooth drum or padfoot vibratory roller (25,000 lbs.)	single drum rollers with a front drum and rear driven sculptured tyres should preferably be used, towed vibratory rollers and a corresponding tractor vehicle are suitable
Minimum test field area	Each calibration area must cover at least 3 partial fields ~20 m long	100 m by the width of the site	Thickness of largest layer 0.2–0.6 m.	300 ft x 32 ft (100 m x 10 m) (minimum at base). Max 1.2 m (4 ft.) thick.	not exceed 150 m without GNSS and the number of tracks side by side should not be higher than 20.
Location Specs	Level and free of puddles. Similar soil type, water content, layer thickness, and bearing capacity of support layers. Track overlap ? 10% machine width.	Homogenous, even surface. Track overlap ? 10% drum width.	Layer shall be homogenous and non-frozen. Protective layers < 0.5 m may be compacted with sub-base.	One calibration/ control strip per type or source of grading material	as uniform as possible
Documentation	Dynamic measuring value; frequency, speed, jump operation; amplitude; distance; time of measurement; roller type; soil type; water content; layer thickness; date, time, file name, or registration number; weather conditions; position of test tracks and rolling direction; absolute height or application position; local conditions and embankments in marginal areas; machine parameters; and perceived deviations	Rolling pattern, sequence of compaction and measuring passes; amplitude, speed, dynamic measuring values, frequency, jump operation, and corresponding locations	—	Compaction, stiffness, moisture, QC activities, and corrective actions weekly report)	Any data characterizing the compaction result: CCC measuring value, travel speed, frequency, jump operation, amplitude and position; Contractor, Client, Construction project, Section, Date, Time, Weather, Soil type or group, Travel direction. Designation of the roller (e.g. serial number), Name of the roller operator
Compaction Specs	The correlation coefficient resulting from a regression analysis must be ? 0.7. Individual area units (the width of the roller drum) must have a dynamic measuring value within 10% of adjacent area to be suitable for calibration.	Correlation coefficient ? 0.7. Minimum value ? 95% of Ev1, and mean should be ? 105% (or ? 100% during jump mode). Dynamic measuring values should be lower than the specified minimum for ? 10% of the track. Measured minimum should be ? 80% of the specified minimum. Standard deviation (of the mean) must be ? 20% in one pass.	Bearing capacity or degree of compaction requirements may be met. Mean of compaction values for two inspection points ? 89% for sub-base under roadbase and for protective layers over 0.5 m thick; mean should be ? 90% for roadbases. Required mean for two bearing capacity ratios varies depending on layer type.	90% of the stiffness measurements must be at 90% of the compaction target value.	*For t ? 0.7 (?) the calibration needs to be enhanced by further comparative measurements or it must be repeated. *Each measuring field for calibration should contain at least three sections with different compaction *Determination of the 10 % minimum quantile TM for the CMV. *A test lot is accepted when the test statistic z ? TM (z = $\mu - 1.28 \sigma$) Coefficient of determination Bxy ? 0.49
Speed	Constant	Constant 2–6 km/h (\pm 0.2 km/h)	Constant 2.5–4.0 km/h	Same during calibration and production compaction	must be maintained at a fixed value (\pm 0.2 m/s)
Freq.		Constant (\pm 2 Hz)	—		constant (? f ? 1 Hz)

table 2.6. Summary of current CCC/IC specifications

Chapter 3.

Quality Assurance of Pavement Earthwork Using Roller-Integrated CCC

The most common approach to quality control in road construction is to carry out a series of periodic in-situ tests (Briaud and Seo 2003). Evaluation of the quality of the compaction is based on the engineering properties of the compacted soil including strength and density.

The most common density-based quality control methods consist of measurements of in situ density and moisture content using the nuclear density gauge, sand cone equivalent test, and water balloon method.

The most common strength-based methods attempt to generate representative measurements of the in-situ modulus or stiffness of the soil. The elastic modulus E [FL^{-2}] is defined as the quotient of stress to strain in the elastic part of the stress-strain curve of a material. The stiffness k [FL^{-1}] is defined as the ratio of the force applied on a boundary through a loading area divided by the displacement experienced by the loaded area. The elastic modulus is a fundamental soil property, while the stiffness is affected by both the soil response and the test approach that is used, as it depends on the size of the loaded area. Therefore, for an elastic material, the stiffness measured with one test will be different from the stiffness measured with another test if the loading areas are different (Briaud and Seo 2003).

The most commonly utilized strength-based in-situ test methods are the: plate load test (PLT), falling weight deflectometer (FWD), light weight deflectometer (LWD), dynamic cone penetrometer (DCP), Clegg-impact hammer, and soil stiffness gauge or GeoGauge (Mooney and Rinehart 2007).

This chapter presents some of the recommended specification options for QA of subgrade, subbase, and aggregate base course compaction using roller-integrated CCC.

The six recommended QA specification options are summarized in Table 3.1 and Figure 3.1.

table 3.1. Summary of specification options.

Roller-Integrated CCC QA Option	Target Measurement Value (MV-TV)	Acceptance Criteria
Option 1: Spot testing of roller-informed weakest area(s)	Not required	Spot-test measurements in roller-identified weakest area(s) satisfy contract spot-test measurement requirements (QA-TV)
Option 2a: Monitoring percentage change in mean MV	Not required	Achieving $\leq 5\%$ change in mean MV between consecutive roller passes
Option 2b: Monitoring spatial percentage change ($\% \Delta$) in MVs	Not required	Achieving the $\% \Delta$ -TV between consecutive passes over a defined percentage of an evaluation section
Option 3a: Empirically relating MVs to spot-test measurements	Based on correlation of MV to spot test measurement: $MV-TV = MV$ corresponding to contract QA-TV ^a	Achieving MV-TV over a set percentage of an evaluation section
Option 3b: Compaction curve based on MVs	$MV-TV = \text{mean MV}$ when the increase in pass-to-pass mean MV in a calibration area $\leq 5\%$	
Option 3c: Empirically relating MVs to lab-determined properties (e.g., Mr)	Based on correlation of MV to lab soil property: $MV-TV = MV$ corresponding to contract QA-TV ^b	

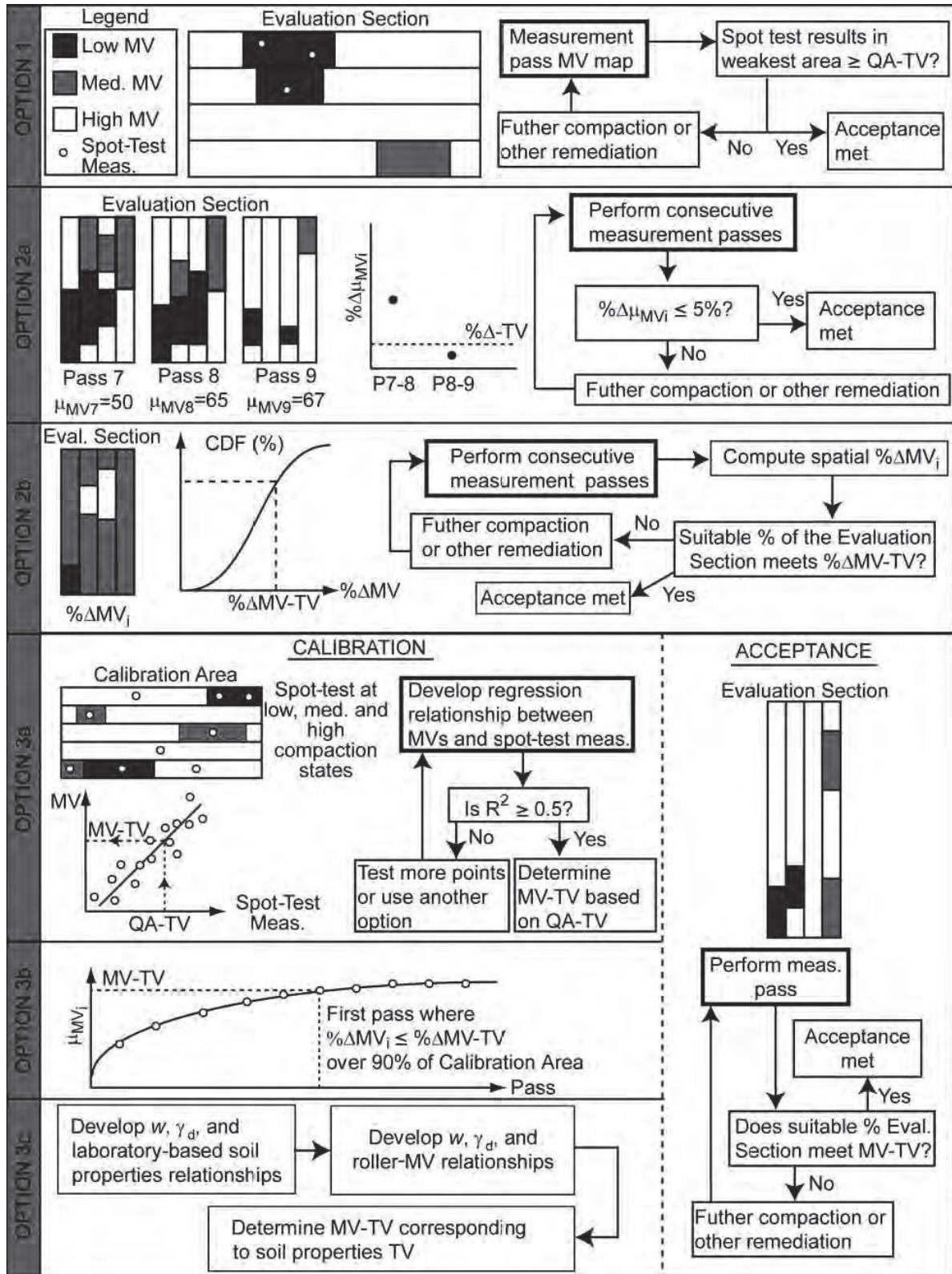
^a Assumption is that QA-TV is spot-test-based measurement of density, modulus, etc.

^b For example, a QA-TV based on Mr.

Options are numbered 1, 2a, 2b, 3a, 3b, and 3c and are distinguished by three principal categories. In Option 1, CCC is used to assist in QA, but acceptance is based on spot-test measurements. Acceptance of Options 2a and 2b is based on roller MVs, but initial calibration of roller MV to spot-test measurements is not required. Acceptance of Options 3a, 3b, and 3c is based on achieving a MV-TV determined via various initial calibration techniques.

Each option can be adopted as the sole method for QA; alternatively, two or more options can be combined to increase reliability. Uniformity criteria discussed in Section 3.9 can be added to any option. Method-based approaches (e.g., using GPS positioning and documentation to record the number of passes) do not utilize roller-based MVs and are therefore not addressed by this specification. However, the implementation of such an approach is straightforward.

table 3.2. Summary of CCC specification options.



3.1 Definitions

Automatic Feedback Control: automatic adjustment of roller *Operating Parameters* such as vibration frequency and amplitude based on real-time feedback from measurement system.

Calibration Area: an area representative of an *Evaluation Section* but typically smaller and used to establish an MV-TV.

Compaction Pass: a static or vibratory roller pass performed during earthwork compaction, not necessarily employing an *Instrumented Roller*.

Evaluation Section: an area of earthwork with consistent properties where acceptance is evaluated.

Instrumented Roller: a roller compactor outfitted with drum vibration instrumentation or other means to compute a *Roller Measurement Value*, onboard computer, and position monitoring equipment.

Layer: a component of the pavement earthwork with distinct soil properties (e.g., subgrade, subbase, or base course).

Lift: a unit of material within a *Layer* that is deposited at one time for compaction. A *Layer* may be comprised of a single lift or multiple lifts.

Measurement Depth: the soil depth to which *Roller Measurement Values* or *Spot-Test Measurements* are representative.

Measurement Pass: a pass performed by an *Instrumented Roller* during which all required information, including *Roller Measurement Values* and machine position, are recorded. *Roller Operating Parameters* must be held constant, and thus no *Automatic Feedback Control* is permitted during a *Measurement Pass*.

MV-TV: a target *Roller Measurement Value* (e.g., the measurement value corresponding to a *QA-TV*).

Quality Assurance (QA): evaluation methods and procedures administered by the owner or owner's representative to ensure that the constructed earthwork meets contract obligations.

Roller Measurement Value (MV): the roller-based parameter used for assessment of soil stiffness during compaction and based on roller vibration measurements.

Spot-Test Measurement: a field test used during earthwork QC and QA that provides a measurement at a discrete location; common examples include the nuclear gauge for

density and moisture and the lightweight deflectometer.

3.2 Notation

The following symbols are used throughout this specification:

A	theoretical vertical drum vibration amplitude
F	excitation frequency of eccentric mass within drum
M_r	resilient modulus (e.g., per AASHTO T-307)
MV_i	spatial <i>Roller MV</i> data from pass i . This is an array of data.
μ_{MV_i}	mean of spatial <i>Roller MV</i> data from pass i
σ_{MV_i}	standard deviation of spatial <i>Roller MV</i> data from pass i
$\% \Delta$	percent difference
$\% \Delta \mu_{MV_i}$	percent difference of the mean of spatial <i>Roller MV</i> data from pass $i - 1$ to pass i (for Option 2a)
$\% \Delta MV_i$	spatial percent difference in <i>Roller MV</i> data from pass $i - 1$ to pass i . This is an array of values.
$\mu_{\% \Delta MV_i}$	mean of spatial percent difference in <i>Roller MV</i> data from pass $i - 1$ to pass i
$\sigma_{\% \Delta MV_i}$	standard deviation of spatial percent difference in <i>Roller MV</i> data from pass $i - 1$ to pass i
v	forward travel velocity of roller
w_{opt}	optimum moisture content

3.3 Important Considerations

3.3.1 Applicable Soil Types

This specification is applicable to cohesive and cohesionless soils and aggregate base materials. Research has shown that current *Roller MVs* are less reliable on cohesive soils and that particular attention must be given to soil moisture content.

3.3.2 Measurement Depth

Current roller-integrated vibration-based measurement systems for 11- to 15-ton vibratory roller compactors provide a composite measure of soil stiffness to depths of 0.8 to 1.2 m (2.6 to 3.9 ft) and three to four times deeper than typical 0.2 to 0.3 m (8 to

12 in) Lifts of subgrade, subbase, or base material. An increase in theoretical amplitude slightly increases the Measurement Depth. Typical spot-test measurements such as the nuclear density gauge and light weight deflectometer (LWD) typically reflect the properties of the 0.2- to 0.3-m (8- to 12-in)-placed Lift of soil, whereas Roller MVs reflect the properties of multiple Lifts. Consequently, sublift soil properties are reflected in Roller MVs much more significantly than in spot-test measurements. Therefore, CCC options that rely on obtaining correlations between Roller MVs and spot-test results are increasingly difficult to implement if the sublift conditions are variable.

Further, as the sublift properties change, so too will the Roller MV and spot-test measurement correlations, even if the Lift material is the same.

3.3.3 Evaluation Section

Acceptance testing for all specification options is performed on Evaluation Sections. An Evaluation Section is an area of production earthwork that exhibits homogeneity, or consistently distributed heterogeneity, both in the longitudinal and transverse directions, as evidenced by the Roller MV map.

An Evaluation Section is commonly the full width of the earthwork section by a length that varies depending on the pace of construction, longitudinal heterogeneity, and other factors (e.g., schedule). Typical lengths can vary from 100 to 500 m (330 to 1,640 ft). A number of factors can contribute to heterogeneity and thus the sizing of Evaluation Sections. A change in borrow material or a transition from a cut to a fill section may induce a distinct change in Roller MV, particularly in the longitudinal direction. In the transverse direction, edge material or shoulders can sometimes exhibit markedly different stiffness behavior. Figure 7.2 provides examples of appropriate and inappropriate Evaluation Sections.

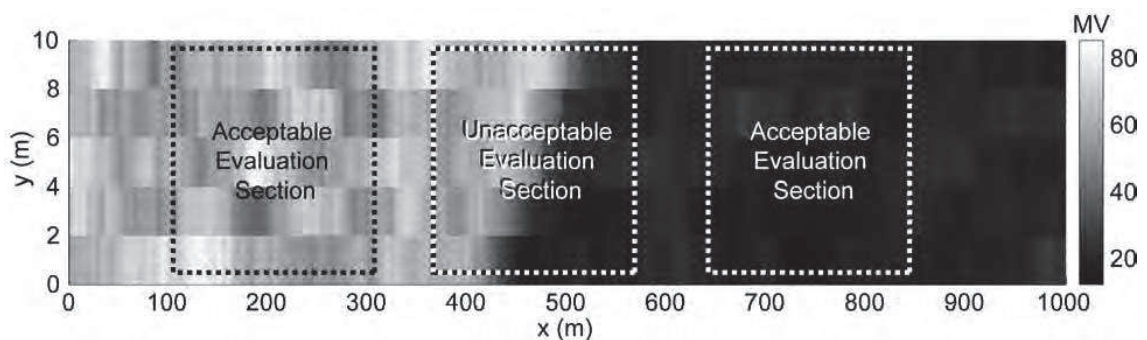


figure 3.1 Acceptable and unacceptable evaluation sections based on roller MV data map.

3.3.4 Verification of Roller MV Repeatability.

Roller MVs must be repeatable (i.e., repeated Measurement Passes over the same, fully compacted material must exhibit similar magnitudes and trends). It is also important to verify the accuracy of roller-mounted GPS position and that a position offset between the receiver and the center of the drum (i.e., where MVs are computed) and/or errors due to data averaging are properly considered.

Accurate position reporting is particularly important for specification options that involve Roller MV correlation to spot-test measurements or spatial comparison of Roller MVs from consecutive passes.

The Procedure to Verify Roller MV Repeatability is:

- 1) Perform two Measurement Passes on a fully compacted test strip at least 100 m (330 ft) long. Measurement Passes should be performed in the same direction, with static passes performed in the reverse direction between Measurement Passes.
- 2). From the two Measurement Passes, compute the spatial percent difference array $\% \Delta MV_i$ per Equation 3.1:

$$\% \Delta MV_i = \frac{MV_i - MV_{i-1}}{MV_{i-1}} \times 100 \tag{3.1}$$

where MV_i and MV_{i-1} represent the MV data array from pass i and pass $i - 1$, respectively. If necessary, linear interpolation may be used to transform the data onto a grid for precise spatial comparison. If the mean of the $\% \Delta MV$ array ($\mu \% \Delta MV_i$) is greater than 5%, the test strip may not have been fully compacted and the procedure should be repeated.

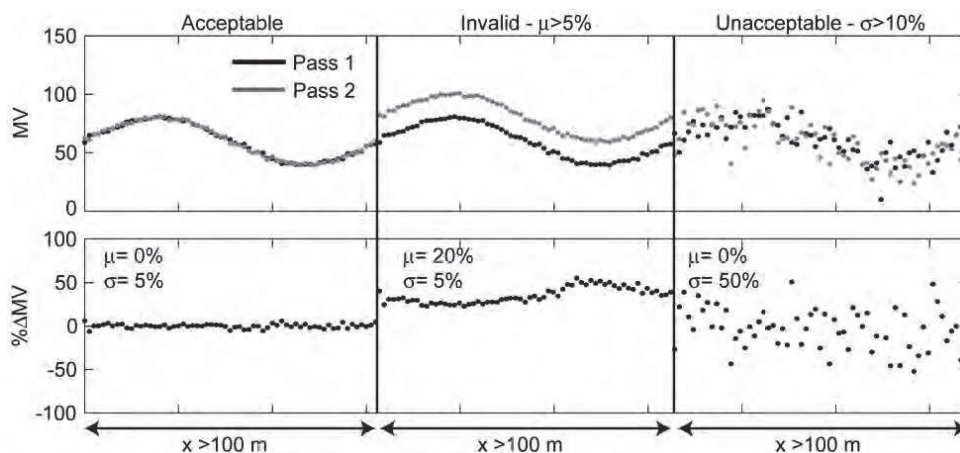


figure 3.2 Roller MV repeatability testing: (left) acceptable repeatability, (middle) invalid test, and (right) unacceptable repeatability.

- 3). Compute the standard deviation of the $\% \Delta MV_i$ array ($\sigma \% \Delta MV_i$). The $\sigma \% \Delta MV_i$ quantifies the Roller MV repeatability. The recommended acceptable maximum $\sigma \% \Delta MV_i$ is 10%, although visual inspection and engineering judgment should be employed when investigating repeatability and when deciding what level of repeatability is required and acceptable on a given project. Figure 7.3 illustrates acceptable and unacceptable levels of $\sigma \% \Delta MV_i$ as well as an invalid test (due to increase in compaction of the test strip).

3.4 In-situ Strength-based test approaches that can be used for compaction QA/QC

An important step in the assessment of CCC and IC systems is establishing a reliable approach for validation of these technologies. Historically, a number of in-situ test methods have been used for QA/QC of the compaction process, falling into two general categories: density-based tests and strength-based tests.

Details about the second one in-situ testing techniques is provided in the following sections.

Strength-based test approaches provide an estimate of the modulus and/or stiffness of a soil layer, by applying a load to the soil and then measuring the resulting displacement response. While such devices can be used to estimate a value for the elastic modulus of the soil layer, which is in theory an independent soil parameter, factors such as stress variability, moisture content, and unknown spatial effects influence the measurement. The effects of stress are primarily due to differences in the applied mean and deviator stress levels, the applied strain level, and the applied strain rate. These factors vary from device to device and they greatly affect the estimation of soil modulus (Briaud and Seo 2003). This complicates comparative analysis of field devices and characterization of subgrade spatial variability (Camargo et al. 2006). Common strength-based tests include the Plate Load Test (PLT), Light Weight Deflectometer (LWD) test, Falling Weight Deflectometer (FWD) test, Dynamic Cone Penetrometer (DCP) test, and the Soil Stiffness Gauge (GeoGauge) test (we will neglect these two last tests).

3.4.1 Plate Load Test (PLT)

The static plate load test (PLT) is a commonly used approach for testing the

performance of pavement and foundation layers in both rigid and flexible pavements. The test involves loading a circular plate resting on the layer to be tested, and measuring the associated deflection of the layer under varying load increments.

Different sizes of load plate can be used for this test; however, for roadway testing, the plates are typically 30.5 cm (12 in) in diameter (ASTM D 1196-93). Typically, load is applied to the plate by a hydraulic jack. The plate must be loaded continuously until all measured settlement has subsided so that the actual deflection for each load increment is obtained. The amount of time required for the preliminary settlement to take place is determined by plotting a time-deformation curve during the test. At the point when the curve becomes horizontal, or when the rate of deformation nears 0.0025-cm/min, the next load increment is applied. According to the ASTM D 1196- 93 testing method, the test should continue until a peak load is reached or until the ratio of load increment to settlement increment reaches a minimum, steady magnitude.

Usually, a PLT is run for two cycles of loading (Figure 2.20), which results in two modulus values, E_1 and E_2 . Normally, E_2 is two to three times greater than E_1 (Forsblad 1980).

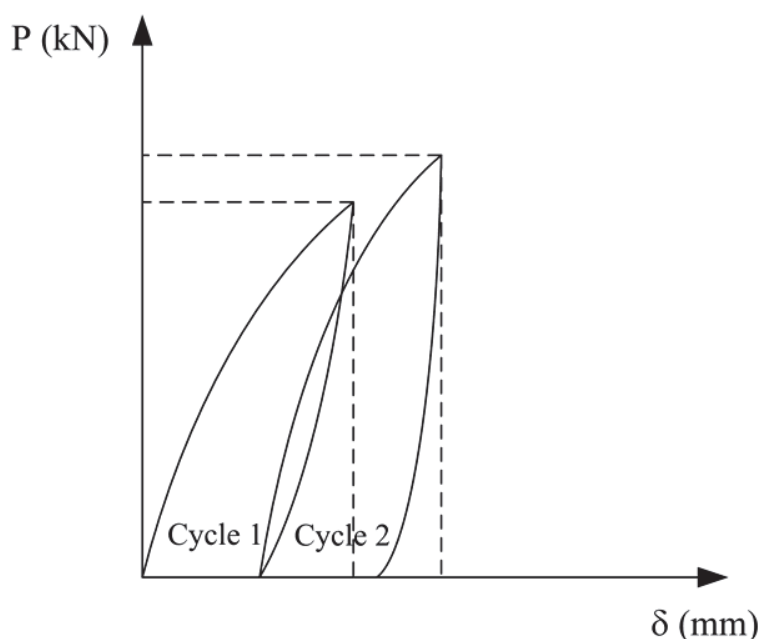


figure 3.3 Typical loading cycles for PLT test

The elastic modulus of the soil layer that is tested is calculated using Equation 2.32 (Alshibli et al. 2005).

$$E_{PLT} = \frac{k \cdot P \cdot (1 - \nu^2)}{r \cdot \delta} \quad (3.2)$$

where, E_{PLT} = Secant modulus for each cycle of loading (Mpa), $k = \pi/2$ and 2 for rigid and flexible plate, P = Applied load (kN), r = Plate radius (m), δ = Deflection of the plate (mm). According to ASTM D 1196, a “rigid plate” is defined as a plate with deflection of less than 0.0025 mm (0.0001 in) from the center to the edge of plate, when the maximum load is applied.

3.4.2 Light Weight Deflectometer (LWD)

The light weight deflectometer (Figure 2.21) induces a soil response by dropping a weight onto a plate resting on the test layer (ASTM E 2583–07). A load cell within the instrument measures the time history of the load pulse and a geophone in contact with the test layer measures the time history of the soil’s velocity. The velocity is then integrated to determine the displacement. The time history files are automatically exported to a data acquisition system, where the peak load and displacement values are used to calculate modulus values. Time history files can also be analyzed using a fast Fourier transform for a more accurate modulus calculation (Hoffmann et al 2003, Camargo et al. 2006).

The elastic modulus of the subgrade soil is calculated from the surface deflection using the following Boussinesq equation (Rahman et al. 2007):

$$E_{LWD} = \frac{k \cdot (1 - \nu^2) \cdot \sigma_0 \cdot r}{z_{ave}} \quad (3.3)$$

where, E_{LWD} = LWD modulus (MPa); $k = \pi/2$ and 2 for rigid and flexible plate, respectively (criteria used to determine plate rigidity are the same as for the PLT discussed above); z_{ave} = Average of three measured deflection at center of the plate (μm); σ_0 = Applied stress (kPa); ν = Poisson’s Ratio; and r = Plate radius (mm).

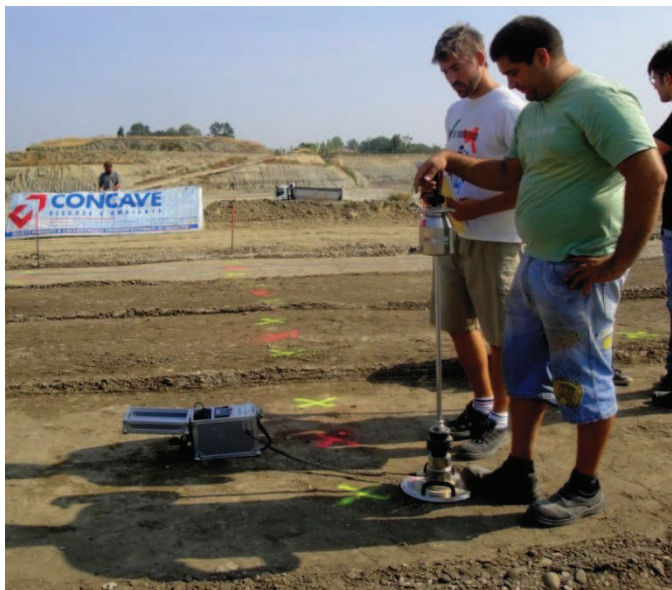


figure 3.4 Light weight deflectometer (300 mm and 200 mm plate)

Generally, there is a good correlation between PLT modulus and LWD modulus (Adam and Kopf 2004). With cohesive soils, a linear relationship is often valid for the entire range of test results. For cohesionless soils, a bi-linear relationship or a logarithmic function shows stronger correlative agreement (Adam and Kopf 2004).

3.4.3 Falling Weight Deflectometer (FWD)

The falling weight deflectometer (FWD), shown in Figure 2.22, is a test device which imparts a load pulse to the soil surface to simulate the load produced by a rolling vehicle wheel (ASTM D 4694). The load is produced by dropping a large weight, and the impact energy from this falling weight is transmitted to the pavement through a circular load plate (typically 300 mm (12 in) diameter). A load cell mounted on top of the load plate measures the load imparted to the pavement surface.

Deflection sensors, usually consisting of geophones or force-balance seismometers that are mounted radially off the center of the load plate, measure the deformation of the pavement in response to the load. Some typical deflection sensor offsets are 0 mm, 200 mm (8 in), 300 mm (12 in), 450 mm (18 in), 600 mm (24 in), 900 mm (36 in), 1200 mm (48 in), and 1500 mm (60 in). The measured deflections at different stations are then used to back-calculate the modulus of the subgrade soil using Boussinesq's equations (Rahman et al. 2007).



figure 3.5 Falling weight deflectometer

3.5 QA Option 1: Spot Testing of Roller-Informed Weakest Area

QA Option 1 utilizes roller-integrated CCC to identify the weakest area(s) of the *Evaluation Section*. The weakest area is defined by the lowest *Roller MVs* recorded during a *Measurement Pass*. More than one weakest area may be selected.

Acceptance is based on spot-test measurements from the weakest area(s) (see Figure 3.2).

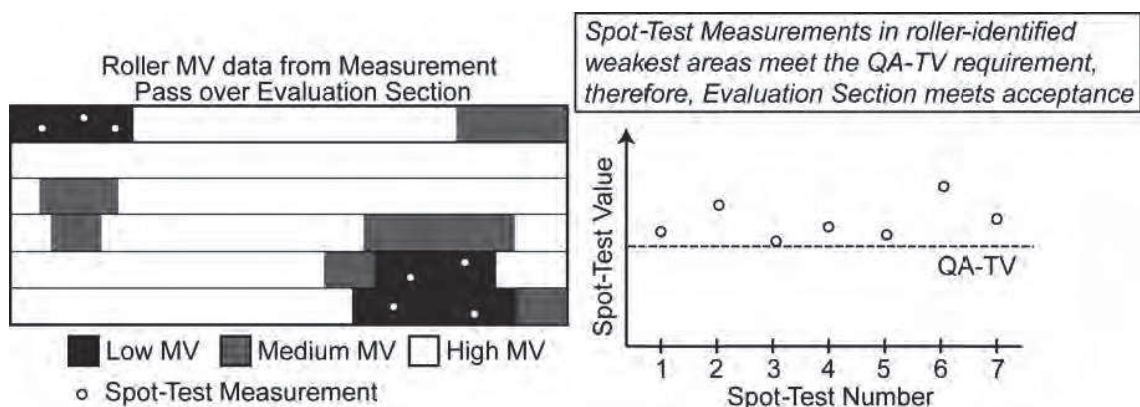


figure 3.6 Acceptance testing via Option 1.

If spot-test measurements from the weakest area(s) meet specified criteria, the *Evaluation Section* meets acceptance. The frequency of spot testing in the weakest

area(s) and acceptance criteria for spot-test measurements should be based on existing spot-test-based QA practice. The selection of Evaluation Sections must be performed in accordance with Section 3.4.3.

An important premise of Option 1 is that there is a positive correlation between *Roller MV* and soil compaction (i.e., the lowest *Roller MVs* correspond to lowest compaction). This positive correlation may not exist if the *Evaluation Section* exhibits localized soil variability (e.g., pockets of high clay content in an otherwise granular material) or significant variability in the sublift material. In cases where the lift and/or sublift material exhibits variability, the correlation between *Roller MVs* and spot-test measurements should be verified. This can be accomplished by comparing spot-test measurements with low, medium, and high *Roller MVs* across the *Evaluation Section*. In addition, low *Roller MVs* can result from fluctuations in machine operating parameters and surface unevenness.

For this reason the weakest area(s) selected for testing should not be based on *Roller MVs* from areas less than 3 m (10 ft) long in the driving direction. Option 1 requires minimal changes to existing spot-test-based QA specifications and should be relatively easy to implement. To improve reliability, Option 1 may be implemented in combination with another recommended option.

3.5.1 QA Option 2: Limiting Percentage Change in Roller MV

QA Option 2 utilizes the pass-to-pass percentage change in *Roller MVs* to determine acceptance of an *Evaluation Section*.

Acceptance is based on achieving a threshold or target $\% \Delta MV_i$ (i.e., $\Delta-TV$) between two consecutive *Measurement Passes* over the same *Evaluation Section*. There are two ways in which Option 2 can be implemented. Acceptance may be based on the pass-to-pass percentage change in mean MV ($\% \Delta \mu MV_i$) of the *Evaluation Section*. Alternatively, acceptance may be based on a spatial analysis of the $\% \Delta MV_i$ data array.

The dependence of *Roller MVs* on driving direction and the influence of soil heterogeneity within the drum length require that *Measurement Passes* must be performed with an identical pass-to-pass *Rolling Pattern*, particularly for Option 2b. The selection of *Evaluation Sections* must be performed in accordance with Section 3.4.3

3.5.2 Option 2a: Monitoring Percentage Change in Mean MV

QA Option 2a involves computing $\% \Delta \mu_{MV_i}$ from two consecutive *Measurement Passes* over the *Evaluation Section* according to Equation

$$\% \Delta MV_i = \frac{MV_i - MV_{i-1}}{MV_{i-1}} \times 100 \tag{3.1}$$

The recommended target value for $\% \Delta \mu_{MV_i}$ (i.e., $\% \Delta -TV$) is 5%. If $\% \Delta \mu_{MV_i}$ between consecutive passes is less than the $\% \Delta -TV$, acceptance is met (see Figure 3.3).

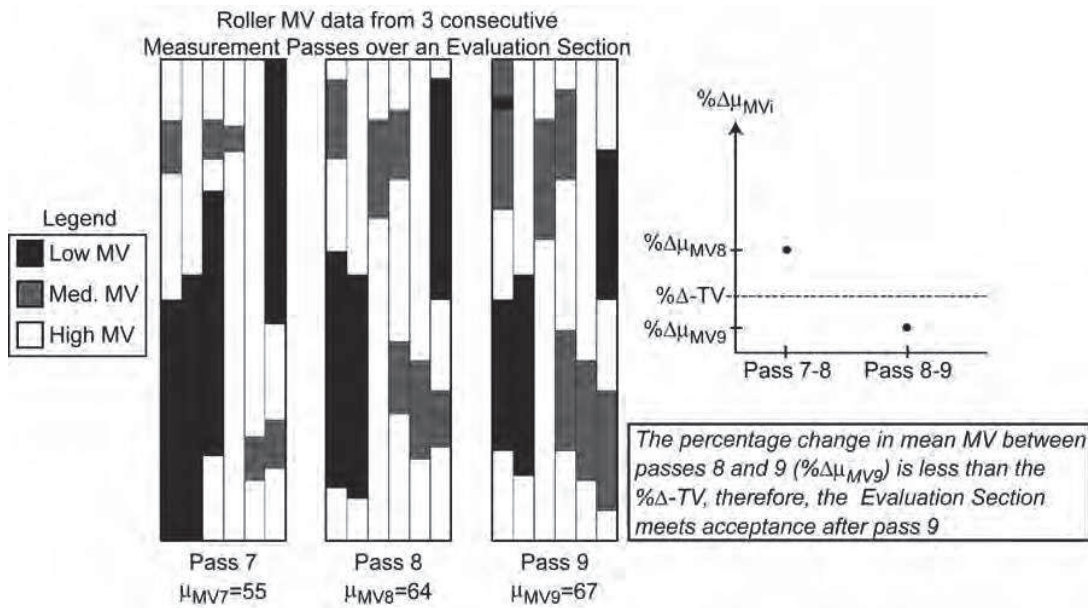


figure 3.7 Acceptance testing via Option 2a.

3.6 Option 2b: Monitoring Spatial Percentage Change in Roller MVs

QA Option 2b involves evaluating the spatial percent change in $\% \Delta MV_i$ from two consecutive *Measurement Passes* over the *Evaluation Section* according to Equation (3.1). This spatial analysis involves transforming the *Roller MV* data onto a fixed grid for direct comparison. The percentage change in *Roller MV* is then computed for each grid location.

The recommended $\% \Delta -TV$ for Option 2b is two times the uncertainty $\sigma_{\% \Delta MV_i}$ determined from repeatability testing (as described in 3.4.4). Acceptance is based on achieving the $\% \Delta -TV$ over a specified proportion or percent area threshold of the *Evaluation Section*, as shown in Figure 7.7. The recommended range for a specified

proportion/percent area threshold is 80% to 95% (e.g., acceptance is met when the *Roller MV* increases by $\leq\% \Delta\text{-TV}$ for 90% or more of the Earthwork Section). The process of transforming spatial *Roller MV* data onto a fixed grid is not trivial and has not been proven fully reliable. The simplest methods (e.g., nearest neighbor gridding, linear interpolation) may be more favorable than the more complex methods (e.g., nonlinear interpolation, kriging) until the geostatistical nature of *Roller MV* data is better understood.

QA Option 2 requires moderate changes to existing construction practice in that two *Measurement Passes* must be performed with similar *Rolling Patterns*. If implemented correctly, Option 2 ensures that compaction has been achieved to the capability of the CCC roller and the selected *Operating Parameters* but does not necessarily ensure that adequate compaction has been achieved. The ability of the roller to produce adequate compaction should be verified before earthwork compaction begins. To improve the reliability of compaction QA, Option 2 may be used in combination with another QA option.

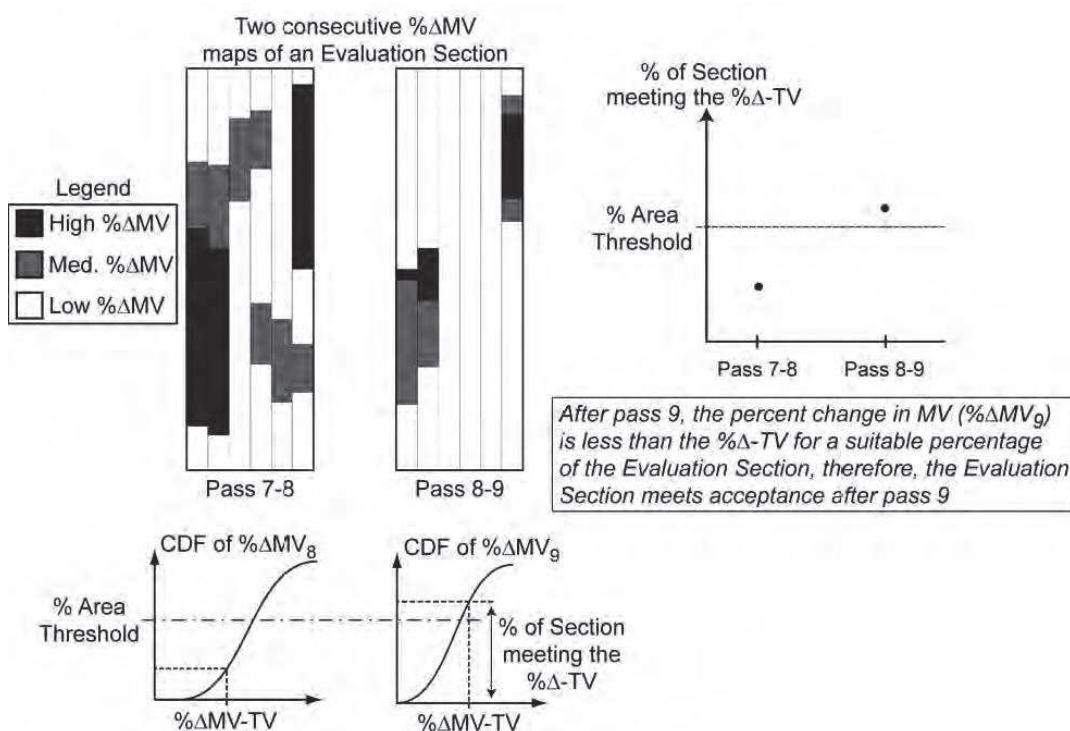


figure 3.8 Acceptance testing via Option 2b.

Chapter 4

Construction and demolition (C&D) materials

4.1. Premise

This section provides some contextual background regarding C&D waste management in Europe and the quantities and composition of waste materials. It briefly identifies the main environmental and sustainability issues associated with C&D waste generation and shows physically, chemically and mechanically characterization performed on the basecourse aggregates on manufactured bound and unbound mixtures that have been performed on field.

4.2. C&D wastes: definition and EU context

Construction and demolition waste is one of the heaviest and most voluminous waste streams generated in the EU. It accounts for approximately 49% of all waste generated in the EU and consists of numerous materials, including concrete, bricks, gypsum, wood, glass, metals, plastic, solvents, asbestos and excavated soil, arising from activities such as the construction of buildings and civil infrastructure, total or partial demolition of buildings and civil infrastructure, road planning and maintenance.

In most European countries in the last decadet here was an increase in the generation of C&D waste and several recent sources provide with estimates of C&D waste arising in Europe (figure 4.1).

Source	Total C&D waste arising (million tonnes)	C&D waste per capita
[WBCSD 2009] (2002 data)	510	1.1
[ETC/RWM 2009](2004 data)	866	1.8
[EUROSTAT 2010] (2006 data)	970	2

Table 4.1. Various C&D working paper in the EU

However, the level of recycling and re-use of CD waste varies greatly (between less than 10% and over 90%) across the Union but it seems very difficult to calculate

recycling rates for C&D waste in Europe.

Two recent sources (UBA 2009 & ETC/RWM 2009) provide recycling and recovery rates of C&D waste in some Member States. UBA 2009 reports recycling rates for 16 countries, representing 64% of the total amount of C&D waste generation they report. ETC/RWM 2009 reports recycling rates for 17 countries, representing 90% of the total amount of C&D waste generation they report. Based on these two samples, average recycling rates for countries where recycling data is available is respectively 86% and 66%.

Those averages recycling rate are a broad estimation with a high uncertainty. However, it looks rather plausible, and within the range of estimates proposed by experts and literature: 30 to 60%.

At a national level, the current situation is as follows:

- 6 countries report recycling rates that already fulfil the Directive's target (Denmark, Estonia, Germany, Ireland, the UK and the Netherlands)
- 3 countries report recycling rates between 60% and 70% (Austria, Belgium, and Lithuania)
- 4 countries (France, Latvia, Luxembourg and Slovenia) report recycling rates between 40% and 60%
- 8 countries report recycling rates lower than 40% (Cyprus, Czech Republic, Finland, Greece, Hungary, Poland, Portugal and Spain)
- For 6 countries, no data was available to estimate the recycling rates (Bulgaria, Italy, Malta, Romania, Slovakia and Sweden)

Construction and demolition waste has been identified as a priority waste stream by the European Union in relation with a growing difficulty to find natural inert materials and a high potential for recycling and re-use of C&D waste, since some of its components have a high resource value.

4.3. C&D waste: composition

C&D wastes typically comprise large quantities of inert mineral materials, with smaller amounts of a range of other components. The following materials are typical:

- concrete;
- bricks, tiles and ceramics;

- wood;
- glass;
- plastic;
- bituminous mixtures and tars;
- metals (ferrous and non-ferrous);
- soils and stones;
- dredging spoils;
- insulation materials (including asbestos);
- gypsum-based materials (including plasterboard);
- chemicals;
- waste electronic and electrical equipment (WEEE);
- packaging materials; and
- hazardous substances.

In addition to C&D waste, other non-hazardous waste materials can be used as recycled in the production of mixtures of aggregates and products in the civil construction branch. Among those, steel slag and wastes from incineration processes are among the most common.

C&D wastes can contain small amounts of hazardous wastes, if not separated at source, the mixture of which can pose particular risks to the environment and can hamper recycling. The management of hazardous components of C&D waste requires special consideration due to their high potential for harm to the environment and human health. Wherever possible they must be minimized through careful selection of materials in the design phase of a project, and the use of non-hazardous substitutes.

4.4. Environment and sustainability issues

The construction industry is one of Europe's largest consumers of natural resources.

Yet, currently, large quantities of these materials eventually end up in landfills, without any form of recovery or re-use.

More efficient use of materials both at the beginning and at the end of their life would make a major contribution to reducing the environmental impacts of construction.

This benefit would be achieved principally through the reduced depletion of finite

natural resources and a reduced dependence on landfill. In addition, efficient use and re-use of materials would also contribute to improving the economic efficiency of the sector and of Europe as a whole.

The need for the improved use of natural resources in this sector has been recognised at the EU level. This is reflected in the challenging target that has been set to increase the recovery and recycling of C&D wastes across Europe (70% by 2020, as noted earlier).

There are considerable opportunities for improvements in the resource efficiency of C&D waste management. This waste stream contains a high proportion of inert materials that are relatively simple to process and that can be used for various secondary applications rather than being disposed of. Note that one of these potential applications is use as structural material at a landfill site. Some inert material is required in landfills and inert C&D wastes could fulfil this function.

C&D wastes also contain many valuable components with high ‘embodied’ environmental impacts (in terms of the investment that has gone into producing them). The re-use or recycling of these components can eliminate the need for further investment in primary production. It would be even better if their use were avoided in the first place, and there are many waste prevention techniques available to the construction sector that can help deal with this issue in order to bring significant environmental, and financial, savings.

Reducing and recycling C&D materials hence conserves landfill space, creates jobs, and can reduce overall building project expenses through avoided purchase/disposal costs. Changing how we think about these materials will create a more sustainable future.

4.5. Research Steps .

Based on these assumptions, the DICAM Roads Department of Bologna University and the Consortium Cave Bologna, Bologna-based company of reference in the production of construction aggregates, have developed an experimental study for the characterization of C&D waste to be used in roads construction. The research has been carried out both in laboratory and on field and C&D materials have been physically, chemically and mechanically characterized to evaluate their use in the production of mixtures for the construction of embankments, foundations and basecourses. Relying on the results, different bound and unbound mixtures have been manufactured.

Having identified the range of products to be used, the research has been developed in three main phases: a first phase of prequalification of the materials in the laboratory, a second one of analysis, formulation and qualification of bound and unbound mixtures and a third phase of testing in work of materials .

In the first phase, carried out in the laboratory on five sorts of fine aggregates, sand and coarse, both recycled and natural, we proceeded to a mechanical physical and chemical characterization

Starting from these results, formulations for the production of bound and unbound mixtures of various types have been defined, suitable for road infrastructure construction industry.

Three unbound mixtures suitable to proceed with the tests have been designed. The mixture analysis by means of laboratory testing procedures allowed a qualitative classification. Two mixtures, made starting from the 5 aggregate source, will be tested on field.

Starting from the same two mixtures then we created two different hydraulically bound mixtures: one with the 1.25% of Portland cement 425 and 1.25% of fly ash and the other one with only 2.5% of cement, both subjected to further laboratory tests so as to obtain a mechanical qualifications before the in-situ tests .

The third phase involved the construction off an experimental field for testing the materials on a 1:1 scale. This has been constructed on a flat area with suitable characteristics of bearing and logistics capacity provided by Consorzio Cave Bologna.

The in-situ testing phase was performed mainly through CCC vibratory roller during the compaction step and deflectometric tools.

4.6. Physical and mechanical properties of the mixtures

The section describes the various laboratory tests carried out according to current European Standars, in order to reach a first pre-qualification of the five basic materials selected for testing in the field.

The aim is to study the appropriate physical and chemical characteristics useful in establishing the appropriate proportions to begin the laboratory analysis of mixtures.

The tests performed are listed below:

- Atterberg limits (CNR UNI 10014: 1964);
- *Particle size distribution-sieving method (EN 933-1);*
- *Shape Index (EN 933-4);*
- *Aggregate Flakiness Index (EN 933-3);*
- *Particle Density Of Filler (EN 1097-7);*
- *Particle Density And Water Absorption (EN 1097-6);*
- *Loose Bulk Density And Voids (EN 1097-3);*
- *Resistance to fragmentation-Los Angeles (EN 1097-2);*
- *Sand equivalent test (EN 933-8).*

4.6.1.Prequalification of the materials

For the purposes of the research, three different aggregates coming from construction and demolition processes and two from waste treatment plants were qualified, subsequently used to the experimental mixture design.

In particular, we analyzed material obtained from selective demolition of concrete structures deprived of any steel bar, non-selective demolition of buildings and other works, from scraps of iron and steel from waste incineration processes of municipal solid waste (Figure 4.1).



Figure 4.1. Materials testing: A. Crushed concrete, B. Mixed Recycled C & D, C. Waste from thermal processes of metal casting, D. and E. Wastes from incineration processes of municipal solid waste.

4.6.2.The Atterberg limits

The Atterberg limits are a basic measure of the nature of a fine-grained soil. Depending on the water content of the soil, it may appear in four states: solid, semi-solid, plastic

and liquid. In each state, the consistency and behavior of a soil is different and consequently so are its engineering properties. Thus, the boundary between each state can be defined based on a change in the soil's behaviour.

In the lab, the Casagrande Liquid Limit Device has been used for determining the liquid limits of soils, described by the specification CNR UNI 10014: 1964 (figura 4.2).



Figure 4.2. Casagrande cup in action.

The results obtained from the tests are reported in Table 4.2. In particular, all the samples are not plastic.

Table 4.2. Percentage values of the limits for each sample.

<i>Atterberg limits</i>			
<i>Sample</i>	<i>Liquid Limit [%]</i>	<i>Plastic Limit [%]</i>	<i>Plastic Index</i>
<u>A</u>	34.07	N.P.	N.D.
<u>B</u>	34.45	N.P.	N.D.
<u>C</u>	31.07	N.P.	N.D.
<u>D</u>	55.27	N.P.	N.D.
<u>E</u>	43.84	N.P.	N.D.

4.6.3. Particle size distribution through sieve

The test requisites of grain size analysis are contained in the European standards EN 933-1/2, which specifies a method, using test sieves (figure 4.3), for the determination of the particle size distribution of aggregates. It applies to aggregates of natural or artificial origin, including lightweight aggregates, up to 63 mm nominal size, but excluding filler.



Figure 4.3. Sieves according to standard 933-1.

The test consists of dividing up and separating, by means of a series of sieves, a material into several particle size classifications of decreasing sizes. The aperture sizes and the number of sieves are selected in accordance with the nature of the sample and the accuracy required.

The mass of the particles retained on the various sieves is related to the initial mass of the material. The cumulative percentages passing each sieve are reported in numerical form and graphical form .

The Figure 4.4 shows the grain size (horizontal logarithmic scale) against percentage distribution (vertical arithmetic scale) of the five constituent materials; A point on the curve indicates the percentage by weight of particles smaller in size than the grain size at the given point. In relation to the particle size then have been designed the various mixtures.

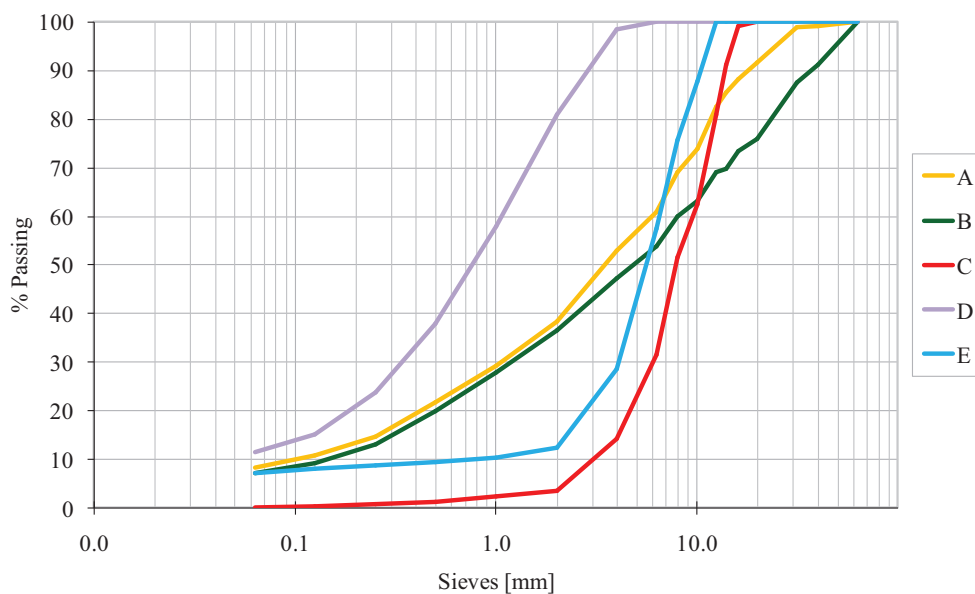


Figure 4.4. Particle size analysis of the sifted aggregates

4.6.4. Tests for geometrical properties of aggregates

A simple method for the examination of coarse recycled aggregates with grain size between 4 and 63 mm is described by the European Standard EN 933-11 through which identifying and estimating the relative proportions of constituent materials.

The proportions of constituent materials in coarse recycled aggregate shall be determined in accordance with EN 933-11 and shall be declared in relevant categories [EN 12620 + A1]. These categories are presented in Table 4.3.

Table 4.3. Categories for constituents of coarse recycled aggregates.

Constituent	Description
Rc	Concrete, concrete products, mortar, Concrete masonry units,
Ru	Unbound aggregate, natural stone and hydraulically bound aggregate
Rb	Clay masonry units (i.e. bricks and tiles), Calcium silicate masonry units, Aerated non-floating concrete,
Ra	Bituminous materials
FL	Floating material in volume
Rg	Glass
X	Other: Cohesive (i.e. clay and soil), Miscellaneous: metals (ferrous and non-ferrous), non-floating wood, plastic and rubber, Gypsum plaster

The portion of each constituent characterizing the specimen is determined and expressed as a percentage by mass, except for the portion of floating particles. For the latter, intended as the particles of material with lower specific weight than water, the relative commodity fraction is not expressed as a percentage by weight, but in volume.

From the analysis of the 5 materials (Table 4.4) used was found that:

- The material A is part of the recycled concrete, or aggregates constructed primarily from fragments of cement conglomerates, also armed, coming from demolition of reinforced concrete works, with a 90% mass of the main component given by concrete and stone material crushed. The 10% is made from scraps of broken masonry construction and coatings;
- The material B comes from rubble or submit aggregates consisting mainly of concrete and crushed stone materials as a percentage greater than or equal to 50% by mass and construction waste of broken masonry with less than 50%;
- The material C is steel foundry slag resulting from thermal processes of

melting metals, the composition of this material is then given by technical sheets provided by the manufacturers and does not require proof of product analysis (the constituent materials are not recognizable to the naked eye);

- The materials D and E are made of the same material derived from the Waste to Energy plants, in different particle-size class, so the test was performed on the bigger speckling size.

Table 4.4. -product analysis, differentiation type per inert.

PRODUCT ANALYSIS							
Sample	Rc	Ru	Rb	Ra	Rg	X	FL
	[% By weight]	[% By weight]	[% By weight]	[% By weight]	[% By weight]	[% By weight]	[% in volume]
A	90%	5%	5%	0%	0%	0%	0%
B	50%	30%	20%	0%	0%	0,01%	0,01%
C	0%	0%	0%	0%	0%	N.A.	0%
D	N.A.	N.A.	N.A.	N.A.	N.A.	N.A.	N.A.
E	0,0%	75,4%	1,5%	0,0%	22,7%	0,4%	3,0%

The Table 4.5 shows the limits required by the reference specifications , the Special Contract Specifications of the Tuscany Region and the one of the Autonomous Province of Trento, which shows how the materials abide by with the requirements., except for material E containing an excessive presence of glass.

Table 4.5. Specification requirements of Autonomous Province of Trento and the Tuscany region.

Components			
lithic materials from any source, crushed stone, concrete, bricks, refractories, ceramics, mortars, plasters, slag and dross		%	> 80
Glass and vitreous slag	separation at the sieve 8 mm (UNI EN 13285/2004)	%	≤ 10
bituminous mix		%	≤ 15
Other mineral waste which is to be admitted in the body recovery road under the current legislation		%	≤ 15 (total) ≤ 5 (single)
perishable materials: paper, wood, fibers, cellulose, organic substances except bitumen, plastics		%	≤ 0,1
Other materials (metals, gypsum, rubbers, etc.)		%	≤ 0,4

4.6.5. Shape Index (S.I.)

The shape index evaluation is defined in reference to the UNI EN 933-4 standard, which provides a methodology for its determination in mixtures of coarse aggregates of any origin. The test method specified in the European Standard is applicable to particle size fractions d_i/D_i [aggregate passing the larger (D_i) of two sieves and retained on the smaller (d_i)] where $D_i \leq 63$ mm and $d_i \geq 4$ mm. (Figure 4.5).

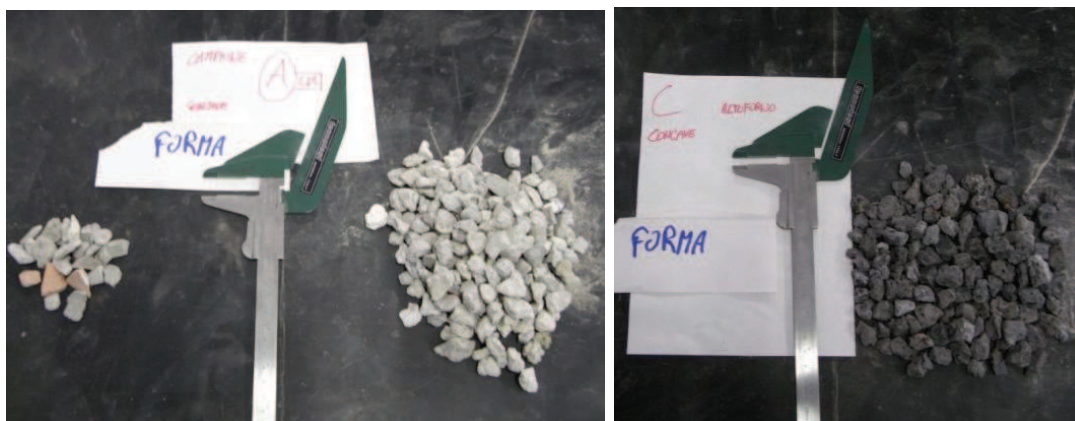


Figure 4.5. Material samples subject to the Shape Index Evaluation.

Individual particles in a sample of coarse aggregate are classified on the basis of the ratio of their length L to thickness E using a particle slide gauge where necessary. According to the shape index value, the reference category is defined as reported in the harmonised standard UNI EN 13242, as shown in Table 4.6.

Table 4.6. Categories for maximum values of the shape coefficient..

Shape Coefficient	Category SI
≤ 20	SI ₂₀
≤ 40	SI ₄₀
≤ 55	SI ₅₅
> 55	SI _{Dichiarato}
No requirement	SI _{NR}

From laboratory tests the results are grouped in Table 4.7; it reports M1 and M2, respectively, the mass of the particle size fraction used and the mass of the not cubic granules, in grams.

Through the two parameters has been obtained a shape index lower than 10% for samples A, B and E.

The sample C has a shape index equal to 0%, reason for which the sample is predominantly composed of cubic granules thus being part of the SI₂₀ category of reference. Regarding the sample D, the particle size is not appropriate for the execution of the test.

Since the Specification gives an upper limit of the shape index of 35% (SI₃₅), the results obtained can be considered fully satisfactory.

Table 4.7. Results of the shape index test.

Shape index (S.I.)			
Sample	M1 [g]	M2 [g]	S.I. [%]
A	500,00	41,20	8,24
B	500,00	45,70	9,14
C	500,00	0,00	0,00
D	N.D.	N.D.	N.D.
E	500,00	42,50	8,50

4.6.6. Aggregate Flakiness Index

The Aggregate Flakiness Index makes reference to the standard UNI EN 933-3;

The test procedure specified in this part of this European Standard is not applicable to particle sizes of less than 4 mm or greater than 80 mm.

The test consists of two sieving operations. First, using test sieves, the sample is separated into various particle size fractions d_i/D_i . Each of the particle size fractions d_i/D_i is then sieved using bar sieves which have parallel slots of width $D_i/2$.



Figure 4.6. Bar sieves.

The overall flakiness index is calculated as the total mass of particles passing the bar sieves expressed as a percentage of the total dry mass of particles tested. If required, the flakiness index of each particle size fraction d_i/D_i is calculated as the mass of particles passing the corresponding bar sieve, expressed as a percentage by mass of that particle

size fraction.(figure 4.6).

Observing the Table 4.8, in accordance with the requirements of the harmonised standard UNI EN 13242, the Flakiness Index defines the reference category. The flakiness index is expressed as a 'category', such as FI₁₅ or FI₃₅, in which the number represents the maximum percentage for the whole sample of aggregate. If the flakiness index is higher than 50% the actual number should be declared.

Table 4.8. Classes for maximum values of the Flakiness Index.

Flakiness Index	Class FI
≤ 20	FI ₂₀
≤ 35	FI ₃₅
≤ 50	FI ₅₀
> 50	FI _{Declared}
No requirement	FI _{NR}

From laboratory tests the results are grouped in Table 4.9 where M1 is the mass of the predominant particle size fraction and M2 the mass of the non-cubic aggregate .

Table 4.9. Results of the flakiness index test.

Flakiness Index Aggregates			
Sample	M1 [g]	M2 [g]	F.I. [%]
A	1107,6	148,5	13,41
B	905,2	112,3	12,41
C	1615,6	54,4	3,37
D	N.D.	N.D.	N.D.
E	711,7	125,4	17,62

From the above it is possible to consider an FI lower than 15% for the first three materials which comply with the reference category. Material E has an index equal to 17.62% still included in the FI₂₀ class whilst it was not possible to perform the tests material D, due to its nature,

Therefore the treated materials appear sufficiently regular in shape: values tending to 0 indicate that the element is cubic while the more increases the value, the more the granule tends to be flaky or to have a prevalent dimension than the other one.

Also in this case the analyzed specifications provide an upper limit of FI equal to 35% (FI₃₅) hence the results obtained can be considered fully satisfactory.

4.6.7. Particle Density Of Filler

The test consists in determining the density of the particles without any surface voids, but including internal voids and water absorption in reference to the standard UNI EN 1097-7.

The measurement of particle density can be done in a number of ways and the pycnometer has been used, a very common precise method useful in characterizing the irregularly shaped soil samples such as the aggregates.

Pycnometer method consists in to place a quantity of a dry, pre-weighed solid sample in the pycnometer and fill the rest of pycnometer with a liquid of known density (typically water), the weight of the pycnometer filled only with the liquid having previously been established. The density of the sample can be determined from the known density of the water, the weight of the pycnometer filled only with the liquid, the weight of the pycnometer containing both sample and liquid, and the weight of the sample. (Figure 4.7). The table 4.10 shows the results for the 5 adopted materials.



Figure 4.7. Pycnometers containing the five samples in deaeration phase.

Table 4.10. Risultati della prova di determinazione della massa volumica reale.

Particle Density Of Filler EN 1097-7										
sample	A		B		C		D		E	
T of test [°C]	29	29	29	29	29	29	29	29	29	29
Specific weight water at Ttest	0,996	0,996	0,996	0,996	0,996	0,996	0,996	0,996	0,996	0,996
Pycnometer [n°]	1	2	3	4	1	2	5	6	3	4
weight	95,60	97,11	96,18	96,47	99,98	100,88	92,40	93,49	99,23	99,05
weight (Piknometer+water) [g]	79,06	77,89	80,33	80,04	79,06	77,89	80,15	78,44	80,33	80,04
Net weight dry [g]	26,16	30,38	25,27	26,11	28,36	31,17	19,37	23,84	29,86	30,00
Volume of materials [cm3]	9,66	11,21	9,46	9,72	7,47	8,21	7,15	8,83	11,00	11,03
particle density [g/cm3]	2,708	2,711	2,672	2,686	3,796	3,795	2,710	2,701	2,713	2,719
Average particle density	2,710		2,679		3,796		2,705		2,716	

4.6.8. (Apparent) Particle Density

The test consists in the determination of particle density of normal weight aggregates in reference to the standard UNI EN 1097-6.

The first five methods are applicable to normal aggregates with a sixth method for lightweight aggregates.

In reference to the specified methods, the apparent particle was carried out in the laboratory by using the pycnometer method for aggregates passing a 31,5 mm sieve but retained on a 0,063 mm sieve (Table 4.11).

Table 4.11. apparent mass density of the five samples.

Particle Density EN 1097-6					
Sample	A	B	C	D	E
T of test [°C]	29	29	29	29	29
Specific weight water at Ttest [g/cm³]	0,99597	0,99597	0,99597	0,99597	0,99597
Piknometer [n°]	4	8	2	B	9
weight (Piknometer+water+material) [g]	2487,79	2143,47	2300,43	2461,42	1999,61
weight (Piknometer+water) [g]	2031,50	1670,50	1711,50	2118,50	1675,70
Net weight dry [g]	743,76	771,68	813,24	592,20	546,85
Volume of materials [cm³]	288,633	299,919	225,218	250,289	223,842
Apparent particle density [g/cm³]	2,577	2,573	3,611	2,366	2,443

4.6.9. Loose Bulk Density And Voids

This test on the aggregates has been conducted according to the European Standard EN 1097-3, which specifies the test procedure for the determination of the loose bulk density of dry aggregate and the calculation of the voids.

The dry mass of aggregates filling a specified container is determined by weighing and the corresponding loose bulk density ρ_b (the quotient obtained when the mass of dry aggregate filling a specified container without compaction is divided by the capacity of that container) is calculated.

The percentage of voids (the air-filled spaces between the aggregate particles in the container) is calculated from the loose bulk density and the particle density.

The test shall apply to both natural and artificial aggregates of grain size up to a maximum of 63 mm.

Table 4.12. Loose Bulk Density And Voids of the five samples.

Loose Bulk Density And Voids EN 1097-3					
Sample	A	B	C	D	E
Volumetric Gross Weight [g]	11115	11002	12467	9157	9760
Tare volumometer [g]	3749	3749	3749	3749	3749
Net Weight volumometer [g]	7366	7253	8718	5408	6011
Volume Volumometer [cm³]	5075	5075	5075	5075	5075
Loose Bulk Density [g/cm³]	1,451	1,429	1,718	1,066	1,184

4.6.10. Density

The different particle densities obtained were then summarized in Table 4.13 ;The percentage of voids (the air-filled spaces between the aggregate particles in the container) is calculated from the loose bulk density and the particle density.

Table 4.13. results of determined particle densities .

Mass Density					
Sample	A	B	C	D	E
ρ_r (real particle density) [g/cm³] EN 1097-7	2,710	2,679	3,796	2,705	2,716
ρ_a (Particle density) [g/cm³] EN 1097-6	2,577	2,573	3,611	2,366	2,443
ρ_m (Loose bulk density) [g/cm³] EN 1097-3	1,451	1,429	1,718	1,066	1,184
V (% Intergranular voids) EN 1097-3	43,7	44,5	52,4	55,0	51,5

4.6.11. Resistance to fragmentation-Los Angeles (L.A.)

This test on the aggregates has been conducted according to the European Standard EN 1097-2 entitled: Tests for mechanical and physical properties of aggregates - Part 2: Methods for the determination of resistance to fragmentation, through the Los Angeles method.

The standard applies to natural, artificial or recycled aggregates used in construction and civil engineering. The treated materials, based on the obtained results , is classified in accordance with the UNI EN 13242 (Table 4.14).

Table 4.14. Classes for Los Angeles Index.

Los Angeles Index	LA Class
≤ 20	LA ₂₀
≤ 25	LA ₂₅
≤ 30	LA ₃₀
≤ 35	LA ₃₅
≤ 40	LA ₄₀
≤ 50	LA ₅₀
≤ 60	LA ₆₀
> 60	LA _{Dichiarato}
No requirements	LA _{NR}

The referenced standard provides two schemes for the determination of resistance to fragmentation of coarse aggregates: Los Angeles test and the impact strength test



Figure 4.8. Rotating cylinder and metal balls used as abrasive mass trial in Los Angeles.

The Los Angeles Machine has been used also to evaluate the Aggregate Freeze-Thaw sensitivity. The standard 1367-1 entitled: (Tests for thermal and weathering properties of aggregates - Determination of resistance to freezing and thawing) establish a test method that provides the necessary information on the behavior of the aggregates when subjected to freezing and thawing cycles.

The test consists in testing samples subjected to 20 thermal cycles with alternate temperatures between -20°C and $+20^{\circ}\text{C}$ and assessing the percentage difference between the Los Angeles test results performed on the treated and untreated material. The results obtained from the tests on the samples under study, with the exception of D with unsuitable grain, have been grouped in Table 3.3.14.

Table 4.15. Test results of Los Angeles.

Sample	LOS ANGELES			FREEZE/THAW TEST		
	Minit. [g]	M fin.[g]	L.A. [%]	Minit. [g]	Mfin. [g]	L.A. [%]
A	5000,0	3440,0	31,20	5000,0	3355,2	32,90
B	5000,0	3228,2	35,44	5000,0	3209,0	35,82
C	5000,0	4034,5	19,31	5000,0	4057,7	18,85
D	N.D.	N.D.	N.D.	N.D.	N.D.	N.D.
E	5000,0	2735,4	45,29	5000,0	2700,2	46,00

From the comparison with the Specification values, which impose a maximum test value equal to 30% of loss in weight, the materials A and B are at the limit of acceptability, the C is suitable, while the E highlights an inadequacy in as composed of inert excessively fragmentable.

In the comparison with the freeze thaw test, differences in loss weight were found, variable from a minimum percentage of 0.38 (sample B) to a maximum of 1.70 (sample A), while the behavior of sample C is substantially unchanged.

In response to a Specification request which does not exceed a difference of 1% between the loss in weight obtained from the two tests, it follows that all materials with the exception of A meet the requirements.

4.6.12. Assessment of fines- Sand equivalent test (S.E.)

This test on the aggregates has been conducted according to the European Standard EN 933-8 that specifies a method for the determination of the sand equivalent value of the 0-2 mm fraction in fine aggregates and all-in aggregates. It applies to natural aggregates.

A test portion of sand and a small quantity of flocculating solution are poured into a graduated cylinder and are agitated to loosen the clay coatings from the sand particles in the test portion. The sand is then “irrigated“using additional flocculating solution forcing the fine particles into suspension above the sand. After 20 min, the sand equivalent value (SE) is calculated as the height of sediment expressed as a percentage of the total height of flocculated material in the cylinder.

The values obtained for the aggregates from the 5 samples are listed In table 4.16.

Table 4.16. Results of the equivalent sand test.

Sand equivalent (S.E.)				
Material	h1 [cm]	h2 [cm]	E.S. [%]	S.E.average [%]
A	13,25	5,00	37,74	37,39
	13,50	5,00	37,04	
B	13,25	3,50	26,42	27,36
	13,25	3,75	28,30	
C	11,50	9,00	78,26	76,89
	12,25	9,25	75,51	
D	14,00	6,25	44,64	46,88
	14,25	7,00	49,12	
E	14,50	8,25	56,90	57,69
	13,25	7,75	58,49	

Minimum specified sand equivalent values for fine aggregate in Specifications of reference is 30% so the aggregates met the test, exception for the sample B with 27.36%, very close to the threshold.

4.7. Study of mixtures for embankment construction

Following the pre-qualification analysis, the five materials (A, B, C, D, E) have been selected and properly combined to constitute 4 optimized mixtures, in terms of mechanical, economical and productive performance, to be installed in the full-scale experimental pavement.

In particular, two unbound and two bound mixtures have been defined. The firsts ones, denominated Y (50% A 50% B) and X (70% B, 30% E) whilst the seconds one J and K, obtained, respectively, from the same unbound mixtures with the addition of hydraulic binders at a rate of 1.25% of Portland cement 42.5 and 1.25% of fly ash for recycling. Here in after the mix design and performance characterization of the mixtures will be described.

4.7.1. qualification and study of the unbound mixtures

three unbound mixtures on which perform mechanical characterization tests have been designed after the pre-qualification analysis of the five materials (A, B, C, D, E),

The test carried out were:

- Identification of grading curve in compliance with grain size provided by the

technical specifications considered (Autostrade del Brennero, Autostrade Venete, ANAS),

- Evaluation of moisture content for the optimum compaction, before and after the Proctor method compaction ,
- CBR test for the evaluation of bearing capacity.

The latter was determined both on saturated sample left to cure in air for seven days, either on samples subjected also to saturation through permanence in water for four days.

The three mixtures, called X, Y, Z are defined in Table 4.4..

Table 4.17. Composition of bound mixtures..

MIXTURE X	MIXTURE Y	MIXTURE Z
50% A, 50%B	60% B, 40% C	70% B, 30% E

4.4.1.1. Particle-size analysis of unbound mixtures

The grading curves of the three selected mixtures , in accordance with the granulometric range of the main specifications, are elencated below. The figures 4.9, 4.10, 4.11 show the different grading curve (defined by a maximum and a minimum curve) with different colors and the grading curve of the mixture (plotted in green) .

As can be noted, the mixtures X and Z appear well graded, while the mixture Y shows a smaller presence of material of size greater than 31.5 mm compared to the other two, due to a higher percentage of passing at the sieves of large diameter .

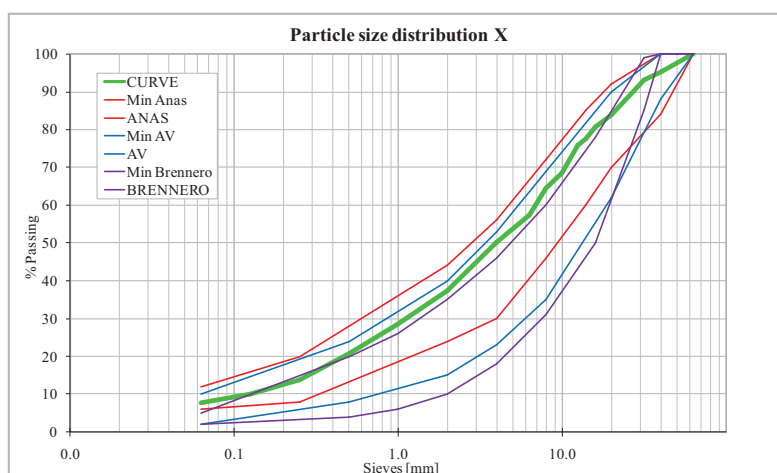


Figure 4.9. Grading curve of mixture X.

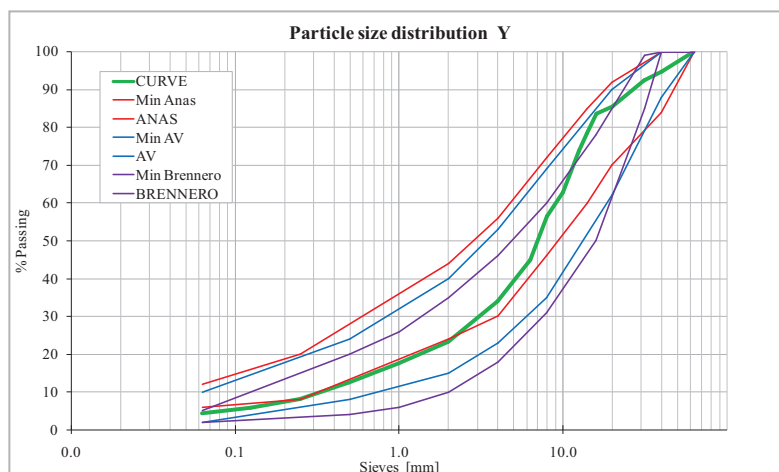


Figure 4.10. Grading curve of mixture Y.

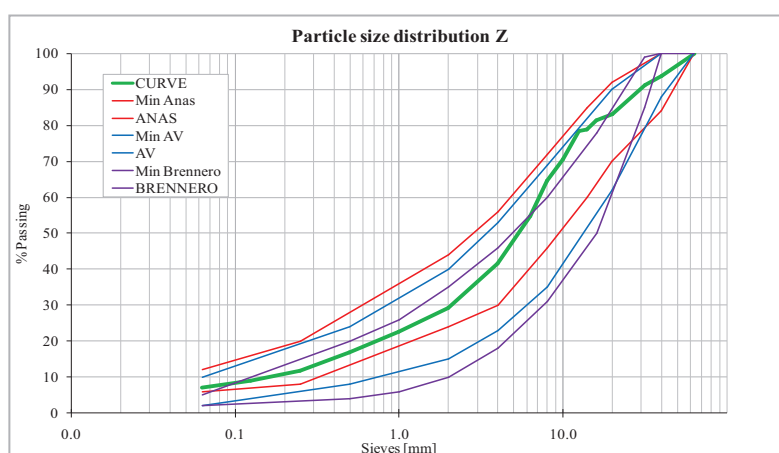


Figure 4.11. Grading curve of mixture Z.

4.4.1.2. Proctor test for the densification of the mixtures

In compliance with the provisions of the reference regulations UNI EN 13286-2, in the laboratory, was thus determined the variation of dry density (γ_d) as a function of moisture present in the sample (Figure 4.12) through the study of Proctor.



Figure 4.12. - Mechanical Equipment for Proctor compaction.

The results are reported in table 4.18.

Table 4.18. Results of compaction .

Compaction AASHO on Unbounded Mixtures			
	X	Y	Z
Maximum dry density [g/cm³]	1,981	2,150	1,906
Optimum moisture [%]	10,9	9,4	10,4

To obtain the optimal maximum compaction according to the optimal content required by the material, the results have been carried out on several specimens with different moisture contents. (Figure 4.13).

These results are of reference for the in situ controls of the degree of compaction achieved which must be equal to at least 90% of the densification obtained through Proctor.

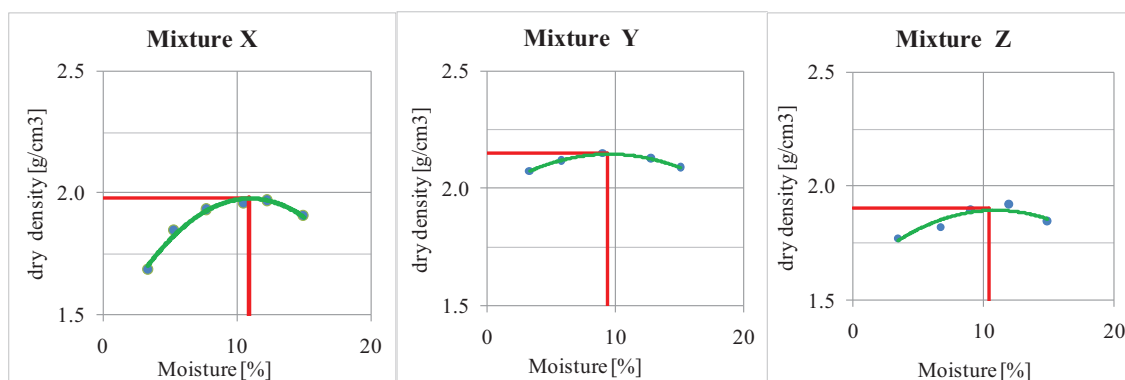


Figure 4.13. - Proctor Curve of the 3 unbound mixtures.

For the three samples the optimum moisture content, corresponding to the maximum value of dry density, lies at an average values around 10%.

4.4.1.3. Pre and post compaction particle size

In order to assess the grain size variation of materials as a result of crushed aggregates subjected to the impulsive Proctor test, it was evaluated the assortment particle size after the test, and the pre and post compaction curve was compared to.

The following tables show graphs of the change in the particle size of the three mixtures. In the graphs that follow are listed:

- The grading curve of reference.
- The theoretical curve, obtained as a combination of the base material curves

according to the amount previously indicated.

- The real pre-compaction curve, obtained in laboratory by mixing of the different materials.
- The post-compaction curve determined by the particle size analysis of the material once it was submitted to Proctor compaction.

From the graphs of Figures 4.14, 4.15 and 4.16 is highlighted a difference between real and theoretical curve due to the size of the grains in relation to the size of the specimen and to the inhomogeneity of the sample.

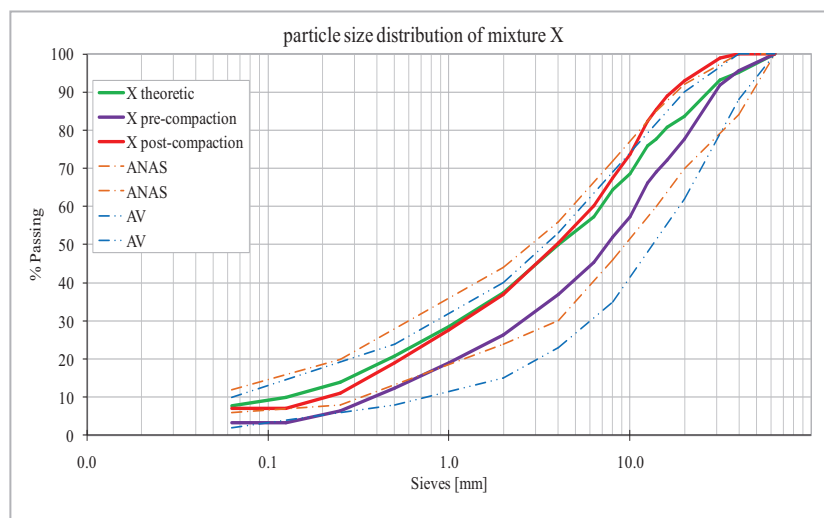


Figure 4.14. - Grading curve pre and post compaction of mixture X.

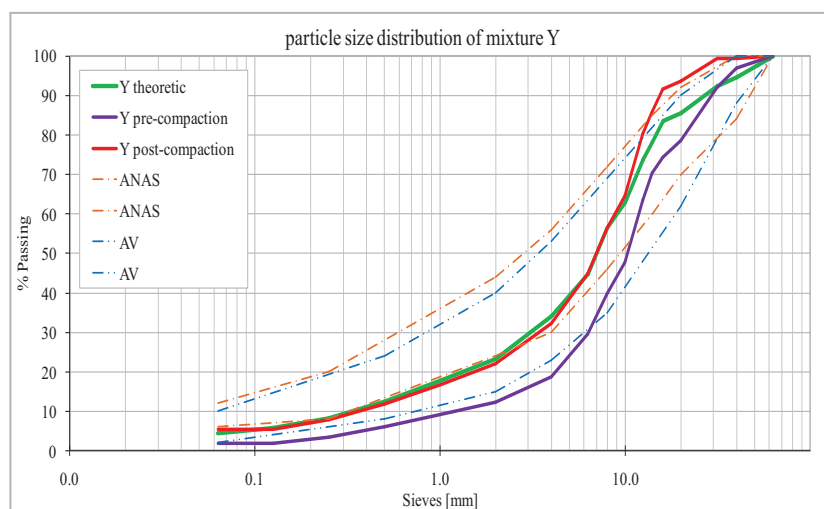


Figure 4.15. - Grading curve pre and post compaction of mixture Y.

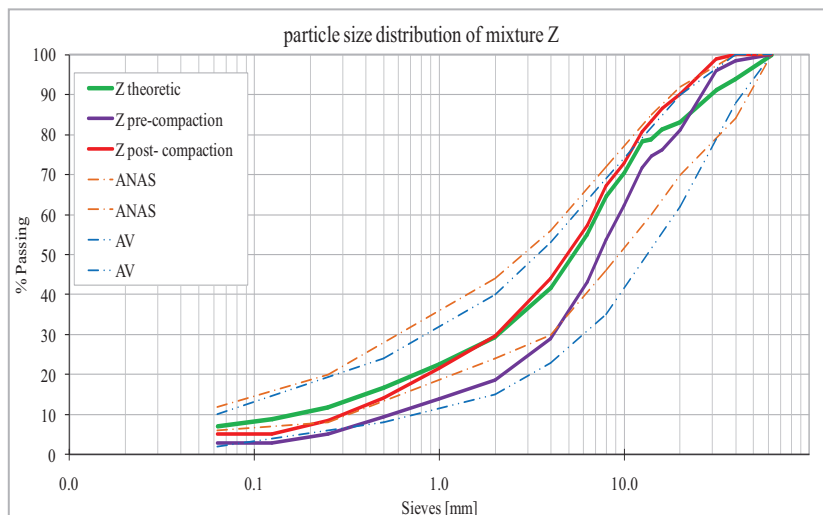


Figure 4.16. - Grading curve pre and post compaction of mixture Z.

In addition there is a shift of the curve after compaction towards the top of the grids for all the compounds, that indicates an increasing fine particle fraction percentage once the Proctor test was performed.

This specifies that the material probably will change its particle size following the passage of the vibratory roller.

4.4.1.4. Californian Bearing Ratio (presaturation)

Once determined the value of optimal moisture content and maximum dry density of each compound, Californian Bearing Ratio tests were performed on the samples with the optimal parameters (Figure 4.17).



Figure 4.17. Samples subjected to the CBR test.

It is a simple strength test that compares the bearing capacity of a material with that of a well-graded crushed stone (thus, a high quality crushed stone material should have a CBR % 100).

In particular, the test was carried out on six samples per mixture, taking as

representative the mean CBR value obtained. The CBR test is described in UNI EN 13286-47 entitled: Test method for the determination of California bearing ratio, immediate bearing index and linear swelling.

Test results are shown in figure 4.18 and table 19.4.

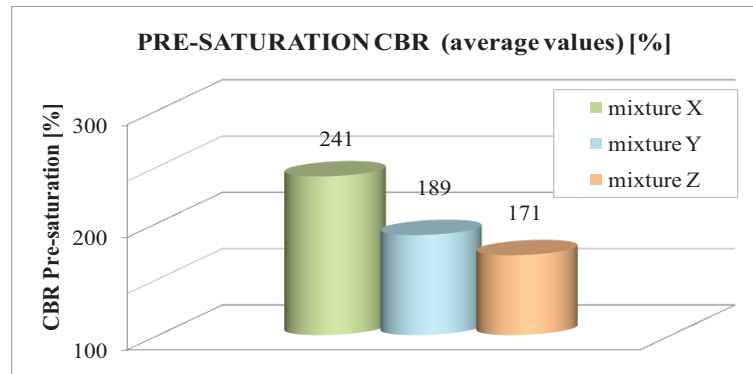


Figure 4.18. CBR test results.

Table 4.19. Final results of the CBR test on samples at optimum moisture.

presaturation CBR test (7 days-curing)			
	Mixture X	Mixture Y	Mixture Z
W [%]	10,9	9,4	10,4
CBR pre-sat [%]	241	189	171

The main Specifications give as CBR value limit a value greater than 50, for road subgrades and basecoarses use, widely respected on the basis of tests carried out.

4.4.1.5. Californian Bearing Ratio (postsaturation).

The final phase relative to the laboratory tests performed consists in the determination of the bearing capacity index and the corresponding swelling by CBR method on the specimens accrued 7 days in air and saturated in a span of 4 days. (Figure 4.19).

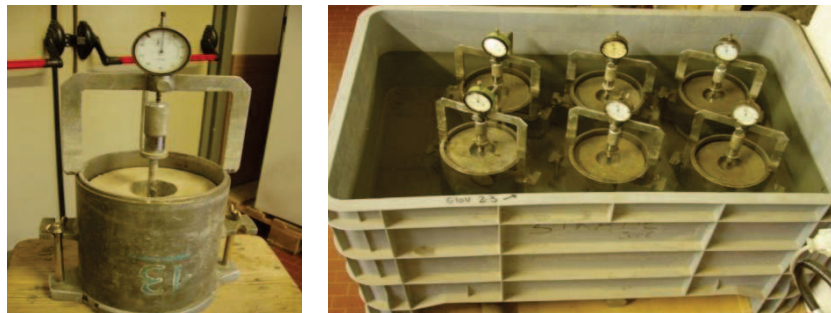


Figure 4.19. Saturated specimens subjected to the CBR test.

The averaged results obtained on the six specimens for any compound are elencated in Table 4.20, with enclosed swelling.

Results of the curing in water of the specimens has seen a decreasing of the CBR values of about 20% for the mixture X and 10% for the mixture Y whilst practically unchanged performance has been ascertained for mixture Z.

Table 4.20. CBR Final results of the saturated specimens..

Post-saturation CBR test			
	Mixture X	Mixture Y	Mixture Z
W [%]	10,9	9,4	10,4
CBR post-sat [%]	196	197	155
Swelling [%]	0,003	0,009	0,003

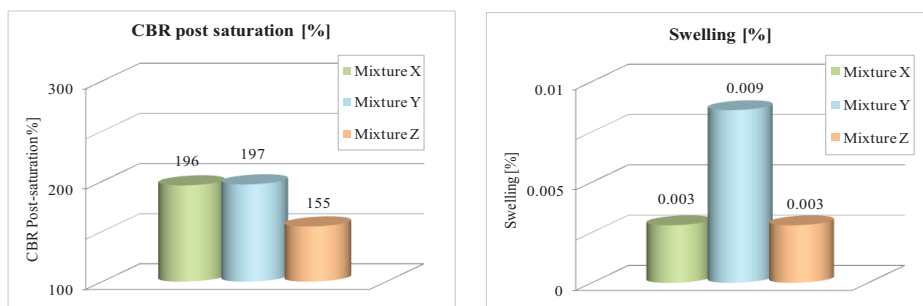


Figure 4.20. Graphic results of the CBR test and post-saturated swelling

The changes do not portend a decay of the bearing capacity. All compounds comply with the limits imposed by the specification.

Comparison between specimens X and Z, which will be used for in-situ tests, subjected to CBR test before and after the saturation phase is displayed in figure 4.21.

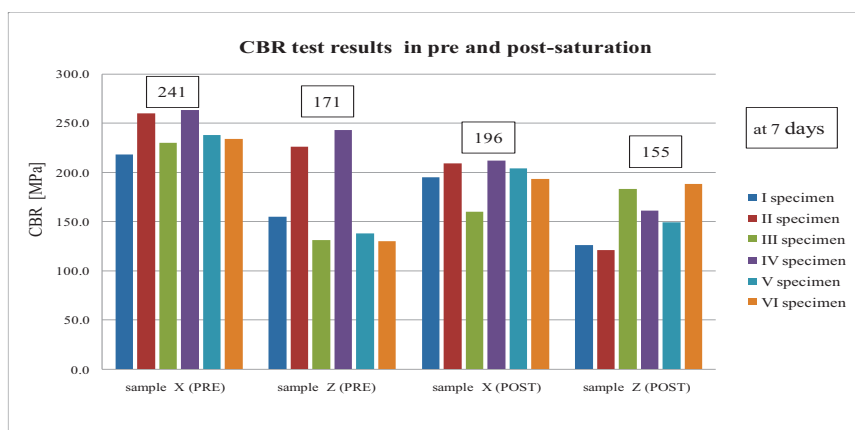


Table 4.21. Comparison between results of CBR test for specimens X and Z.

4.7.2. Qualification of the bound mixtures

A hydraulically bound mixture (HBM) can be defined as a mixture comprising an aggregate with a controlled grading and one or more hydraulic binders that have been mixed together using a technique that produces a homogenous mixture.

In this paragraph the two bound mixtures J and K, respectively obtained from the unbound one X, Z with addition of Portland cement 42.5 (1.25%) and fly ash (1.25%), have been mechanically characterized to assess its use in foundations and road bases construction.

The same unbound mixtures were blended with a percentage of cement equal to 2.5%, that is with no use of recycled fly ash as binder, to assess its influence on the mechanical performance. Such sample were analyzed only with tests at 7 days.

In the first analysis was verified compliance of the granulometric distribution with the reference ranges for bound mixtures of Autostrada del Brennero, Autostrade Venete, ANAS, the Autonomous Province of Trento and the Tuscany Region.

It has been defined an optimum moisture content equal to the one of the respective unbound mixtures with the addition of a percentage point of water for cementitious binder hydration.

The analysis work on the mixtures has been performed through the following tests:

- California Bearing Ration CBR to determine the mechanical strength , not routinely used to bound mixtures, but made just to have a comparison with the unbounded one;
- Not confined compression (CELL), in accordance with the European Standard EN 13286-41;
- Indirect tensile strength TI, according to the UNI EN 13286-42;

All tests were performed on saturated samples cured in air for 7 days (Table 4.22).

Table 4.22. Composition of the bound mixtures

Mixture	Aggregates	Binder
J	50% A, 50% B (X)	1,25% Cement425
K	70% B, 30% E (Z)	1,25% Cement 425

4.7.2.1. Grading curve analysis of the bound mixtures

The grading curves analysis of the three selected mixtures, in accordance with the granulometric range of the main specifications is reported in the following figures 4:21 and 4:22; The curve of the mixture in question is plotted in green

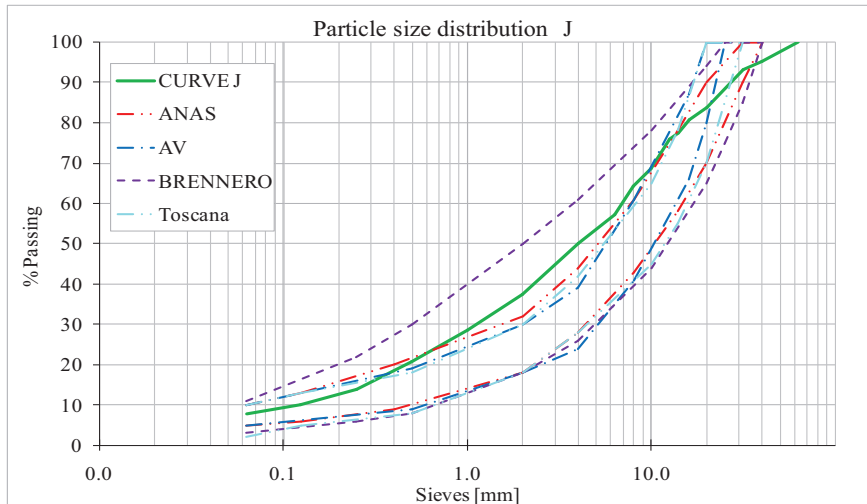


Figure 4.21. Grading curve of bound mixture J.

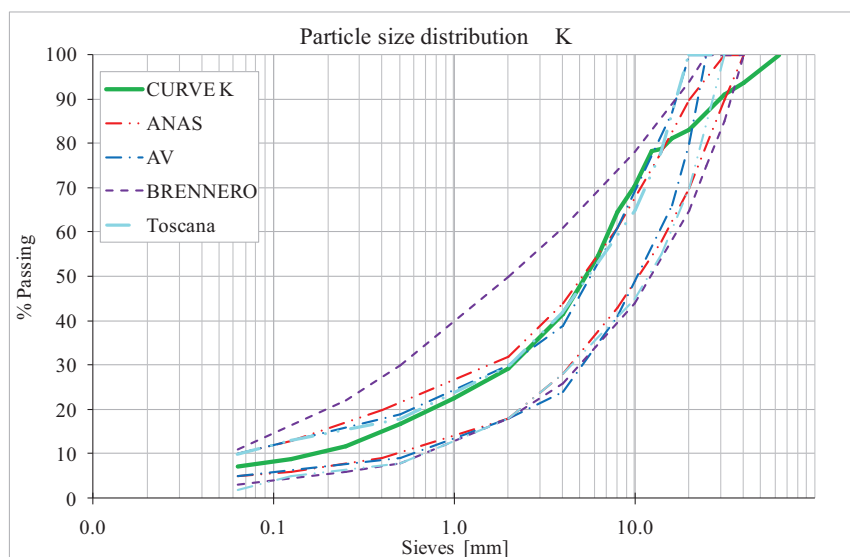


Figure 4.22. Grading curve of bound mixture K

The grading curves of mixtures J and K are well graded and in accordance with the reference granulometric range.

4.7.2.2. CBR test for the bound mixtures

As for unbound mixtures, the test was performed on six specimens per mixture and the

average values was adopted. In Table 4,24 and 4,22 the figure show the results obtained.

Table 4.23. CBR final results on specimens at optimum moisture content.

CBR PRE-SATURATION (7-day curing)				
	Mixture J	Mixture K	Mixture J	Mixture K
W [%]	11,8	11,4	11,9	11,4
CBR [%]	480	332	621	355

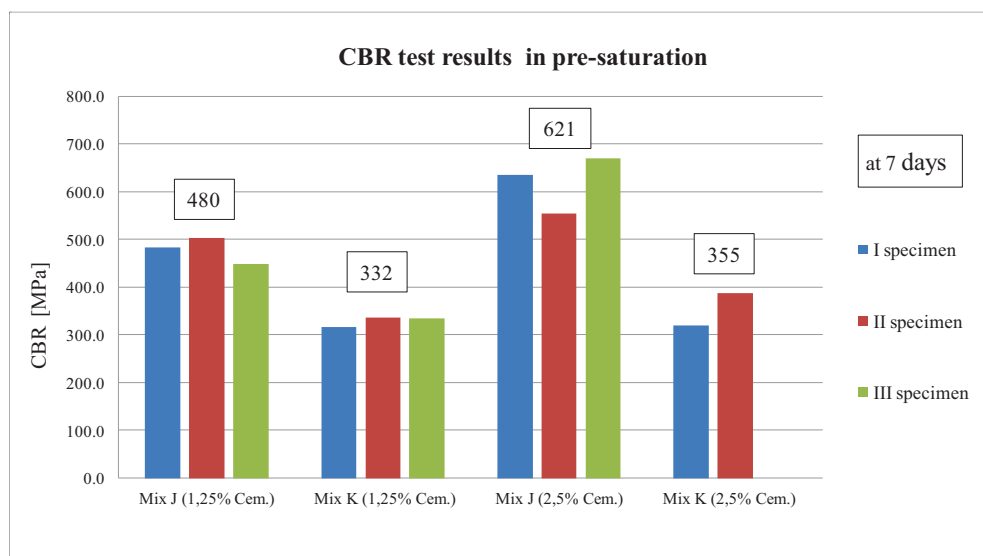


Figure 4.23. CBR test results.

The addition of Portland cement and fly ash in the unbound mixtures X and Z previously analyzed, increases by almost double the CBR values of mixtures. This test is not expected by specification for bound compounds but allows a comparison to assess the cementitious binder effectiveness compared to the unbound mixture.

The same tests were carried out after 28 days of curing on the three samples, but not for the specimens containing only Portland cement. The results are reported in table 4.25.

Table 4.24. CBR test results of specimens at 28 days of curing

CBR PRE- SATURATION (28 day-curing air)		
	Mixture J	Mixture K
W [%]	11,8	11,4
CBR [%]	495	402

We note an increase in values of CBR values of both the mixtures following the

maturation of the cementitious binder.

4.7.2.3. Compressive strength of hydraulically bound mixtures

The test was performed according to the UNI EN 13286-41 CNR BU 29/72. It specifies a method for the determination of the compressive strength of hydraulically bound mixtures specimens. This standard applies to specimens made from either laboratory or production mixture with a maximum aggregate size of 31,5 mm.

In accordance with this, compressive strength testing was undertaken on cylinders of a 2:1 or 1:1 height to diameter ratio (H:D) (shown in Figure 4.24).



Figure 4.24. compressive strength test on on samples of bound mixture.

Specimens were subjected to a continuous and uniform loading so that failure occurred within 30 to 60 seconds of the test commencing. Results outside this period were discarded. The strength datasets were expressed in MegaPascals (MPa).

As for unbound mixtures the test was performed on six specimens for each mixture and average CELL value was adopted. In this case the test was performed on both the samples with and without fly ash, to evaluate the influence of this on the mixture performance. The results of the vertical compression tests with free lateral expansion have been reported in table 4.26.

Table 4.25. final results of the CELL test on the specimens at optimum moisture.

compressive strength test at 7 days				
	Mixture J	Mixture K	Mixture J	Mixture K
W [%]	11,9	11,4	11,9	11,4
Compressive strength [MPa]	2,86	2,42	3,46	3,65
Displacement [mm]	3,41	3,29	3,75	3,18

The specifications require a deformation modulus including between 2 and 3,5 therefore

both the mixtures J and K fulfill the requirements.

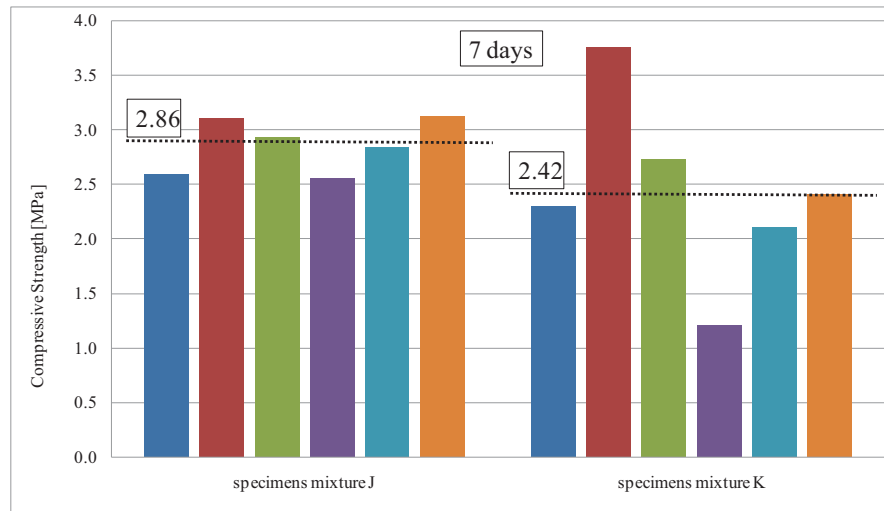


Figure 4.25. Results of CELL test on the specimens with 1,25 % of fly ashes.

4.7.2.4. Indirect tensile strength of hydraulically bound mixtures

Indirect tensile strength test procedures is described in UNI EN 13286-42.

A cylindrical specimen is loaded diametrically across the circular cross section. The loading causes a tensile deformation perpendicular to the loading direction, which yields a tensile failure. By registering the ultimate load and by knowing the dimensions of the specimen, the indirect tensile strength of the material can be computed.

the test requires specimens of a minimum H:D ratio of 2:1. The exact minimum height to diameter ratio is a function of the maximum aggregate size and specimen diameter. (figura 4.24).



Figure 4.26. Mixed specimen loaded on equipment.

The values of IDT strength may be used to evaluate the relative quality of cementitious mixtures in conjunction with laboratory mix design testing and for estimating the potential for rutting or cracking.

The results, averaged on six samples, have been reported in table 4.26. Also the tests accomplished on three specimens with 2.5% of cement are shown.

Table 4.26. Final results of ITS test of specimens at optimum moisture at 7 days.

Indirect tensile strength at 7 days				
	Mixture J 1,25% fly ash.	Mixture K 1,25% fly ash.	Mixture J 2.5% Cem.	Mixture K 2.5% Cem.
W [%]	11,9	11,4	11,9	11,4
Indirect Tensile	0,31	0,21	0,49	0,33
Displacement [mm]	0,82	1,02	0,77	0,62

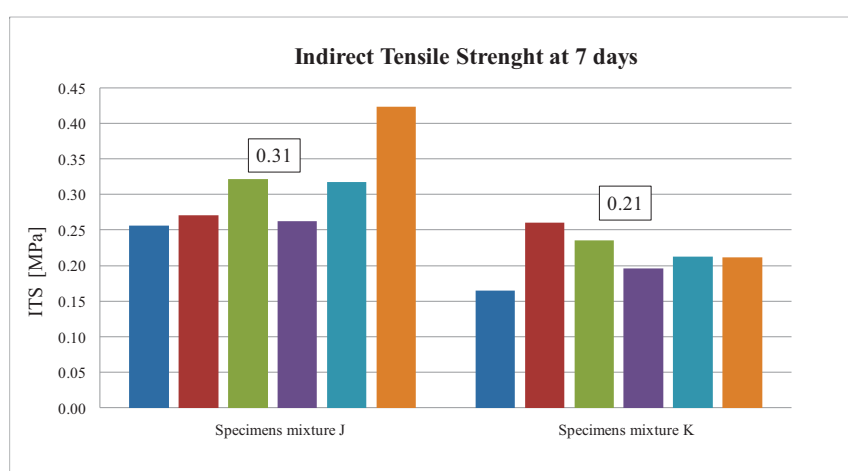


Figure 4.27. Final results of IS test on samples with 1,25% of Cement and 1,25% of fly ashes

The specifications require strength values comprised between 0.25 and 0.35 MPa, therefore, it can be noted that the mixture J responds to specifications requests, while for the mixture K the requirement is achieved only for the blend linked to 2, 5% cement. The same tests were carried out after 28 days of curing. The results are reported in table 4.27 and visible on figure 4.28

Table 4.27. ITS test final results at 28 days of specimens .

Indirect Tensile Strength at 28 day-curing		
	Mixture J 1,25%Cem. 1,25% Ash	Mixture K 1,25%Cem. 1,25% Ash
Indirect Tensile Strength [MPa]	0,35	0,28
Displacement [mm]	0,97	0,73

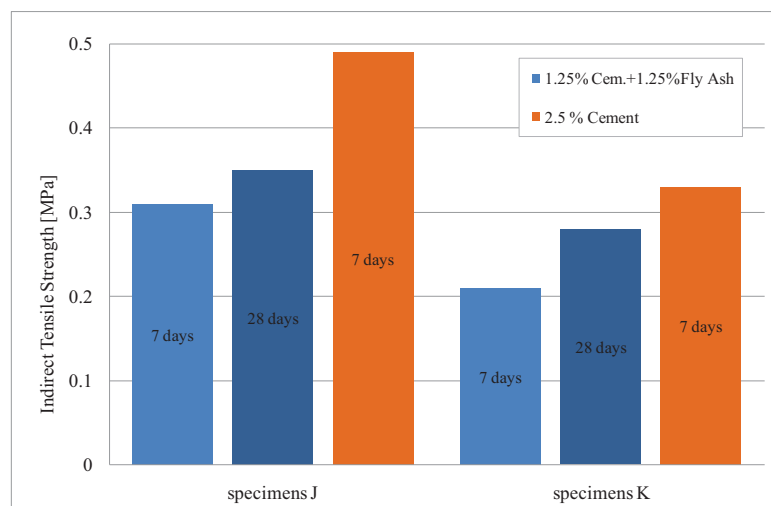


Figure 4.28. Average final results of ITS test at 7 and 28 days (this last only for specimens with fly ashes)

In particular, considering the gap $0,25 \div 0,35$ MPa as reference values to 7 days for indirect tensile test, we see that only the mixture J fully abide by the specification, while the mixture K needs a greater curing period to meet the requirements imposed on indirect tensile strength as can be seen from Figure 4.27.

As regards the results of the indirect tensile test at 28 days, the test values also meet the requirements imposed by the specifications, which foresees a range from 26 to 50.

Chapter 5

Test Field & Data Analysis

5.1 Premises

This chapter focuses on the test field setup, the implementation phases, strength-based in-situ testing and analysis of the EVIB value along all the layers of the field during compaction tests performed in Continuous Compaction Control (CCC).

5.2 The Test field

A test pad was constructed in an aggregate quarry provided by Concave in September 2012 at Trebbo di Reno, Bologna; as shown in Figure 5.1.



Figure 5.1. Plan of the mining area and location of the tests field .

The construction of a full-scale experimental field has several purpose briefly listed:

- To evaluate under real field conditions the bearing capacity characteristics of waste materials object of study arising from construction and demolition (C&D) , in single and double layer.
- 2) To understand the optimal conditions of C&D waste uses in the construction

of compacted base or subbase.

- 3) to evaluate the effectiveness and reliability of measurement instruments used to estimate pavement structural capacity, and their iteration

The field test simulates a 10 x 30 m road section consisting of:

- a subgrade lift necessary to obtain a homogeneous laying surface
- An unbound materials lift (X and Z, respectively referred to as M1 and M2 for all subsequent analyzes)
- A second one of bound materials (J and K, called M3 and M4) has been laid out.

Figure 5.2 shows the distribution of materials: if the subgrade is uniform, layer 1 is divided into two subarea while layer 2 should preferably be analyzed into quarters; therefore must be considered, for this latter, four different types of fields were constructed which allows the direct performance comparison of bearing capacity under differing conditions.

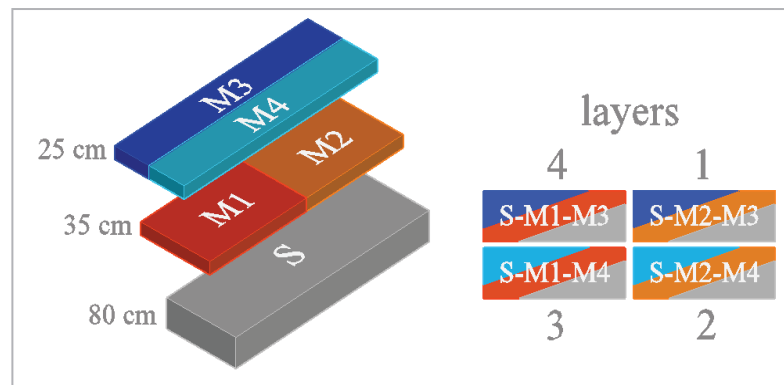


Figure 5.2. stratigraphy of the field tests.

5.2.1 Constructing the Embankment

The embankment was constructed to an approximate total final height of 1,4 m, by compacting three thick lifts.

The subgrade is a layer of reclaimed material (70-80 cm) consisting of virgin natural material of class A1 (UNI 10006) with good mechanical properties and bearing capacity.

The unbound materials M1 and M2 (X and Z) were laid out on the subgrade with a thickness of 30 cm (layer 1). The laying of M1 and M2 divides transversely the field in two areas 15m long and 10m width.

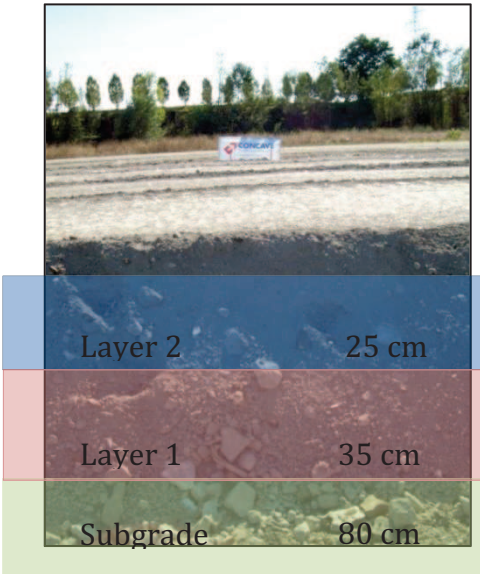


Figure 5.3. Section of the embankment and relative thicknesses of the layers.

Using the Bomag compactor, each lift was compacted in a series of passes using four side-by-side lanes (the roller width was 2.1 m , the test pad width was 10 m, which left approximately 15 cm of overlap at the edges of each compacted soil “lane”).

For each lift, between 4 and 7 compactor passes were performed to achieve the desired compaction level.

Before beginning construction, the designated area was marked by building a non-reinforced concrete curb in proximity of the centreline, at the level of the subgrade, parallel to the shorter side; Its function was to clearly separate the two halves of the field and to assess and understand the settlement caused by compaction and how the presence of underlying rigid sections may influence stiffness modulus measured on the overlying layers.



Figure 5.4. Position of the concrete curb.

Before beginning construction, the designated area was marked by installing grade stakes at approximately 3.0 m intervals (also in correspondence of the concrete curb) on either sides of the construction pad.

5.2.2 Subgrade

The subgrade is a reclamation lift consisting of material with good mechanical characteristics and bearing capacity; The purpose of such a layer is to prevent the materials of the underlying layers, already present on site of unsuitable mechanical characteristics (or not notes), influencing the testing of the materials that are object of study. Even on the subgrade were however carried out the bearing capacity characterization tests were carried out on the subgrade for the constituent layers of the embankment in order to qualify the materials.

The reclamation operation has resulted over a first stratum of native soil to an average thickness of 70-80 cm and a second phase of spreading of good quality material (gravel) resulting in satisfactory homogeneity, in terms of load-bearing capacity. The gravel material has been placed with a cross fall of 2% to allow for the rainwater runoff.

To facilitate the localization of the tests in the field it was decided to divide the field into four quarters (I, II, III, IV) and each quarter split in half (figure 5.6). each sub areas is identified by a roman numeral (I, II, III, IV) preceded by the letter S indicating the subgrade.

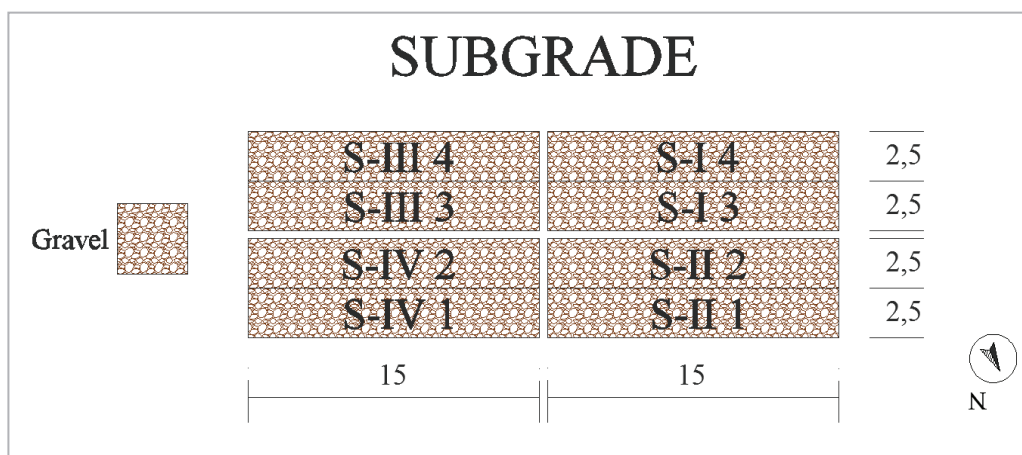


Figure 5.5. Division of the subgrade in areas and subareas.

5.2.2 Layer 1 (Unbound materials)

The unbound materials M1 (50% Concrete - Mixed Recycled 50%) and M2 (70% Mixed Recycled - 30% AG Matrix) have been placed on the subgrade with a thickness of approximately 35 cm, after the compaction, . Spreading took place, as shown in Figure 5.6, taking care to make a clear division between the two materials to half of the long side corresponding to the position of the concrete curb. The two symmetrical areas are then exactly rectangular 10 m wide and 15 m long..

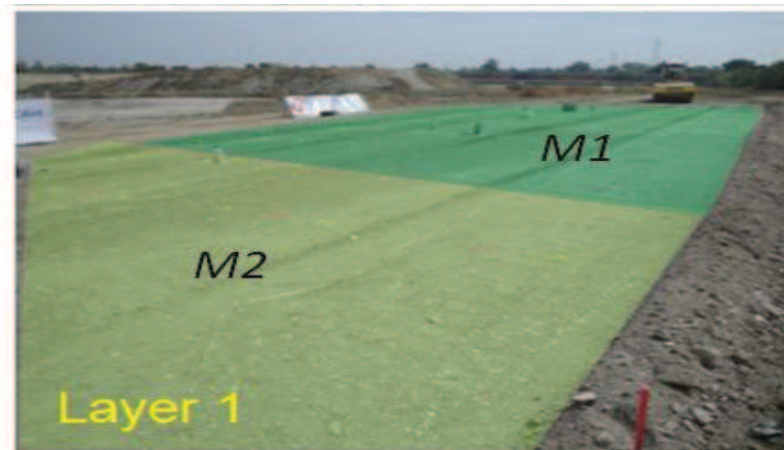


Figure 5.6. Disposition of the two unbound materials.

The compaction was carried out along four parallel lanes 30m long and 2.5m wide. Every subarea of field is represented by a number (1,2,3,4) preceded by the letter "L1" (layer 1), as well as each line.

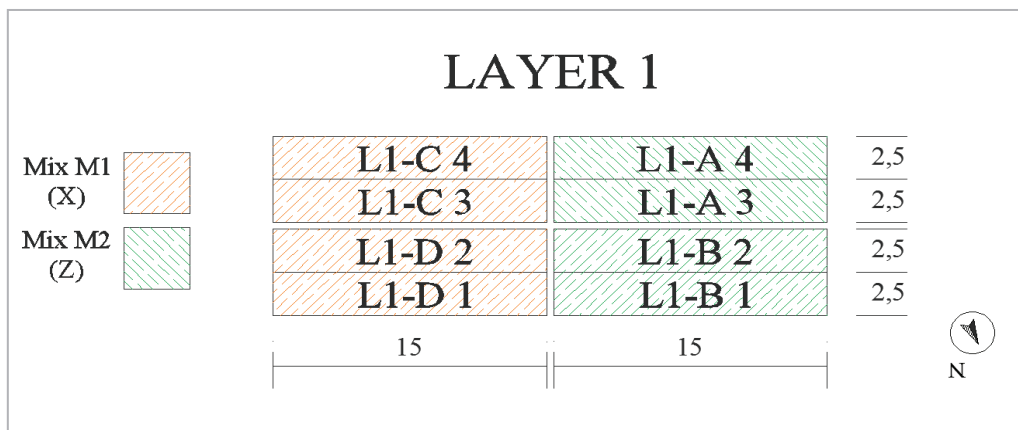


Figure 5.7. Division of the layer 1 in areas and subareas.

5.2.3 Layer 2 (bounded materials)

The bound materials M3 (M1 mixture added with binder) and M4 (M2 mixture added with binder) were spread above the unbound materials with a compacted thickness of 30 cm.

The spreading took place, as shown in Figure 5.8, taking care to make a clear division between the two materials at the middle of the shorter side for the whole length of the field. The two areas are then exactly rectangular and symmetrical of dimensions 15 x 30 m.



Figure 5.8. Disposition of the two bound materials

Every subarea is represented by a capital letter between A and D preceded by the letter “L2” (Layer 2), then each lane is identified by a number between 1 and 4. Four combinations then occur (shown in the figure 5.9, respectively from the bottom left, clockwise): M1-M4, M1-M3, M2-M3 and M2-M4.

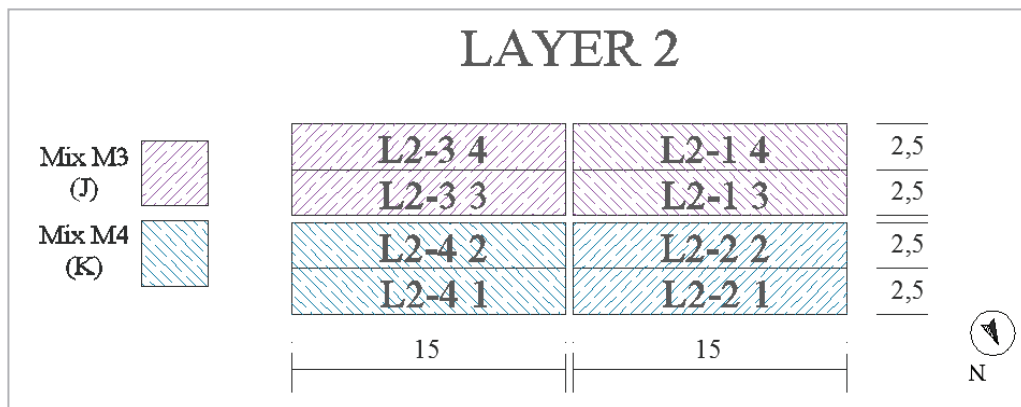


Figure 5.9. Division of the layer 2 into areas and subareas.

5.2.3 Equipment .

Several methods of construction have been employed for the preparation and construction of the test field as shown in Figures 5.10.



Figure 5.10. Construction and testing devices.

An excavator has been used to remove 70-80 cm of the native material then reclaimed; were then utilized to construct each lift Dump Trucks were used to transport the material from the plant to the site and to place fill for spreading by the on-site bulldozer. After spreading each lift, a water truck was driven through the test area as needed to adjust the moisture content of the fill material to achieve optimum compaction.

Upon completion of loose-lift material placement and moisture conditioning, each layer was compacted using a 15 ton heavy Bomag BW213 vibratory smooth drum roller, equipped with a BCM5 system. The roller drum was 2.1 m wide, and had an operating weight of 12.525 kg.

Compaction was performed by adopting a number of predetermined rolls for each lift and manually setting the amplitude vibration (0.7 mm or 1.9), at a vibratory frequency of 28-30 Hz in order to obtain, for that configuration of compaction (energy, thickness, humidity), the maximum possible densification of the placed materials, avoiding superficial decomposition phenomena.

In addition to the CCC measurements conducted during the mechanical compaction of materials, a series of deflectometric tests were performed through the use of Light Weight Deflectometer (LWD) equipments , in addition to density and moisture testing (Figure 5.11).



Figure 5.11. roller passes and test phases for each lift.

There are several types of LWD in existence around the world, and many prototypes have been developed. In particular, the LWD Good Practice Guide identifies two main classes, both used for measurements in the test field:

- Class 1 (C1): This equipment permits a variable drop height, and incorporates both a velocity sensor to measure deflection (also termed a ‘geophone’), and a load measuring sensor (load cell) for the recording of the time histories of the pulses under the cell (ASTM 2583-07).
- Class 2 (C2): is of the type with a fixed drop height, and incorporates an accelerometer based sensor to measure deflection (mounted rigidly within the middle of the bearing plate). It does not incorporate a load cell, and assumes a constant peak force on impact (TP BF-StB Part 8.3).

The employed device C1 includes a load cell and allows a specific load by setting the drop height depending on the type of layer investigated.

The device C2 adopted on our field requires a nominal peak force (calibrated by the manufacturer) equal to 7.07 kN for a mass of 10 kg, and 10.60 kN for one of 15 kg

heavy. Such forces are considered acting on the top of the plate, and it is assumed constant for the calculation of vertical pressures under the load cell.

The load pulse is applied with a semisinusoidal transient pulse length. The length of the device C2 has a period of about 16 to 18 milliseconds, while for C1 is approximately 28 to 30 milliseconds.

On the last day, thanks to support provided by the Bologna Department of Civil Chemical Environmental and Materials Engineering, a falling weight deflectometer (FWD) was also added to the in-situ testing methods that were used.

The (FWD) is a testing device used by civil engineers to evaluate the physical properties of pavement. FWD data is primarily used to estimate pavement structural capacity for 1) overlay design and 2) to determine if a pavement is being overloaded.

For each lift, 24 test stations were established at ≈ 3 m intervals along the centreline.

The phases of testing on the 3 layers were performed by following the same predetermined grid.

The layers were subjected to physical and deflectometric investigations to check the load bearing capacity. The tests performed on site, once the lift is compacted, are:

- Compaction and optimal moisture content test.;
- Grain size (with removal of material);
- Light Deflectometre Test with accelerometre (LWDz) e a geophone (LWDd);
- Tests with Falling Weight Deflectometre FWD;

The experimental tests have been performed on specific field stations as shown in the figures 5.12, 5.13, 5.14.

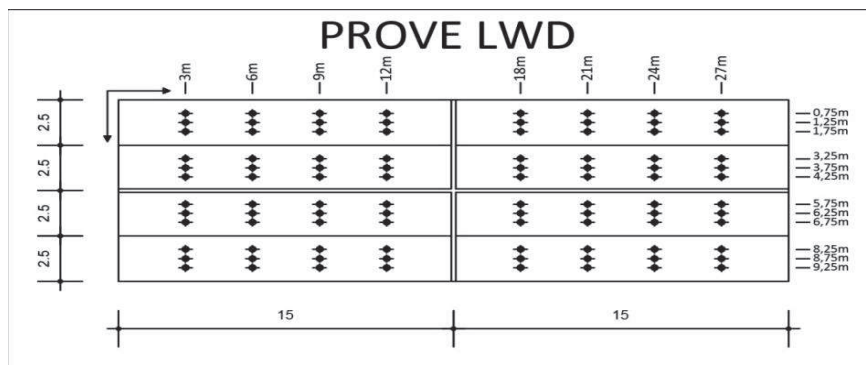


Figure 5.12. Spot stations of the LWD test

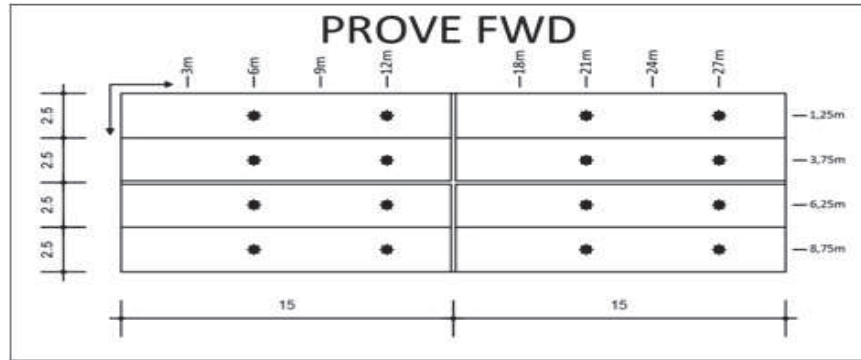


Figure 5.13. Spot stations of the FWD test

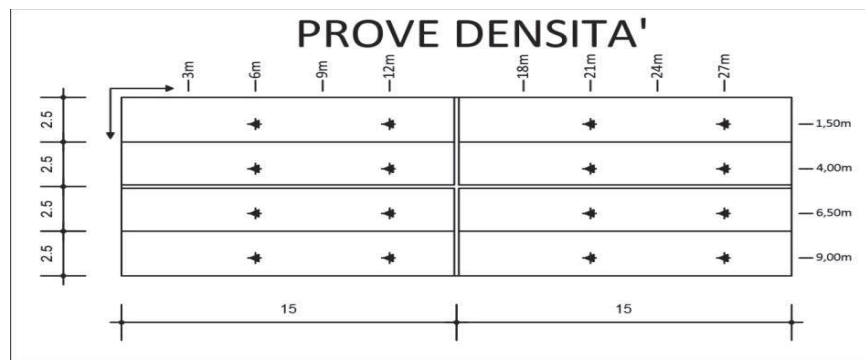


Figure 5.14. Spot stations of the in situ density test

5.3 Factors that may have influenced the measured data

Some significant natural factors had the potential to influence the in-situ test results and associated CCC measurements during the field study. Weather conditions were the first contributing factor, which caused variability over time with respect to the in situ moisture content of the soil. Daytime temperatures were in the range of 20° C during the study, which had the tendency to dry the soil over time.

Another factor which had the potential to impact the measured values was the existence of some cobbles and steel bars in the mixture material that could be a potential source of variation in the recorded data. Manual “rock-picking” was performed periodically in the fill area to try to remove these cobbles when they were encountered.

However, the potential presence of these types of rocks in the fill material should be noted, as they can influence the measured test results.

5.4 Data Analysis

The Aim of this analysis is the evaluation of the load bearing capacity of the mixtures and the monitoring of the degree of compaction achieved for each construction phase of the embankment, observed and analyzed from different points of view.

In particular, the homogeneity of the EVIB value over the entire field and the use of different roller vibration amplitude to investigate a different thickness of pavement has been evaluated, and the behaviour of different mixtures under investigation has been compared.

Given the vast amount of data to be analyzed, each diagram is identified by a standard model shown in figure 5.15: the three surfaces, in perspective view and divided into subarea, indicate the first three layers, and each quarter a configuration materials, while the planimetric figure indicates which lines or part of field the diagram refers to, allowing, in this way, a simple and immediate understanding of the area under examination.

For the example in figure 5.15, we are considering the II and IV subareas, of layer 2, in particular the whole lane 2

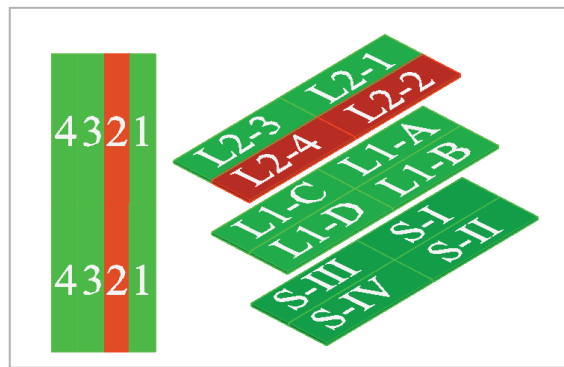


Figure 5.15. Standard model displaying the area and subareas.

The single-drum roller BOMAG, equipped by the Terrameter measuring system BTM, collected real-time Evib value during compaction in addition to the documentation of the number of passes, the vibratory frequency, the amplitude of the roller drum, and the speed of the roller. (figure 5.16)

It is therefore possible to create a graph for the Evib data against the distance with 10 cm precision with the help of mappings identifying the whole investigated area.

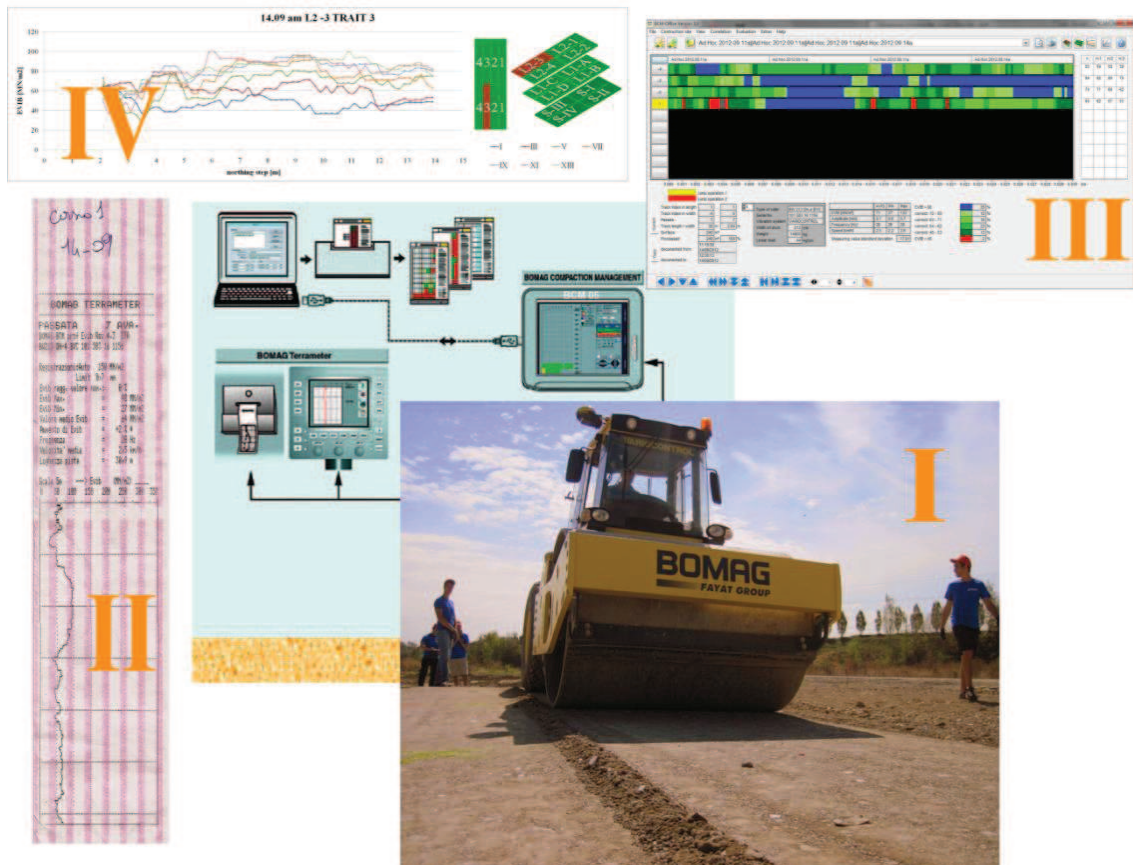


Figure 5.16. working phases: from the compaction to the data analysis.

In order to monitor the degree of compaction achieved by the material for each single pass, graphs correlating the average Evib value between consecutive compactor passes were created.

If the values between successive passes are similar, the average vibratory modulus approaches the line of 45 degree . The optimum compaction, understood as the maximum compaction degree attainable by material in those conditions of compaction, is reached when two consecutive passes do not record a change in value.

Due to the presence of the concrete curb in proximity of the centreline of the field and seen the possibility of contamination of the materials for the initial and final stretch of the field, these areas were not taken into account in the calculation of the average values of the quality analysis of the materials; In particular, the first two meters of the field were excluded, the last stretch (1 meter) and the area affected by the element (considered 14 to 17 meters) on all the passes.

An example of the accomplished "cleaning" work is visible in figure 5.17.

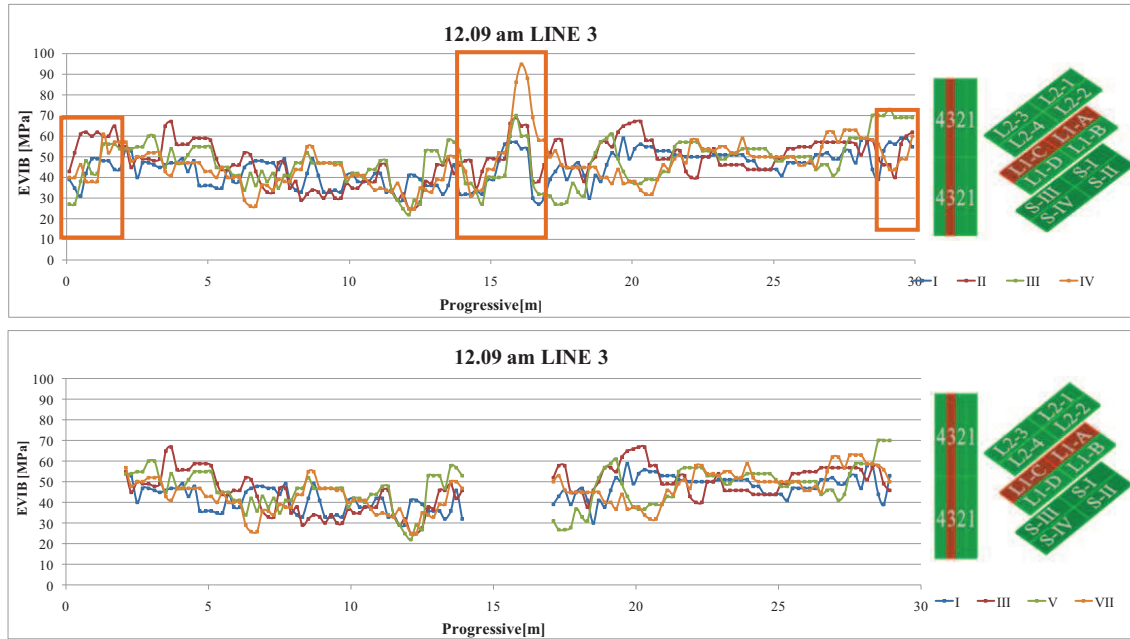


Figure 5.17. example of deregistration of "unreliable areas".

From here on, it was possible to analyze the field tests in several ways: the entire field, each quarter of the field (forth) and each half of a quarter (eighth).

5.4.1 Analysis of passes

The presence of more than one mixture employed for the lifts L1 and L2 did not allow a generalized analysis of the test field except for a comparison of results obtained from various compositions of mixtures used.

In the three day of test an amplitude of 0.7 mm (manual 2) was always applied in the morning, while also manual 5 (1.9 mm), and in sporadic cases, manual 7 (2.5 mm) have been used in the afternoon, to better understand the action in depth of the dynamic compaction.

5.4.2 Data analysis of the 11-09: layer S

Load bearing characterization tests of the material were performed even on the subgrade.

The diagrams and tables below give more keys of the EVIB measurement value on the whole subgrade. This investigations have been made primarily for subareas but it is considered appropriate to report the results of the entire field.

The diagram show the EVIB value in relation to the average distance between the four

passes is shown in Figure 5.18; A weak sections is clearly noticeable between 3m and 6m and 21m to 23 m of the field , weakness were also observed in some cases also for the upper layers, while the highest values are around 50 MN/m².

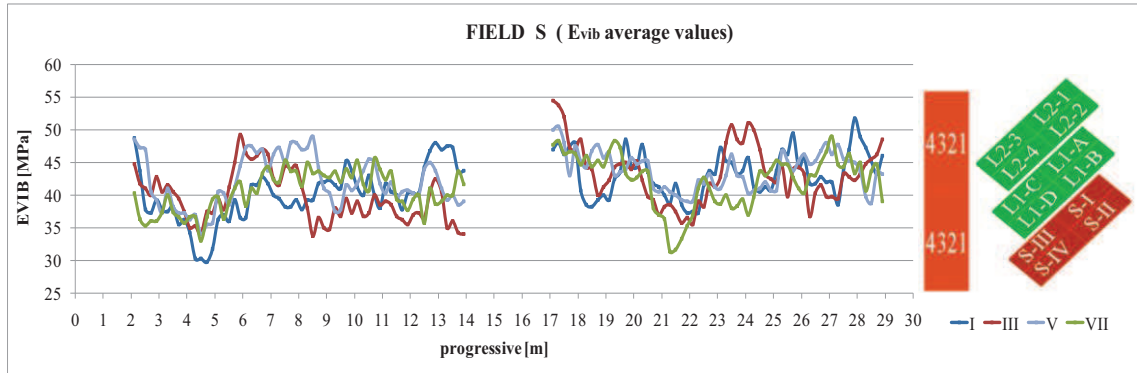


Figure 5.18. Evib average values for the whole subgrade S.

The comparison between the average values for each pass and the increments between successive module, is shown in the table 5.1. The field is examined at intervals of 3 m and the negative differences, highlighted in the table, show the zones in which the next pass results to have a "decompaction" effect .

table 5.1. Difference between consecutive passes along the subgrade

	Evib average calculated in the range Δ Y [MPa]				ΔEvib average calculated in the range Δ Y		
	Pass I	Pass III	Pass V	pass VII	I-III	III-V	V-VII
3-5 m	36.6	39.3	39.5	36.9	2.70	0.22	-2.58
5-8 m	39.0	44.1	44.8	41.5	5.12	0.70	-3.28
8-11 m	41.1	37.5	42.9	43.2	-3.58	5.45	0.31
11-14 m	43.3	37.3	40.9	40.1	-5.97	3.65	-0.87
17-20 m	43.5	46.2	46.1	44.9	2.73	-0.08	-1.23
20-23 m	41.2	39.1	41.6	38.2	-2.15	2.57	-3.37
23-26 m	44.3	45.8	42.8	41.3	1.43	-2.92	-1.50
26-29 m	44.5	42.5	44.7	43.9	-2.05	2.17	-0.74

	I	III	V	VII
Variance	7.867	13.215	4.871	7.665
Average	41.66	41.44	42.91	41.26

Both the table 5.1 and the figure 5.19 show a steady compaction degree between consecutive passes, with average values around 41.5 MPa;

In the comparison between the first and the last compaction, the EVIB value is even lower for the latter though with a difference of about 1%.

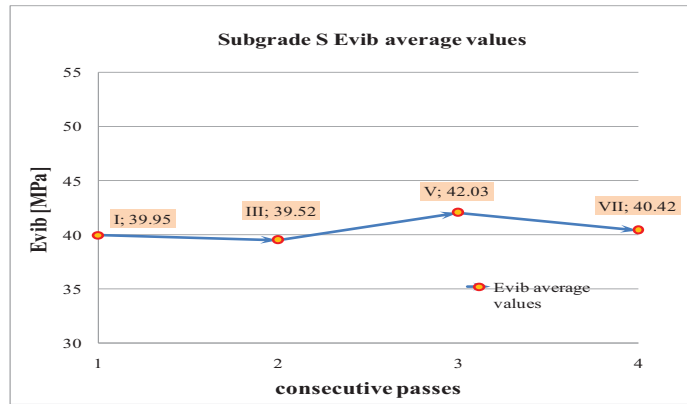


Figure 5.19. behaviour of the subgrade for the different passes

By comparing the passes it has been established that the achievement of the optimum compaction degree of the materials by the third pass with insignificant, if not counter-productive, effects for the following pass.

This behavior is also confirmed by the compaction path on the subgrade, shown in Figure 5.8, where the last point is placed under the line of 45 ° to demonstrate the ineffectiveness of the last dynamic compaction.

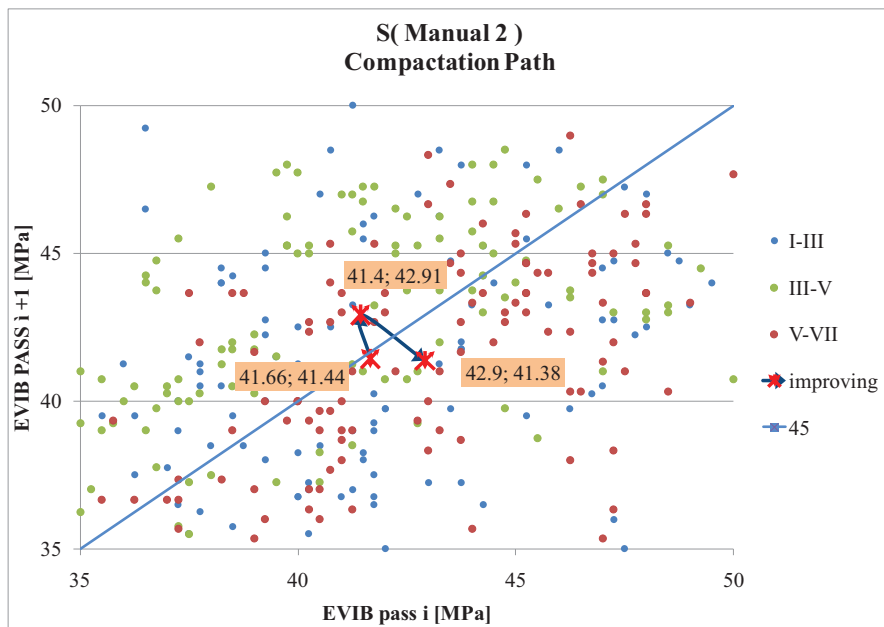


Figure 5.20. compaction path of the substrate

5.4.3 Layer L1 (mixtures M1 and M2)

The unbound materials M1 and M2 have been applied with thickness, after compaction, of about 30 cm (layer 1). The spreading was carried out similarly to the previous layer, taking care to make a clear division between the two materials in correspondence of the concrete curb.

On the application of the two mixtures, laying on two symmetrical areas 10m x 15 m in size, it was deemed to evaluate them separately: the first area consists two subareas of the field named L1-C and L1-D composed by the mixture M1 and the second half of the field by L1-A and L1-B with the laying of the mixture M2.

The measured values along the layer L1 in all its extension is shown in Figure 5.9: the first part (mixture M1) exhibit a decrease of the compaction degree towards the center of the field, an opposite behaviour compared to the other half of the field (composed of the mixture M2).

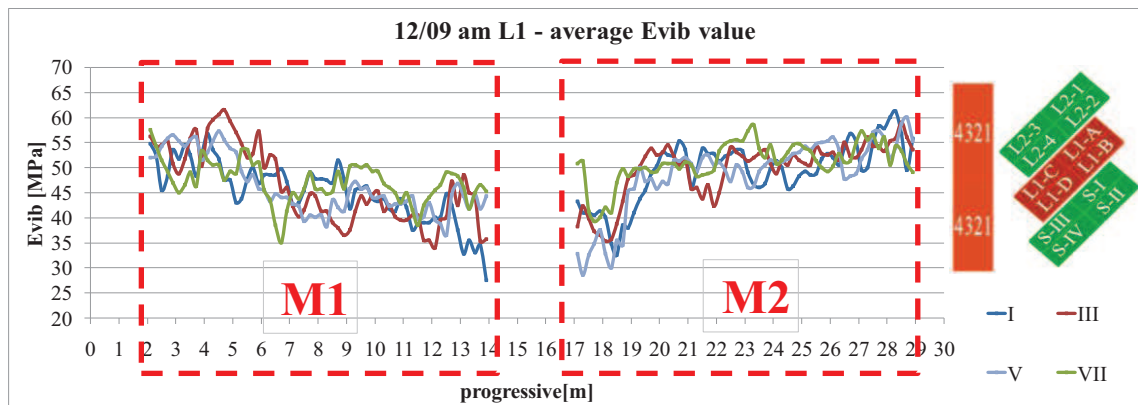


Figure 5.21. Evib average values for the whole layer L1.

The Table 5.2 and the figures 5.22, 5.23, deal with the first quarter of field where the unbound mixture shows similar behaviour with respect to the subgrade, with average bearing capacity of around 46 MPa and a total increase of only 2 MPa. Between the first and the last pass. However variances much higher in modulus than those concerning the subgrade are deduced from the table 5.2, indicating a more pronounced dispersion of values around the mean value.

table 5.2. difference between consecutive passes for the substrate

	Evib average calculated in the range ΔY [Mpa]				Δ evib average calculated in the range ΔY [Mpa]		
	pass I	pass III	pass V	pass VII	I-III	III-V	V-VII
3-5 m	51	56	55	50	4.18	-1.03	-4.62
5-8 m	47	49	45	46	2.03	-4.15	1.35
8-11 m	45	41	43	47	-4.22	2.35	4.07
11-14 m	38	40	42	45	2.62	1.98	2.72

Variance	32.746	52.352	31.928	4.633
Average	45.25	46.40	46.19	47.07

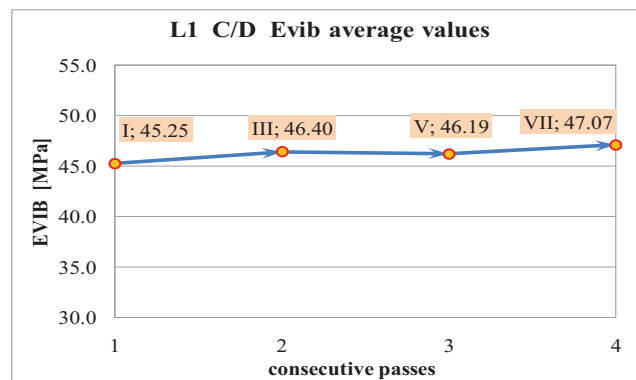


Figure 5.22. behaviour of the subgrade along with the different passes

The compaction path for the first half of layer 1 reinforces the analysis made right now; the three comparisons differ very little among them remaining at around the line of 45 °

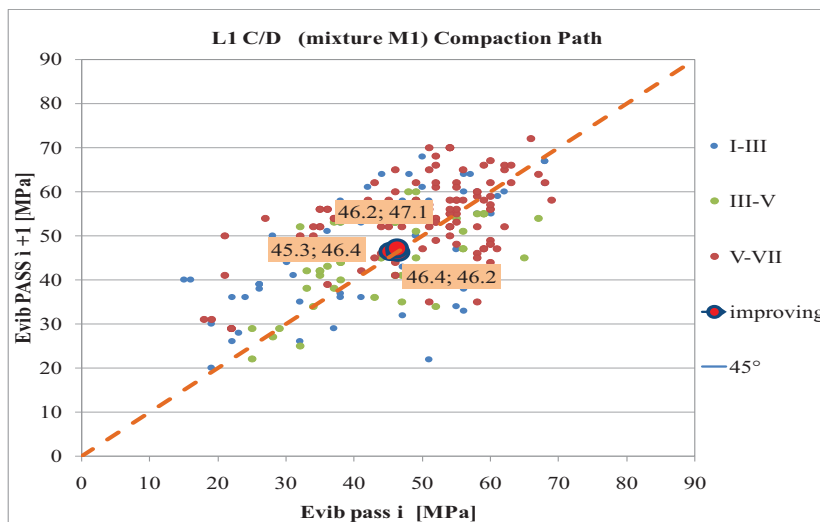


Figure 5.23. Compaction path of the area L1 C/D

The behaviour of the mixture M2 is similar to that one to mixture M1: also in this case

the optimum compaction is already achieved with the first two passes and the total increase is only 2 MPa for which the figures 5.24 will also be respectively characterized by an almost flat path for the average EVIB values and figure 5.14 by a compaction path with characteristic points very close to each other.

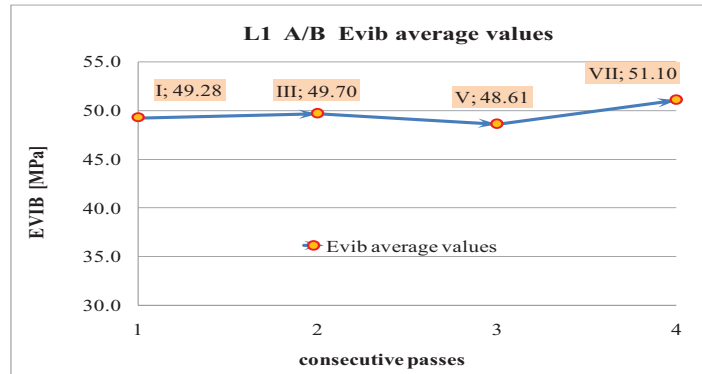


Figure 5.24. Behaviour of different passes for the L1 A/B area.

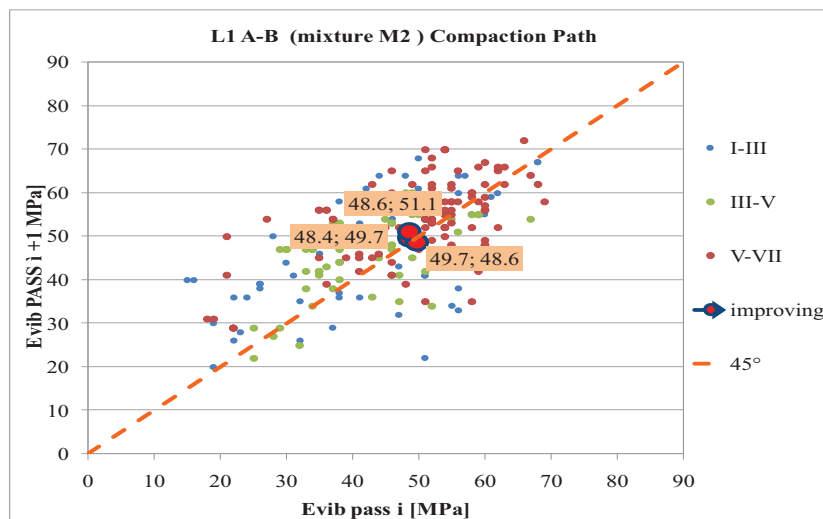


Figure 5.25. Compaction path of the area L1 A/B

5.4.4 Layer L2 (mixture M3 and M4)

The bound mixtures M3 and M4 were spreaded over the unbound mixture with a compacted thickness of 25 cm (layer 2).

The two symmetrical areas, 30 long and 5 m wide, obtained by longitudinally placing the mixtures along the centreline of the field, entail, when the construction took place, four different lift configurations already indicated in the introduction of this chapter.

Figures 5.26 and 5.27 show the average EVIB values for the two lanes composed by different mixtures in order to have an overall view of the whole field and a simple

comparison between materials.

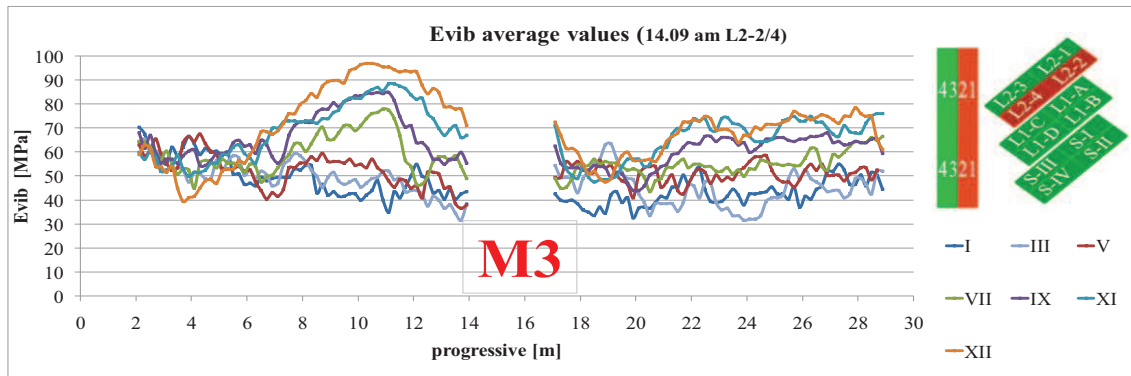


Figure 5.26. Evib average values for the half of field L2-2/4 (mixture M3)

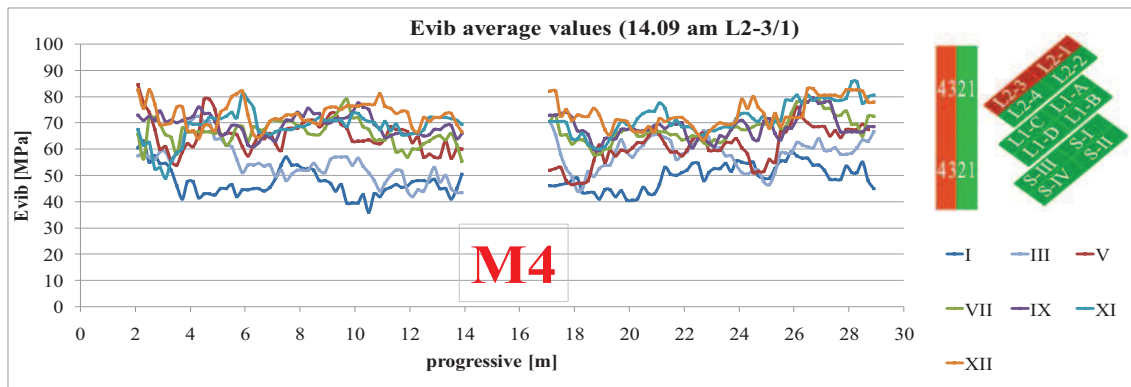


Figure 5.27. Evib average values for the half of field L2-3/1 (mixture M4)

At first glance, the mixture M3 seems to have greater importance in particular for the last pass but, beside to show the highest values, with peaks value above 90 MPa from 9 to 10 meters of field, also have greater instability with intervals that reach 50 Mpa; For half of the field L2-2/4 it is evident how the latter passes worsen the degree of compaction of some parts of the field, in particular between 2m and 5 m and 18m and 20m. The analysis of the various compaction paths for the four field parts, offers a clearer view of the layer 2: it denotes a sharp difference between the internal and external lanes of each area for both the employed mixtures, with an increase in stiffness of the structure in the central areas more confined (lanes 2 and 3) with respect to the outer lanes placed with the same materials. In order to prove as set out above , Figures 5.15 and 5.16 show compaction paths for separate lanes of the same area, in this case for the area L2-1.

The path to the lane 3 appear regular with a gradual approach to the 45 degree line and

a more and more reduced stiffness growing between consecutive passes, demonstration of the approach to optimum compaction.

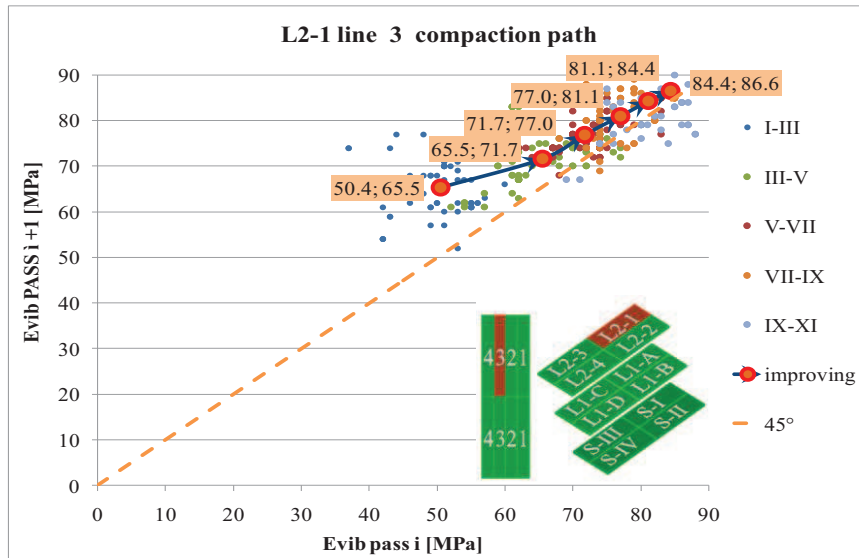


Figure 5.28. Compaction path per half of lane 3, L2-1 subarea.

The same can not be said for the outer lane (lane 4) with a compaction path confused and a general increase of stiffness less pronounced.

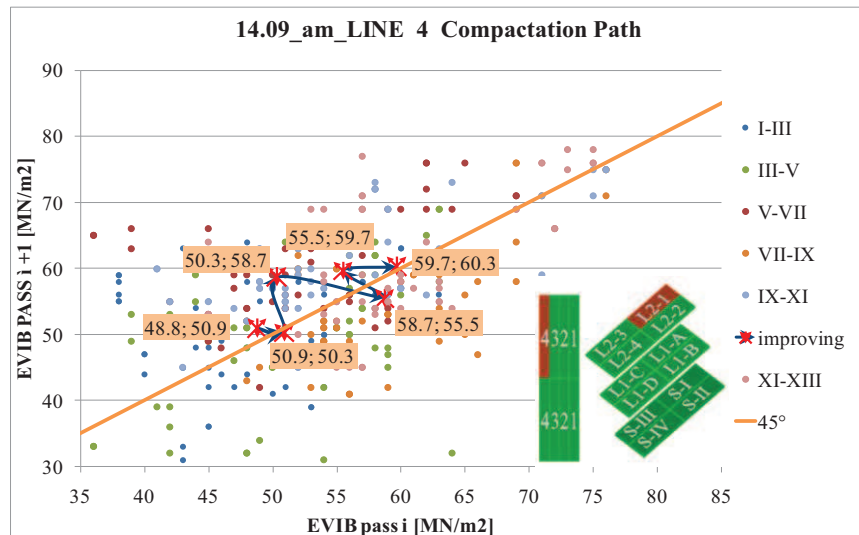


Figure 5.29. Compaction path for half of lane 4, L2-1 subarea.

Then the two figures show very similar initial EVIB modulus, around 50 MPa, but paths that differ with the achievement of the appropriate bearing capacities of a road coarsebase exclusively in the central field areas: above 80 MPa for the inner lane and even 60 MPa for the external one.

This leads to disregard the lateral lanes in the analysis of optimal mechanical capacity for the mixtures realized and to make a careful confinement of the embankments about the use of such mixtures as road pavement material.

The same behaviour is evident for all the four areas of the layer 2, with a different bearing capacity between the central and the lateral lanes ; Such behaviour is not found in the first pass and is highlighted with increasing stiffness of the structure.

It is therefore considered sufficient to show, through the figures 5.30 and 5.31, one of the two areas relating to the mixture M3, in particular the area L2-3.

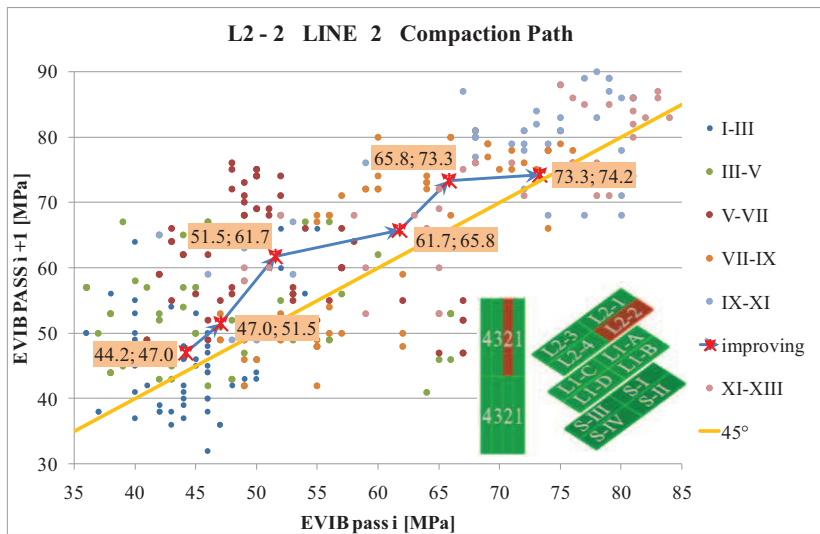


Figure 5.30. Compaction path for half of lane 2 , L2-3 subarea

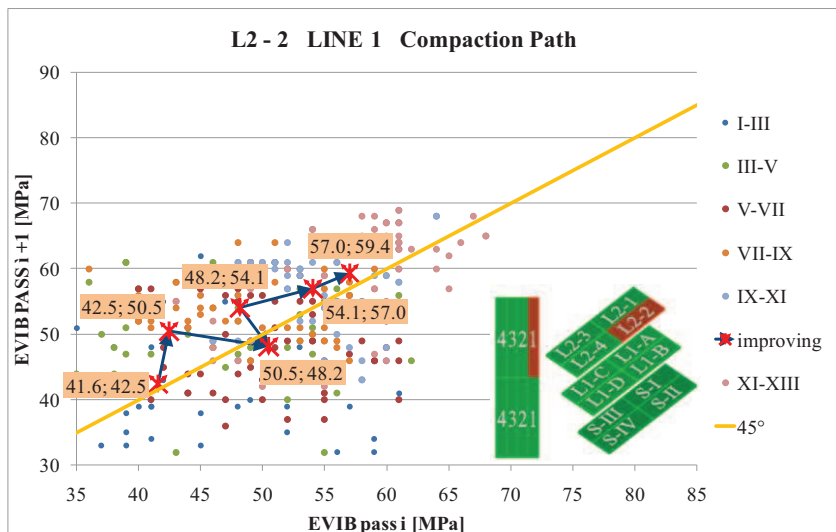


Figure 5.31. Compaction path for half of lane 1 , L2-2 subarea

Regarding the validity of the number of passes it can be said that the optimum compaction is roughly achieved at the seventh roller pass to the center lanes while the same is not valid for the lateral ones whose trend of the compaction paths (CPs) shows an optimum value already at the third pass and negative effects for the successive pass .

5.5 Mapping of Evib values

For the study of the homogeneity of bearing capacity through the vibration EVIB value analysis, we proceeded to the creation of two-dimensional maps of the surface characterized by colours indicating the compaction degree of the surface through the use of the software Surfer;

The two sensors applied to the Bomag drum detect a frequency of EVIB measurements every 10 cm for each lane 2.1 m wide; the data set is adequately presented via Excel spreadsheets; This allowed the interpolation of the values by Surfer and the construction of adequate mappings .

These maps have been created for all the roller passes of the backfill and take into account the whole field, including the area corresponding to the concrete artefact and the initial and final portion, previously excluded for the purposes of data analysis.

Each mapping will also be accompanied by tables showing the mean of EVIB values

The three lifts are first individually analyzed and then an overall view of the entire test field has been given.

5.5.1 .Layer L2

The mapping of EVIB values, measured by BOMAG Single drum rollers over the entire lift L2, shows a stiffness increase of the whole field to a succession of the roller passes, especially for the two center lanes (figure 5.32).

Those latter in fact show a more marked increasing compared to the outer lanes, and final values ranging from 74 to 86 MPa, over which a greater sensitivity in regard to the presence of the artefact along the centreline, already visible from the second passage of the roller in dynamic mode .

The influence depth in manual 2 is therefore higher than 60 cm in thickness made of the configuration L1/L2 (30 +25).

Noteworthy is the anomaly mentioned above, about the first part of the pad: as the map

denote, the stiffness of the considered area is initially higher than the rest of the field, and then it slowly reduces with the successive passes, probably because of the movement of the backfill material towards the outside of the field during the passage of the rubber wheels and the vibration of the roller besides the slight initial slope, with consequent thickness reductions.

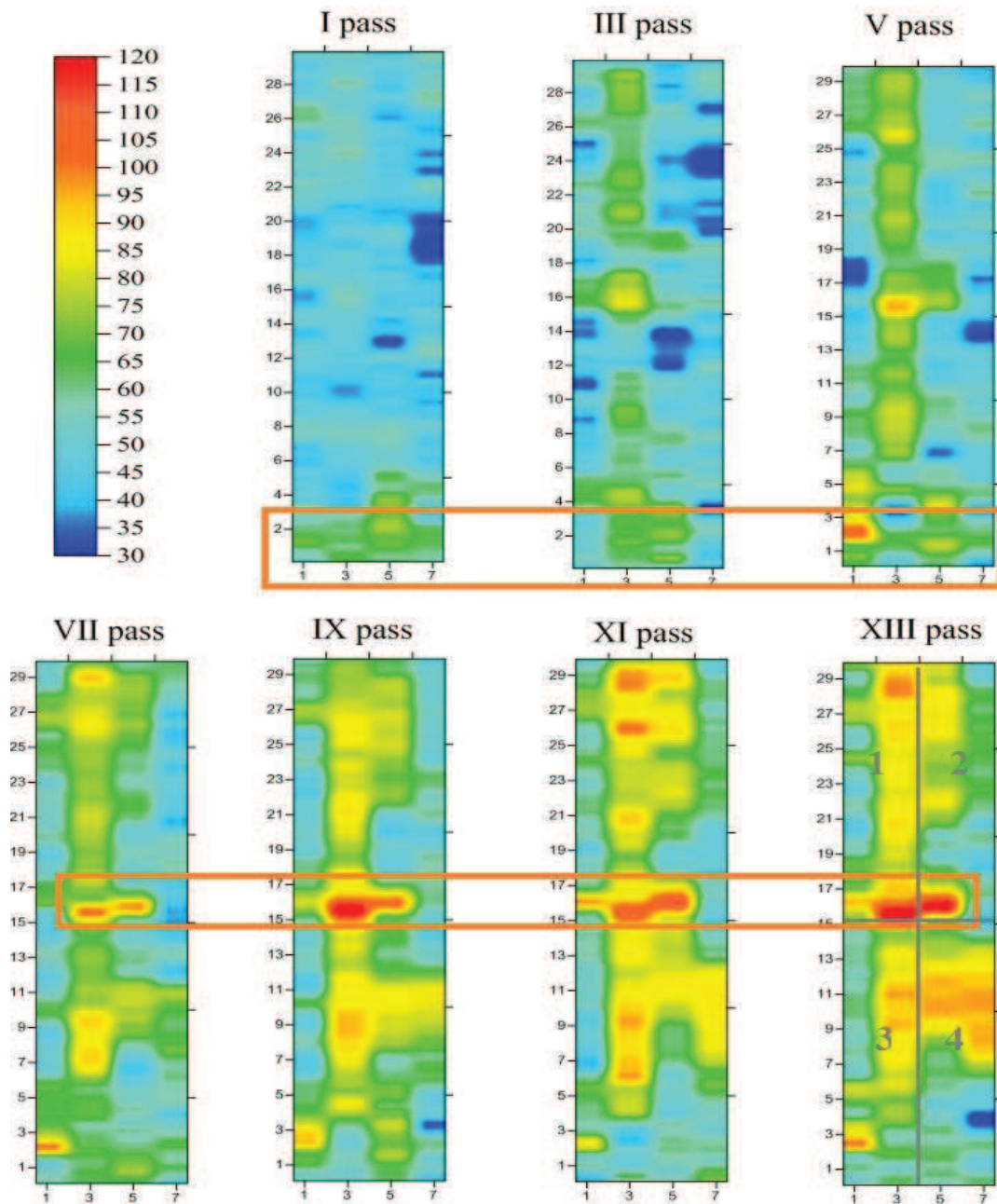
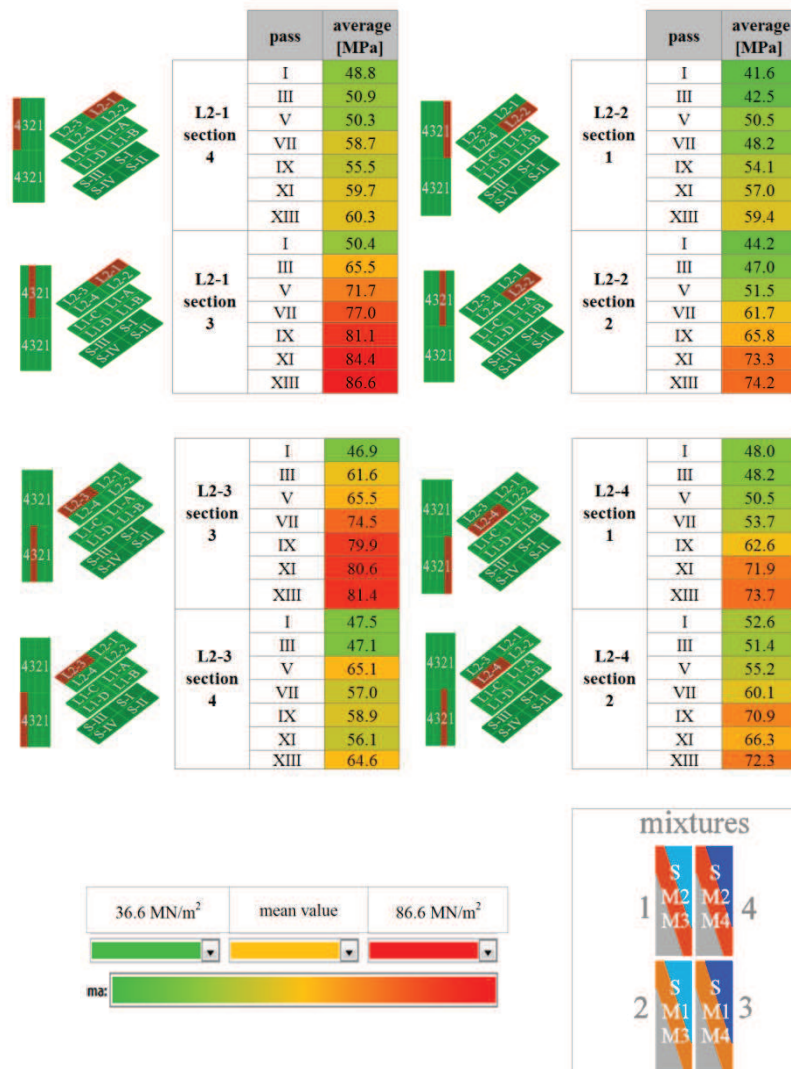


Figure 5.32. Evib mapping of the layer 2

Table 5.3 deepens and simplifies the general reading of the layer 2:

table 5.3. E_{vib} average values of the eighth of the layer 2 for each pass.



It can be deduced that:

- If at the first pass all lanes show a general stiffness modulus which stood at about 45-50 MPa, the subsequent compaction instead shows a completely different behaviour between the lanes, in particular, as already mentioned, between the inner and outer lanes; except for the area L2-4, whose lanes reach the same degree of compaction (about 73 MPa).
- If the outer lanes are omitted, M3 shows better mechanical capacity with respect to M4, in particular configuration M2-M3 with a dynamic module E_{vib} above 85 MPa.

Unlike the mappings, the tables of the Evib average values for subarea regarding the three lifts have the same colour scale ranging from the minimum value of the subgrade S to the maximum of L2.

5.5.2 Layer L1

For the compaction of the middle layer L1 four forward vibratory passes were considered sufficient, in addition to the four backward static passes, as illustrated in section 5.2.5, since achieving compaction degree in a few passes.

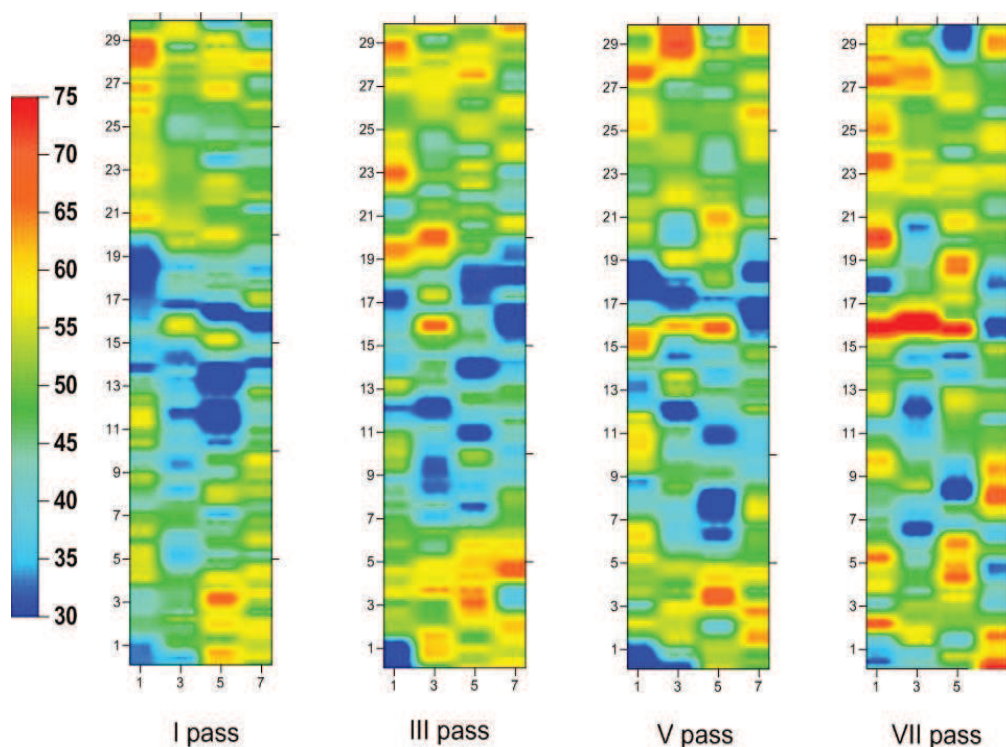


Figure 5.33. Evib mapping of the layer 1

The scale of the values in figure shows a reduction of the average values of the unbound layer respect to L2; demonstrating the soundness of the binders in the mixture compared to unbound materials; upper and lower limits of the colour scale is not the same used for the layer 2 so as to permit a more adequate interpretation of the layer and to highlight the impact of the concrete curb on the field.

The mapping shows an irregular trend, in particular for the first three compactions, with modest values for the central lanes of the field (blue coloured areas), and more consistent and regular for the initial and final part of the field (verifiable through yellow-green coloured area).

The apparent weakness of the central zone is resized in the fourth pass in which the influence of the centerline artefact is also visible.

The final pass of the field shows in any case different weak areas with EVIB values lower than 35 MPa, in particular for the first half of the field.

With the help of the tables 5.4 and 5.5 it is also possible to find a stiffness range between about approximately 45 and 55 MPa and one, albeit minimal, most load-bearing capacity of the unbound mixture M2 (70% B, 30% E) compared to M1 (50% a 50% B), with a maximum for the lane 4.

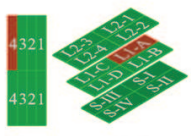
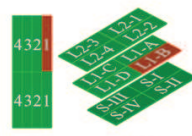
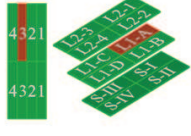
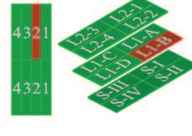
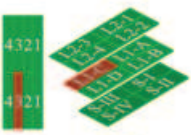
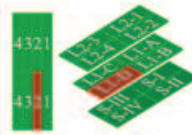
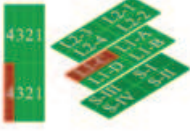
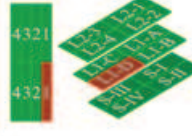
		pass	average (MPa)			pass	average (MPa)
	L1-A section 4	I	51.6		L1-B section 1	I	47.1
		III	53.1			III	46.2
		V	48.8			V	47.3
		VII	55.9			VII	47.5
	L1-A section 3	I	48.5		L1-B section 2	I	49.9
		III	52.0			III	49.7
		V	48.8			V	49.6
		VII	49.4			VII	51.7
	L1-C section 3	I	40.6		L1-D section 2	I	42.5
		III	42.8			III	46.8
		V	45.6			V	41.8
		VII	41.4			VII	47.5
	L1-C section 4	I	48.6		L1-D section 1	I	49.3
		III	48.2			III	47.8
		V	49.2			V	48.2
		VII	51.2			VII	48.2

table 5.4. E_{vib} average modulus per pass for the eighths of the layer 2.

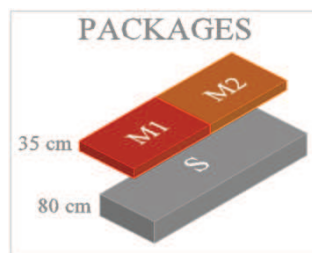


table 5.5. E_{vib} average modulus per pass for the mixtures of the layer 1.

The two mixtures show an average gap of about 2-3 MPa, residual difference which allows to deem equivalent the two mixtures with regard to bearing capacity.

5.5.3 Subgrade S

As for the layer L1, four dynamic passes were deemed sufficient for the subgrade, with the exception of the first lane (3 passes), previously compacted three times in manual mode 2 with the use of GPS positioning system, not mentioned in this discussion.

The value scale for S is the same applied to L1 because of similar E_{vib} range values despite these are more concentrated around the average value as evidenced by variances just reported

Even if the weakest areas (in blue) decrease anywhere, apart the firsts meters, it is not evident a particular growth of value along the pass progression, with a average values around 40-45 MPa..

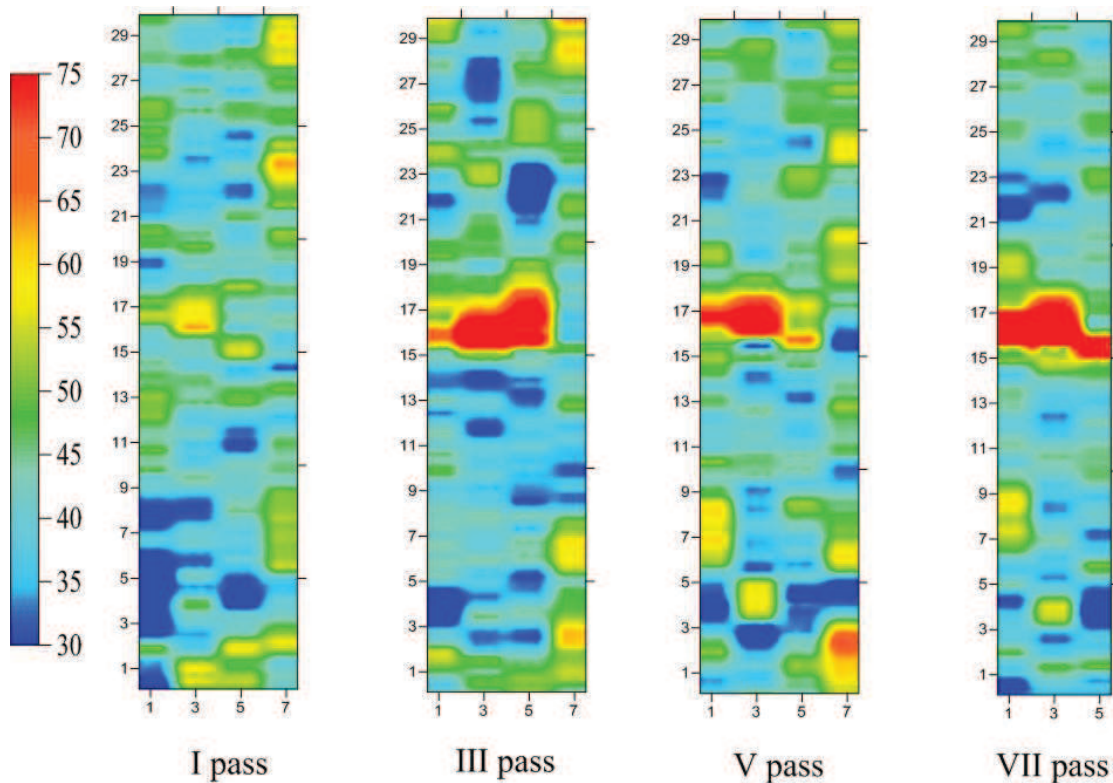


Figure 5.34. E_{vib} mapping of the substrate.

By examining the table 5.6 we have confirmation of the hypothesis, with practically null

average increases on almost all the subareas..

The EVIB average values along the first lane are, 5-6 MN/m² higher than the remaining lanes, slightly invalidate of a few percentage points the results over the whole field.

The table shows the less satisfactory value in correspondence of the fourth dynamic compaction (41.4 MPa), which no longer takes account of the first lane.


Although the material does not show particular increases of the bearing capacity during the entire compaction process, we can hypothesize that the third pass in manual 5 (hence with amplitude 1.9 mm) performed with GPS system, has also influenced the virgin material below, slightly improving the overall stiffness degree of the entire lane.

table 5.6. E_{vib} average modulus of the eighths of the subgrade S

		pass	average (MPa)			pass	average (MPa)
	S-IV section 1	I	45.9		S-II section 1	I	48.9
		III	45.7			III	46.4
		V	45.8			V	48.8
		VII	/			VII	/
	S-IV section 2	I	38.7		S-II section 2	I	41.0
		III	36.6			III	41.7
		V	38.4			V	44.0
		VII	38.0			VII	43.6
	S-III section 3	I	38.8		S-I section 3	I	41.3
		III	37.3			III	41.1
		V	40.0			V	41.2
		VII	39.5			VII	40.5
	S-III section 4	I	36.5		S-I section 4	I	42.4
		III	38.5			III	42.6
		V	43.9			V	41.3
		VII	43.7			VII	42.6

table 5.7. E_{vib} average modulus per pass of the whole substrate S

BACKGROUND	
FINAL VALUES	
pass	average
I	42.8
III	42.3
V	43.8
VII	41.4



5.6 Comparison between the layers

This section deals with the comparison of dynamic stiffness modulus between the three overlapped layers.

The Figure 5.35 shows the comparison between the higher average Evib value passes for each lift: the third pass for the subgrade and the last pass for the remaining layers, as documented by the tables 5.8 provided of colour scale.

The last graph gives a general overview of the compaction efficiency throughout the experimental field, then we can confirm the following:

- The several analysis procedures corroborate the efficiency of the compaction, particularly for mixtures M1 and M2 used for the surface lift whose modules vary within the range 60-80 MPa for the last pass.
- They also shows a steady growth in the dynamic module, demonstrating the importance presence of hydraulic binder in the mix design to achieve adequate road foundation bearing capacity values.
- The unbound mixtures M1 and M2 employed on layer L1 show little stiffness percentages rate during the entire phase of tests, not exceeding the limit of 60 MPa as for the virgin excavated natural material of the subgrade S.

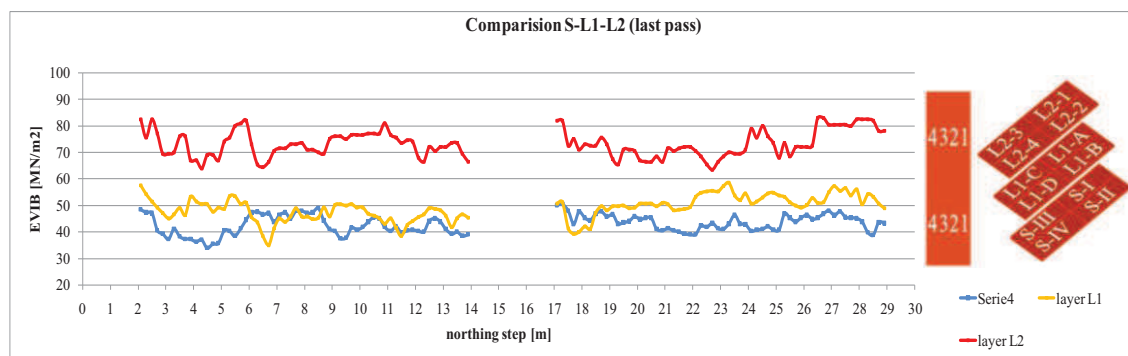


Figure 5.35. EVIB values for the more relevant pass of each layer.

table 5.8. EVIB averages each pass of each layer.

Subgrade		L1		L2	
FINAL VALUES		FINAL VALUES		FINAL VALUES	
pass	average	pass	average	pass	average
1	42.8	1	47.3	1	47.5
3	42.3	3	48.3	3	51.8
5	43.8	5	47.4	5	57.5
7	41.4	7	49.1	7	61.4
				9	66.1
				11	68.7
				13	71.6

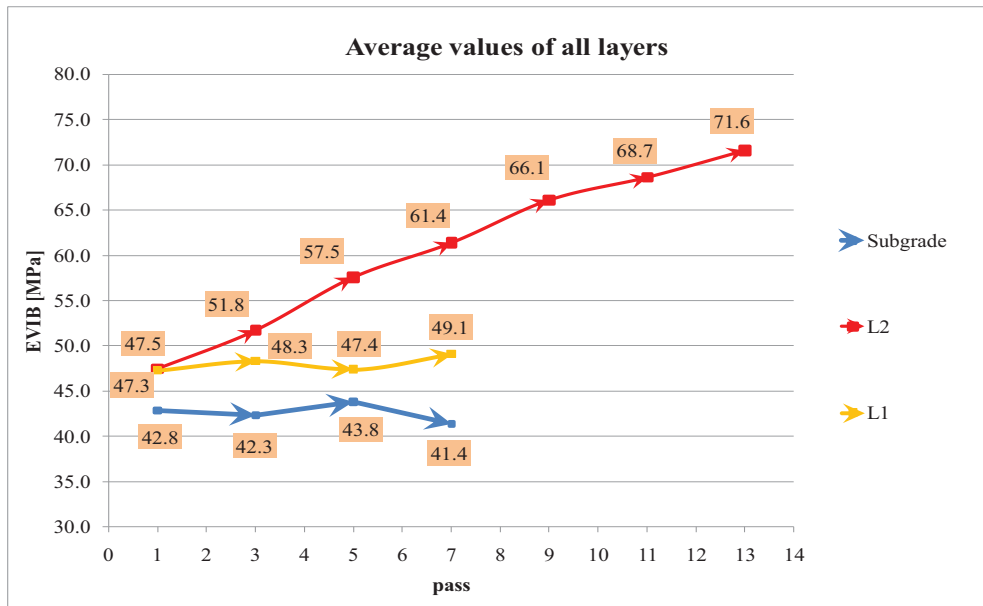


Figure 5.36. Summary sheet of all the test field

5.7 Depth of measurements.

Individual fixed amplitude (0.7 and 1.9 mm) dynamics compaction passes have been performed several hours after the initial compaction, to deepen and better understand the behavior of analyzed lift, when varying influence depth, from 50 cm to over 1 meter.

The figures below show the results obtained at the lane 1 for the three layers. Similar results were also obtained for the other lanes.

An amplitude of 1.9 mm (defined manual 5 in the Bomag system) leads to a deeper compaction compared than 0.7 mm (manual 2) and this is inferred from the comparison of three lifts:

- For subgrade S, the drum amplitude 0.7 mm implies a greater stiffness due to the low influence depth: in this way only the considerate lift, 80 cm thick, undergoes compaction being more rigid than the manual mode 5 whose amplitude affected the virgin material stiffness far less: the measurements obtained in-fact are very low, exceeding 20 MPa only in correspondence of the concrete curb.

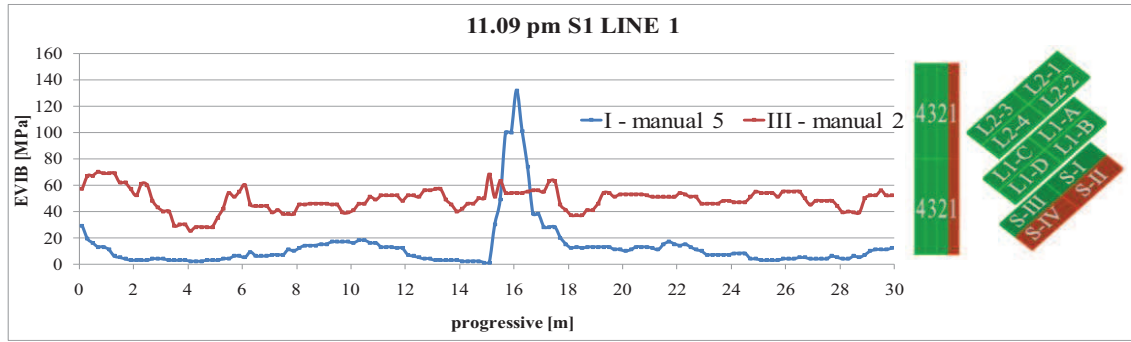


Figure 5.37. EVIB values results with different roller amplitude, substrate S

- For the subsequent lifts L1 and L2 is clear the opposite effect: the presence of underlying backfill layers involves the survey of a greater stiffness for the compaction in manual 5 compared to that in manual 2, this is due to a greater investigation thickness but made up with lifts of good mechanical properties.
- The EVIB values in manual 2 (0.7 mm) show a steady growing rate with a gap of about 20 MPa between lifts.; those in manual 5 (1.9 mm) sharply increase between the subgrade and the intermediate lift (with an average increasing EVIB value of approximately 120 MPa), while about 15% is the gap between L1 and L2.

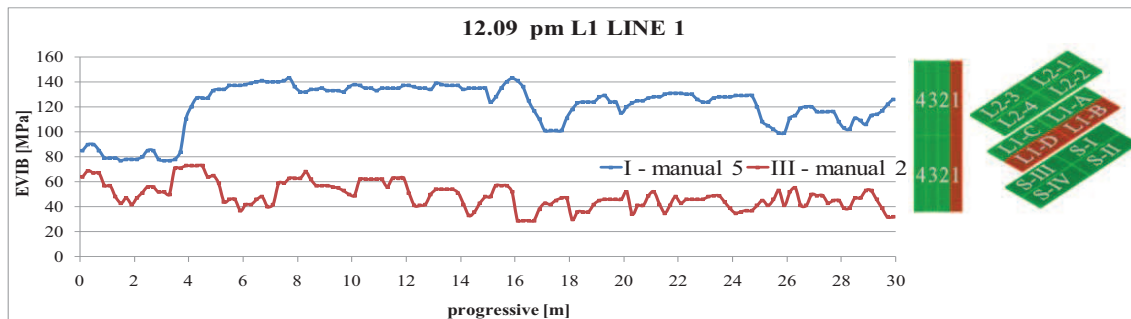


Figure 5.38. EVIB values measurements over the layer 1 in different manuals

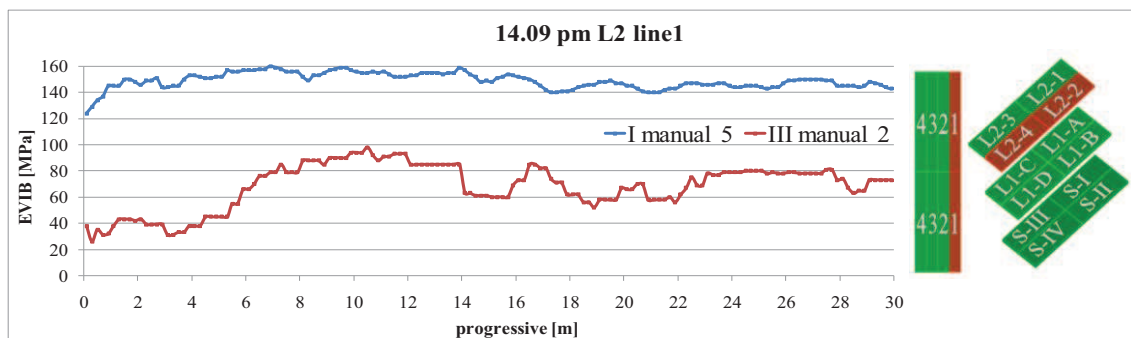


Figure 5.39. EVIB values measurements over the layer 2 in different manuals,

From what has just been exposed, using the VARIOCONTROL fixed amplitude vibration it is possible to influence considerable thicknesses of lifts and subgrade depending upon the selected roller amplitude.

Therefore appears unsuitable to use high amplitudes dynamic compaction in case of subgrade where the power compaction is wasted because of the underlying poor quality material.

For the upper layers of the embankment instead the greater amplitudes allow the roller compactor to also cover the applications of heavier compactor machine in such a way to compact significantly higher depths.

It is interesting to note that the investigated volume by CCC system increases with the passage of the roller: via the diagrams of Figure 5.31 it can be seen as peaks stiffness due to the curb at the centreline placed at the level of subgrade, become pronounced for both lifts L1 and L2, the latter situated at 35 cm from the artefact.

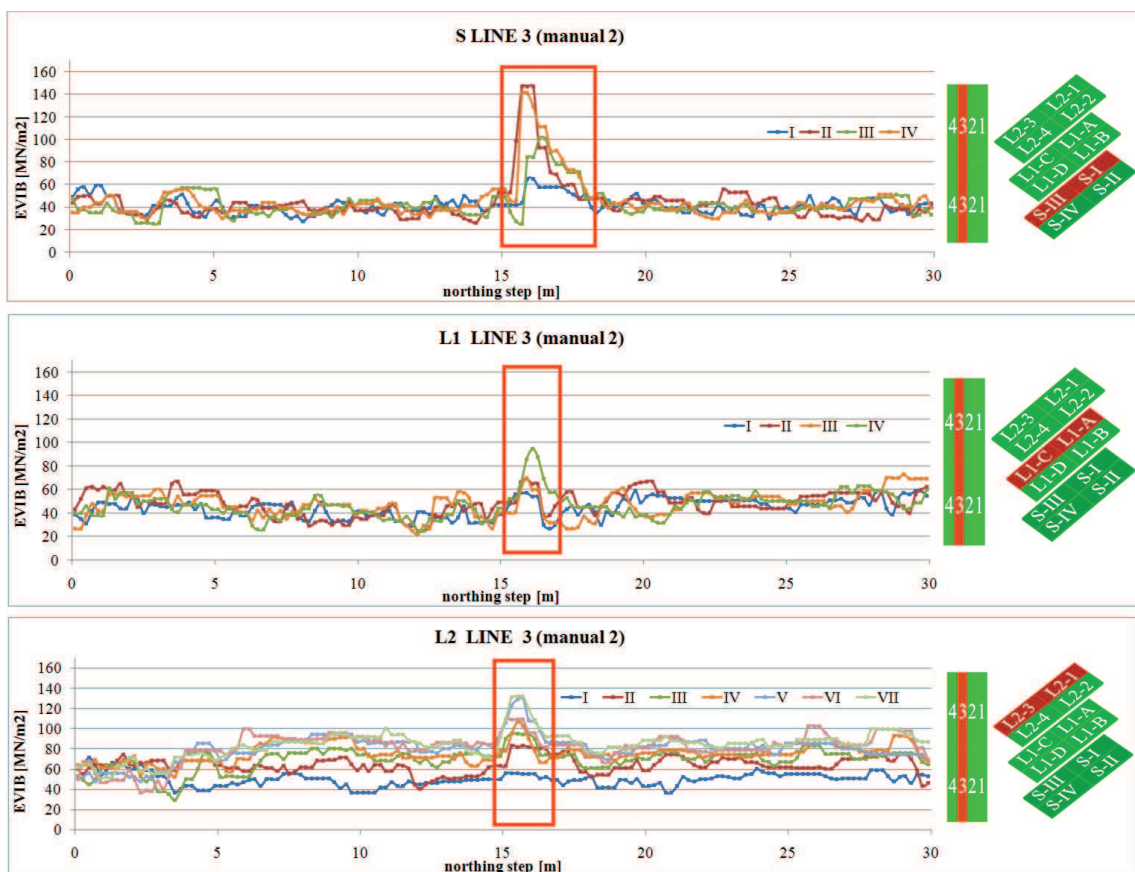


Figure 5.40. EVIB values measurements, in manual 2, over the whole test field ,

Chapter 6

Study of the compaction

6.1. State of Practice

The most common approach to quality control in road construction is to carry out a series of periodic in-situ tests. Evaluation of the quality of the compaction is based on the engineering properties of the compacted soil including strength.

The most common methods attempt to generate a new strength-based method by using vibratory proof-rolling quality assurance and final acceptance of earthwork compaction. Using this approach, a heavy truck (the smooth drum Bomag in our case) is driven at walking speed along the alignment measuring representative measurements of the in-situ modulus or stiffness of the soil.

In this last chapter implementation of the recommended quality assurance have been performed through some of the strength-based methods described in chapter 4: in particular, we refer to Specification Options 2a and 2b which have been deemed the most suitable for the experimental field application.

The performed analysis is presented in this chapter in the form of paragraphs, each of which referent to a specific control method.

Basecourse L1 and L2 have been analyzed on the entire pad, with the exclusion of the areas considered inadequate for the purpose of research and often pointed out: the first metre and the last 2 m of the field and area above the concrete curb.

6.2. Acceptance using specification option 2a

Acceptance for Option 2a is based on the percentage change in the mean MV $\% \Delta \mu_{MV_i}$ from consecutive passes over an Evaluation Section according to the equation:

$$\% \Delta \mu_{MV_i} = \left(\frac{\mu_{MV_i} - \mu_{MV_{i-1}}}{\mu_{MV_{i-1}}} \right) \cdot 100$$

Acceptance is met when $\% \Delta \mu_{MV_i}$ is less than the target percentage change ($\% \Delta -TV = 5\%$ for the case study presented here, similar to Austrian CCC specifications)

For the application of acceptance for option 2a, it was decided to evaluate the percentage change of MV values between consecutive passes in the entire strip, to provide an overview, but also for subareas or sections 3 m long in such a way to evaluate in more detail the performance of $\% \Delta \mu_{MV_i}$ for every material configuration.

The evaluation of $\% \Delta \mu_{MV_i}$ was performed on odd pairs 1-3, 3-5, 5-7, 5-9, 9-11 and 11-13 because the intermediate passes (2, 4, 6, 8,10,12) were static passes.

Option 2a requires constant roller operating parameters for measurement passes.

6.2.1. Analysis of the percentage change $\% \Delta \mu_{MV_i}$

Acceptance for Option 2a was applied starting from the measurements in real-time of the vibratory passes along the lifts L1 and L2, by using Excel spreadsheets

It is evident, with reference to the following figures, that the measurements performed involves the whole field test, then the proposed tables simply provide an example of how the available data have been treated; in this case, are shown the tables in reference to one of the subarea of the field for the layer 2, exactly the fourth L2-1.

The first step consists in calculating the MV (average EVIB value in our report), assessed both for the whole subarea and for interval of 3 m (Figure 6.1).

table 6.1. MV for intervals of 3 m and for the field

Evib average calculated in the range ΔY							
	pass I	pass III	pass V	pass VII	pass IX	pass XI	pass XIII
3-5 m	56	59	64	61	66	59	61
5-8 m	49	54	57	61	65	68	69
8-11 m	45	51	62	70	77	75	83
11-14 m	45	44	54	60	65	73	79
Variance	25.79	37.77	22.85	20.45	31.81	53.28	98.82
Average	48.73	52.08	59.08	62.93	68.08	68.73	73.00

The next step consists of determining the percentage change $\% \Delta \mu_{MV_i}$ between consecutive passes by using the average values given above (figure 6.2).

table 6.2. difference in absolute value of the MV for 3 m sections.

	Evib average calculated in the range ΔY					
	I-III	III-V	V-VII	VII-IX	IX-XI	XI-XIII
3-5 m	3.28	5.30	-3.27	4.55	-6.80	2.32
5-8 m	4.70	2.92	4.67	3.27	3.07	1.00
8-11 m	6.52	10.45	8.02	6.92	-1.47	8.00
11-14 m	-1.12	9.37	5.95	5.87	7.80	5.80

Starting from the realization of the latter table has been possible to proceed with the Acceptance for Option QA 2a through the creation of the table 6.5 showing $\% \Delta \mu_{Mvi}$ and scatter plots (figure 6.5) that illustrate $\% \Delta \mu_{Mvi}$ trend between consecutive passes.

table 6.3. for sections of 3 m and final average results.

	I-III	III-V	V-VII	VII-IX	IX-XI	XI-XIII
3-5 m	5.89	8.98	-5.08	7.45	-10.37	3.94
5-8 m	9.56	5.41	8.22	5.31	4.74	1.47
8-11 m	14.61	20.44	13.02	9.94	-1.92	10.66
11-14 m	-2.46	21.16	11.09	9.85	11.92	7.92

$\% \Delta$ Evib average						
6.87	13.46	6.50	8.18	0.95	6.23	

The $\% \Delta \mu_{Mvi}$ development rate is therefore proposed for the four fields investigated , (Figure 6.1, Figure 6.2, Figure 6.3, Figure 6.4). which also describe the threshold considered optimal, ie 5%.

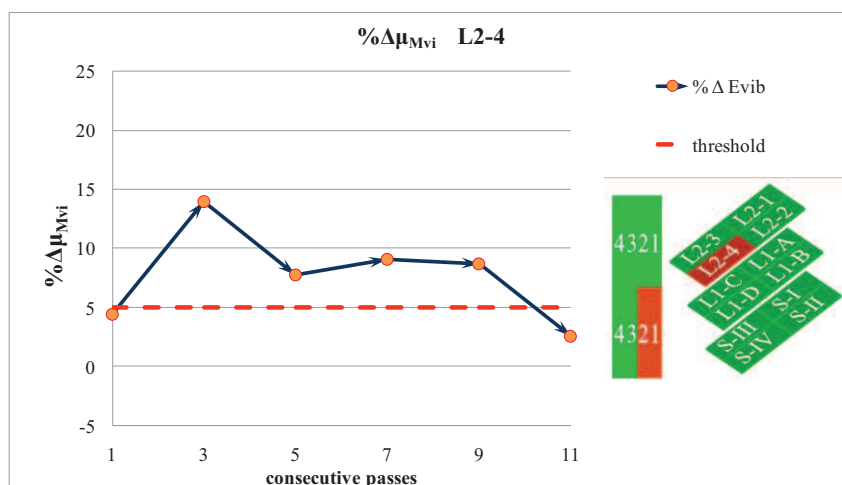


Figure 6.1 quality control QA 2a for the area L2-4.

Each diagram is accompanied by the corresponding graph with the average dynamic modulus for each pass, so as to include also the relative growth of the degree of compaction of the concerned area. (

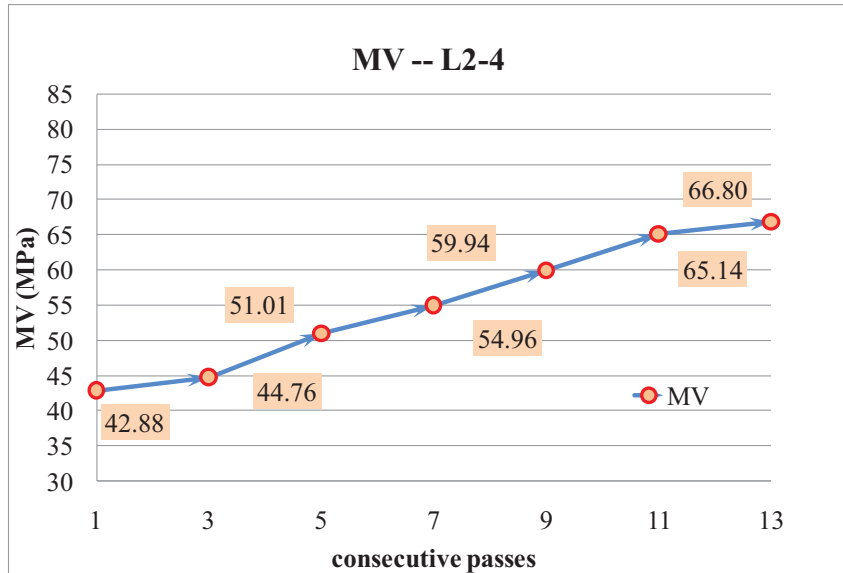


Figure 6.2 MV per pass, area L2-4 .

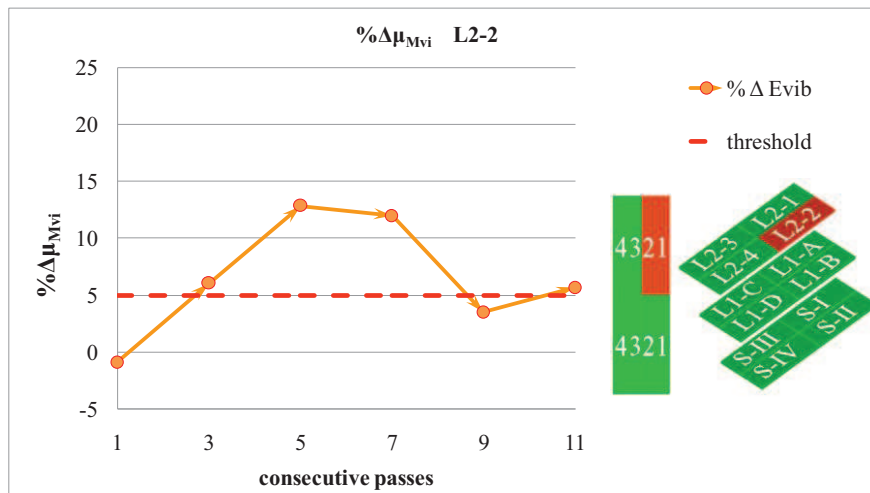


Figure 6.3 – quality control QA 2a for the area L2-2.

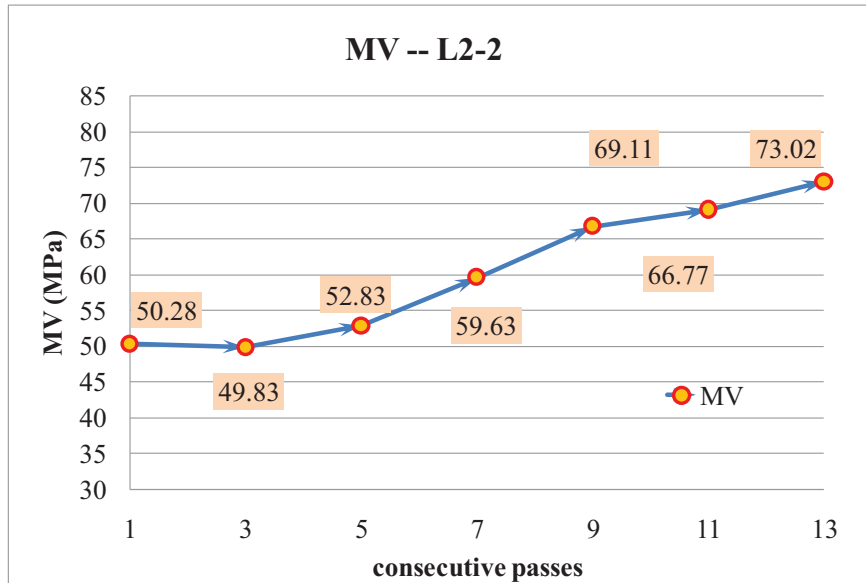


Figure 6.4 – Evib average modulus per pass –L2-2 area

From the graphs and table shown above it is possible to draw the following important considerations regarding the mixture M3:

- For the area L2-4 and L2-2 the achievement of the threshold of 5% already from the second pass. We note in fact as the values achieved are in many cases and not only for the final pass, lowest of 8-10%.
- This is undoubtedly an indication of the goodness of the compaction method; But with the succession of passes the percentage change in MV ascends above the threshold for intermediate passes to descend again the 5% between the fifth and the seventh pass.
- During the passes in question, the bound mixture suffers a rearrangement, probably due to an interstitial water rising, which causes a greater effectiveness of the compaction thanks to the reaction of the hydraulic binder with water.

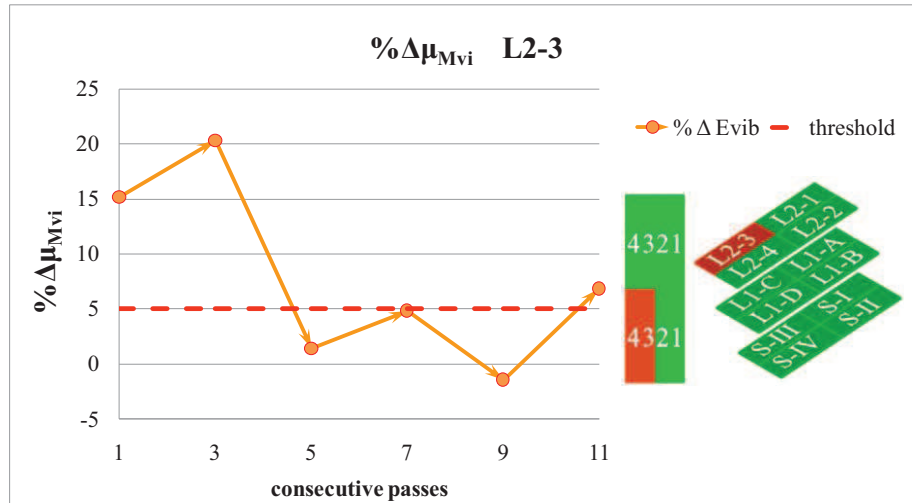


Figure 6.5 – quality control QA 2a for the area L2-3.

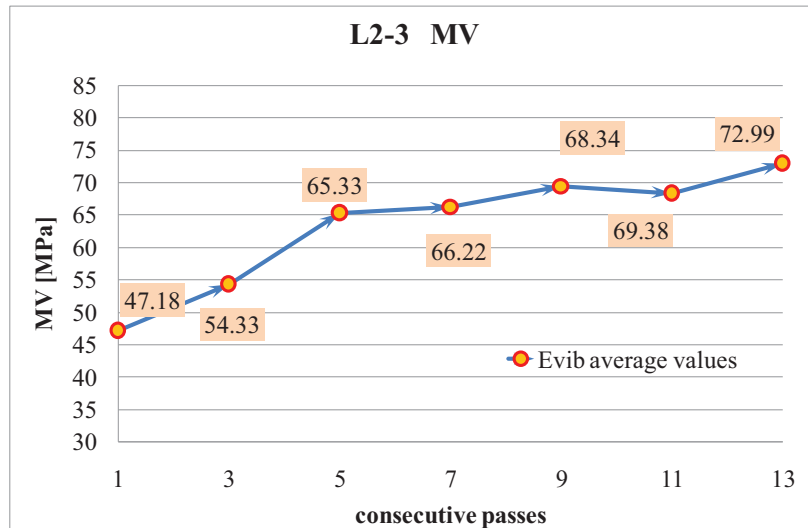


Figure 6.6– Evib average modulus per pass –L2-3 area

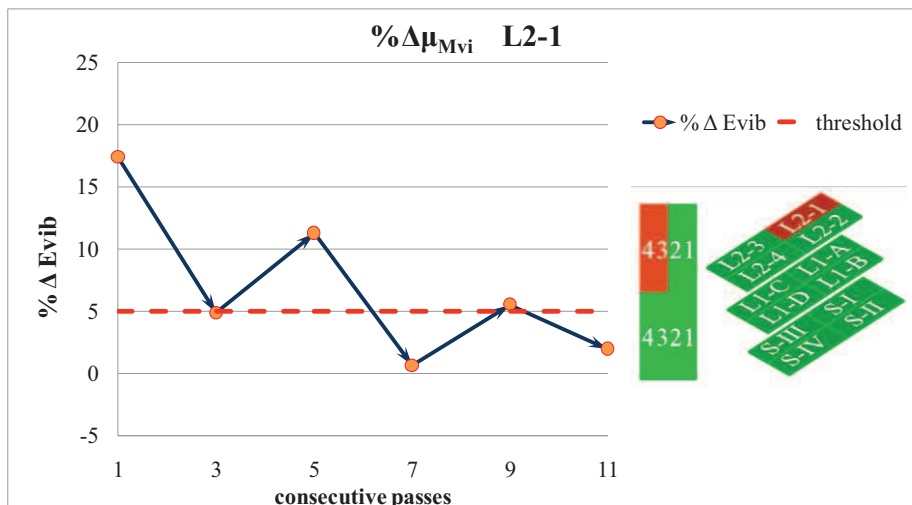


Figure 6.7 – quality control QA 2a for the area L2-3.

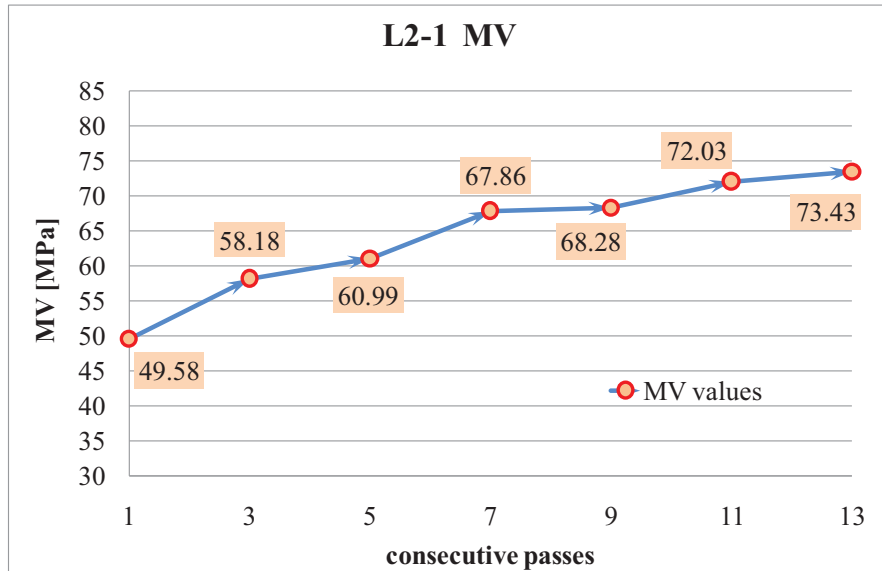


Figure 6.8– Evib average modulus per pass –L2-1 area

- For the material M4 the two subareas drop below the threshold only in the comparison of passes 5-7 .
- Between passes 9 and 11 of L2-3 a negative MV value is visible, symptom of a counterproductive compaction even if the last pass confirms the tendency of the field to an increase of the mechanical properties of mixture.
- The final consideration with respect to the bound layer materials leads to observe how the 5% used as threshold is not restrictive and difficult to reach in our case; Indeed another pass of measurement would have required at least , with the aim of confirming the trend line of the two mixtures, although this would further burdened on the implementation timing of the test field .

The same Acceptance for Option 2a has been applied to the middle layer L1, for each lane and for the two halves of the field (Figure 6.10, 6:11), composed of the unbound mixtures M1 and M2, respectively, on the subarea L1 C/D and L1 A/B.

This lift show has been compacted with only 4 vibratory passes (1,3,5,7) considerate enough for optimum compaction of the unbound layers.

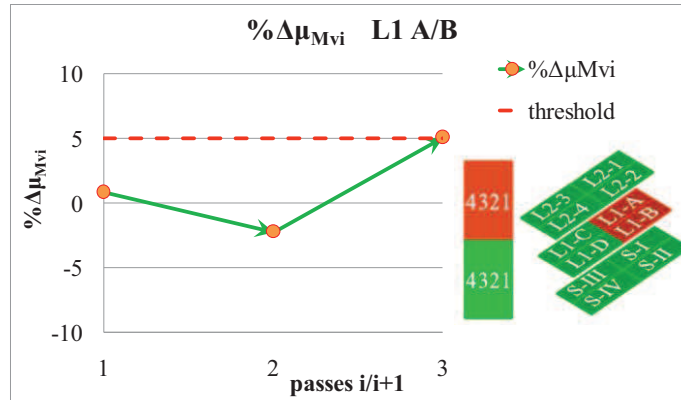


Figure 6.9 – quality control QA 2a for the area L1-A/B (mixture M1)

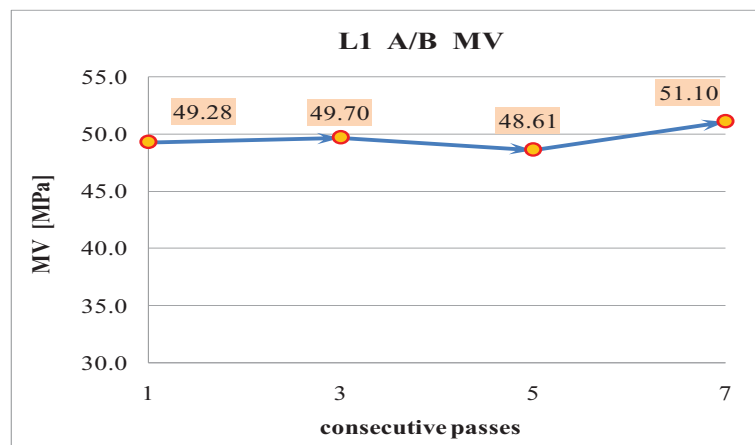


Figure 6.10 – E_{vib} average values per pass on the area L1-A/B (mixture M1)

For unbound materials M1 and M2, Acceptance for Option 2a shows values below the threshold of 5%, everywhere all over the field, confirming the low validity of further compaction, in this case expensive and in some areas counterproductive as demonstrated in both the materials between the II and III pass. with negative $\Delta\mu_{Mvi}\%$.

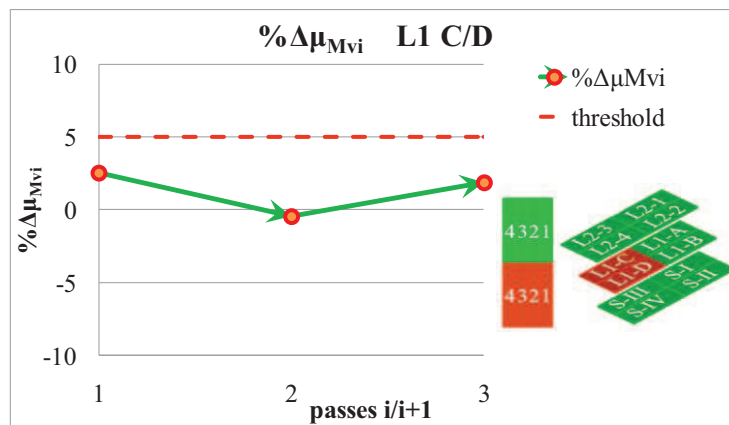


Figure 6.11 – quality control QA 2a for the area L1-C/D (mixture M2)

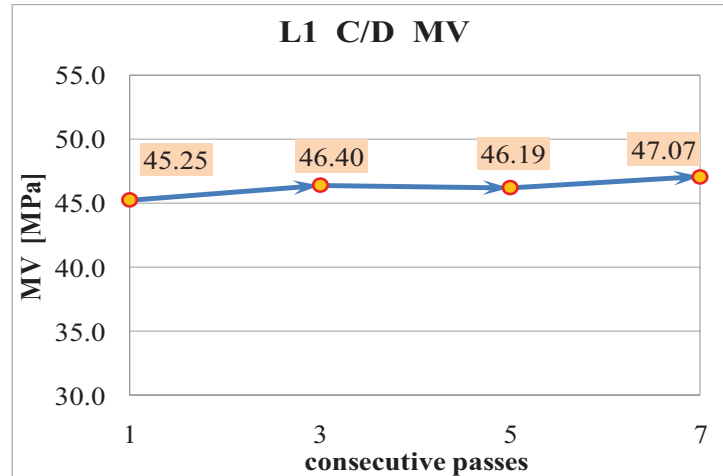


Figure 6.12 – E_{vib} average values per pass on the area L1-C/D (mixture M1)

For subgrade S acceptance testing were not undertaken since it simply provides the stable foundation needed to support the additional C&D material layers and separate it from the native material.

6.3. Acceptance using specification option 2b

Acceptance for Option 2b is similar to that previously exposed but is based on the spatial percentage change in MV_i between consecutive passes $\% \Delta MV_i$ rather than the percentage change in mean MV of the entire Evaluation Section per Option 2a.

Starting from the equation:

$$\% \Delta MV_i = \frac{MV_i - MV_{i-1}}{MV_{i-1}} \cdot 100$$

Acceptance is met when $\% \Delta MV_i \leq \% \Delta -TV$ for a specified percentage of the Evaluation Section ($\% \text{Area-TV}$), according to the equation:

$$\% \Delta MV_i = \frac{MV_i - MV_{i-1}}{MV_{i-1}} \cdot 100$$

The analysis continues with the creation of a graph that expresses the cumulative values $\Delta MV_i\%$ and the $\Delta -TV$.

Per Section 3.34, the recommended $\% \Delta -TV$ is two times the $\sigma_{\% \Delta MV}$ determined from repeatability testing with a maximum $\% \Delta -TV = 20\%$. However, higher $\% \Delta -TV$ may be used at the discretion of the engineer of record.

The optimal value considered is 10 % for this case study; Therefore, $\% \Delta\text{-TV} = 20\%$ was set. The $\% \text{Area-TV}$ was set at 80%.

The first step was, at the same way of what was done for the previous method, to calculate, via Excel spreadsheet, the percentage change $\% \Delta \text{MVi}$ (An example is given in Table 6.6).

Table 6.6 – difference in absolute value of the EVIB modulus for 3 m lane.

	progressive [m]	% ΔEVIB					
	2-14 m	I-III	III-V	V-VII	VII-IX	IX-XI	XI-XIII
2-5 m	2.10	-8.51	-2.33	2.38	5.43	-11.76	-1.67
	2.30	-2.96	-10.69	10.26	-4.65	-7.32	10.53
	2.50	0.83	0.83	1.64	8.06	-9.70	0.83
	2.70	1.68	8.26	-15.27	7.21	-3.36	-6.09
	2.90	3.51	0.85	-5.04	-1.77	-6.31	3.85
	3.10	0.91	0.00	9.01	-5.79	-7.89	-1.90
	3.30	-15.32	0.00	4.76	3.64	-5.26	0.00
	3.50	-8.55	0.00	-4.67	8.82	5.41	-23.08
	3.70	-15.32	21.90	-17.19	10.38	-9.40	-25.47
	3.90	-28.57	40.00	-21.05	15.24	-17.36	-18.00
	4.10	-18.90	25.24	-30.23	35.56	-15.57	-19.42
	4.30	-13.56	32.35	-17.78	-1.80	-5.50	-12.62
	4.50	-20.33	29.59	-11.02	-3.54	-3.67	-8.57
	4.70	-18.33	23.47	-7.44	0.89	-1.77	-12.61
4.90	-6.61	4.42	-9.32	11.21	-6.72	-15.32	

Naturally, the procedure has been performed for all the measurement passes performed. The same operation was then adopted for subareas of the same material since that main objective of this treaty is to analyze the behavior of the placed four .

Also for this control therefore the two halves of the field for the layer L1 (with mixtures M1 and M2) and the other two for the layer L2, will be treated however, perpendicularly placed to the underlying mixtures in order to four material compositions , as repeatedly highlighted previously.

6.3.1. Layer 2

Considering the cumulative distributions evaluation of the $\% \Delta \text{MVi}$ data on each subarea is possible to investigate in more detail the behavior of different materials subjected to successive compaction cycles.

Below results obtained for the subareas of the field layer 2 are reported , leaving out, measurement pass pairs from I-III to VII-IX because of not significant, and showing only the one relative the last pass pair over the Evaluation Section.

Figures 6.12, 6.13, 6.14, 6.14 shows % Δ MVi for passes 9 and 11.

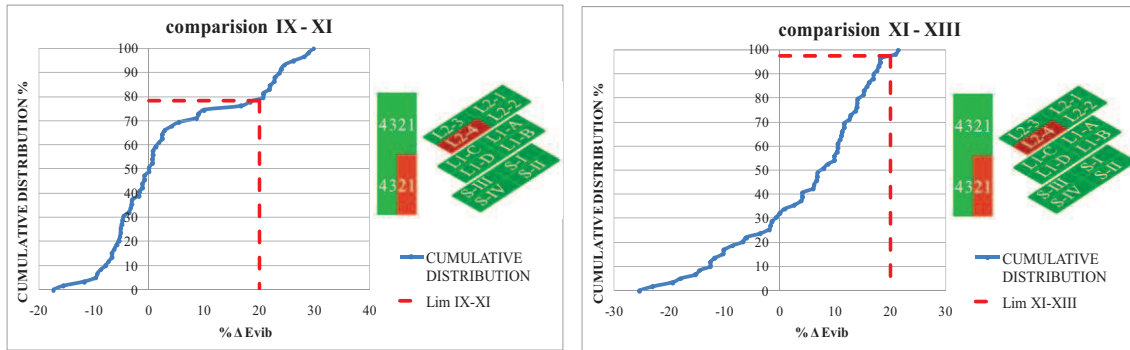


Figure 6.12 - QA2b for the composition M1/M3

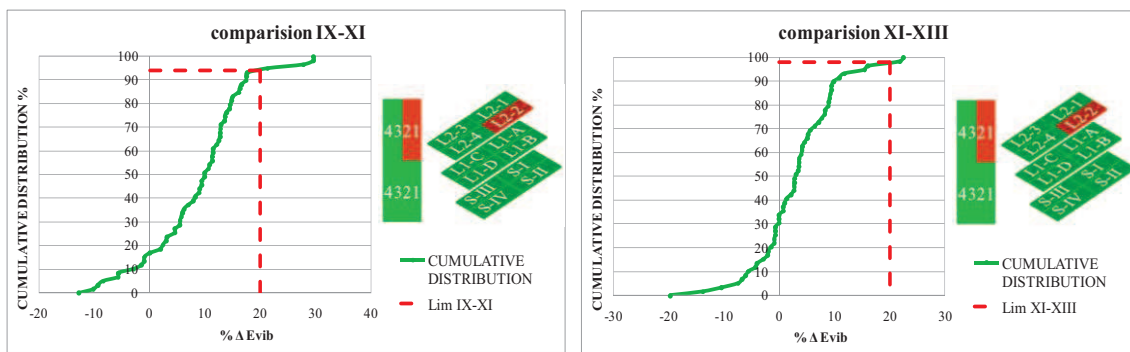


Figure 6.13 - QA2b for the composition M2/M3

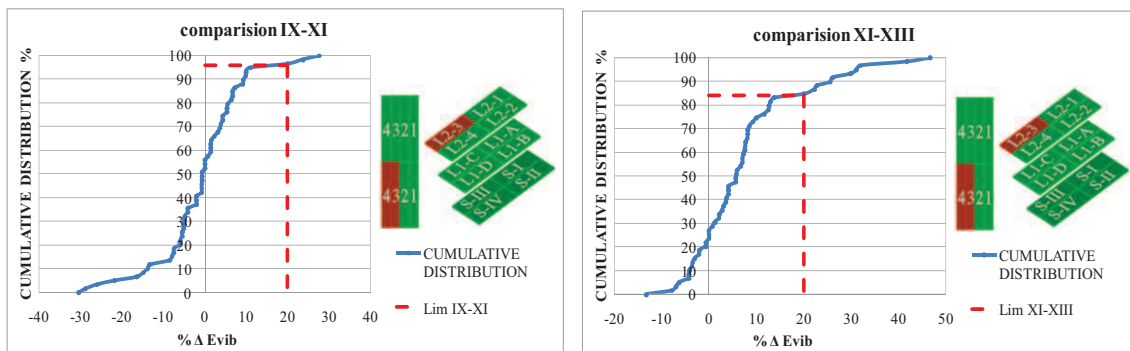
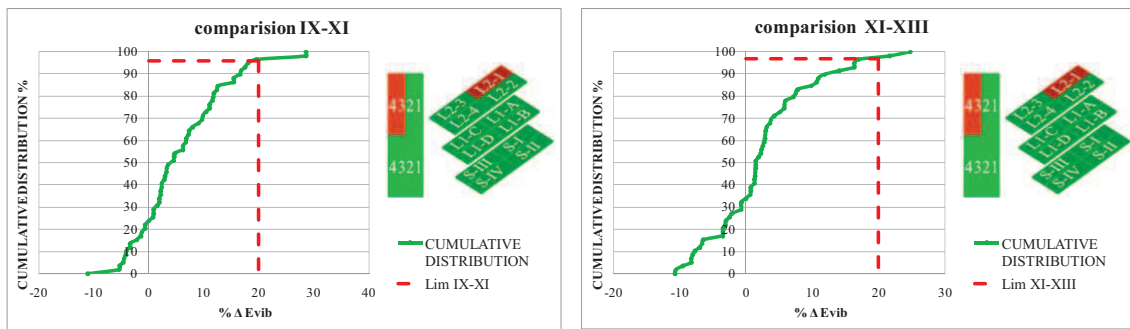


Figure 6.14 - QA2b for the composition M1/M4



From the graphs it appears that all of the composition materials met the $\% \Delta$ -TV after pass 9, except for the comparison 9-11 for M1/M3 (79%).

In the comparison between the two evaluation sections over 15 meters of progression have nearly 100% of the cumulative values below $\% \Delta$ -TV, and would have met even the threshold value of 10%. , demonstrating the validity of the compaction. The first half of the field do not meet contract QA requirements for the pass pair 9-11 which has even a 50% decreasing values that reach Δ MVi% -30%, significantly improving for the last two passes. Overall the test field then met acceptance based on Options 2a.

Figure 6.16 presents $\% \Delta$ MVi data for passes 9, 11, 13, the last two Measurement Pass pairs over the Evaluation Section.

The research was completed with $\% \Delta$ MVi mappings in order to have an appropriate visual feedback of the areas that meet the acceptance; The white areas indicate $\% \Delta$ MVi increments in the range 0-20% and can therefore be considered acceptable, in green we indicate areas with negative $\% \Delta$ MVi lower than -10% while in red areas with increasing Δ MVi% greater than 20%.

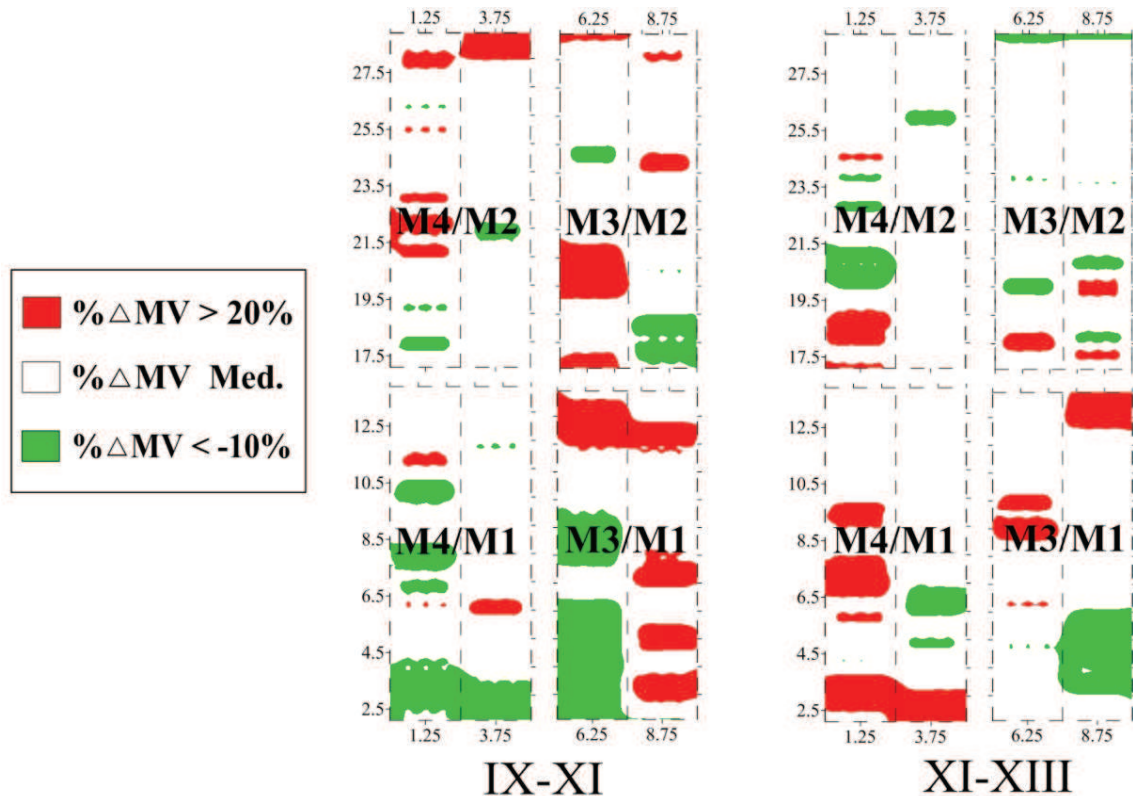


Figure 6.16 - Mapping of $\% \Delta$ MVi values for the layer L2 (Passes 9-11 and 11-13)

It looks evident that the second half of the evaluation section appear less coloured in

both passes pairs demonstrating the validity of the test as already mentioned, in particular for the subarea composed by M4/M1: the areas with negative $\% \Delta MV_i$ (in green) along 9-11 passes exceed the threshold of +20% in the pass 11-13 (in red).

6.3.2. Layer 1

The same quality assurance method for the layer 1 has been applied.

The test field has been divided into two evaluation sections due to different unbound mixture and results are illustrate in Figure 6.17 and 6.18

The graphs show both the reference threshold $\% \Delta TV$ equal to 20% and 10%.

Only the pass 3-5 met the control method for the threshold of 10%, while more than 85% of the $\% \Delta MV_i$ for the entire layer 1 does not exceed the reference threshold of 20% demonstrating the validity of the compaction.

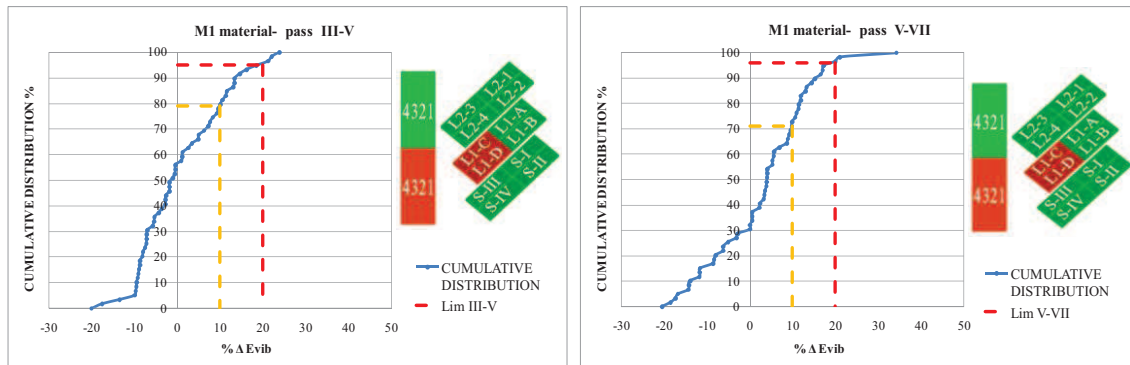


Figure 6.17 - QA2b for the mixture M1

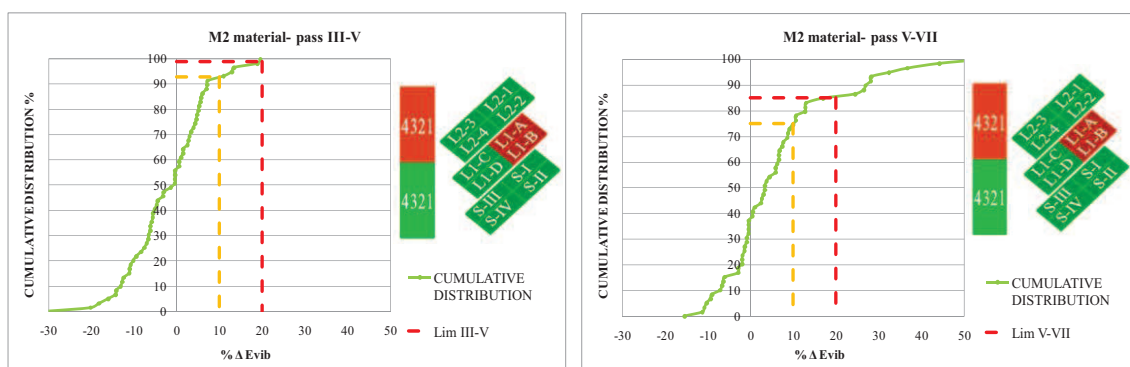


Figure 6.18 - QA2b for the mixture M2

Despite the results achieved through the Acceptance for Option 2b appear fairly satisfactory we have also take into account the percentage of negative $\% \Delta MV_i$ indicating a "decompaction" of the interested area: this are upper the -50% for the

second to last passes 3-5 and -30% in the last comparison 5-7.

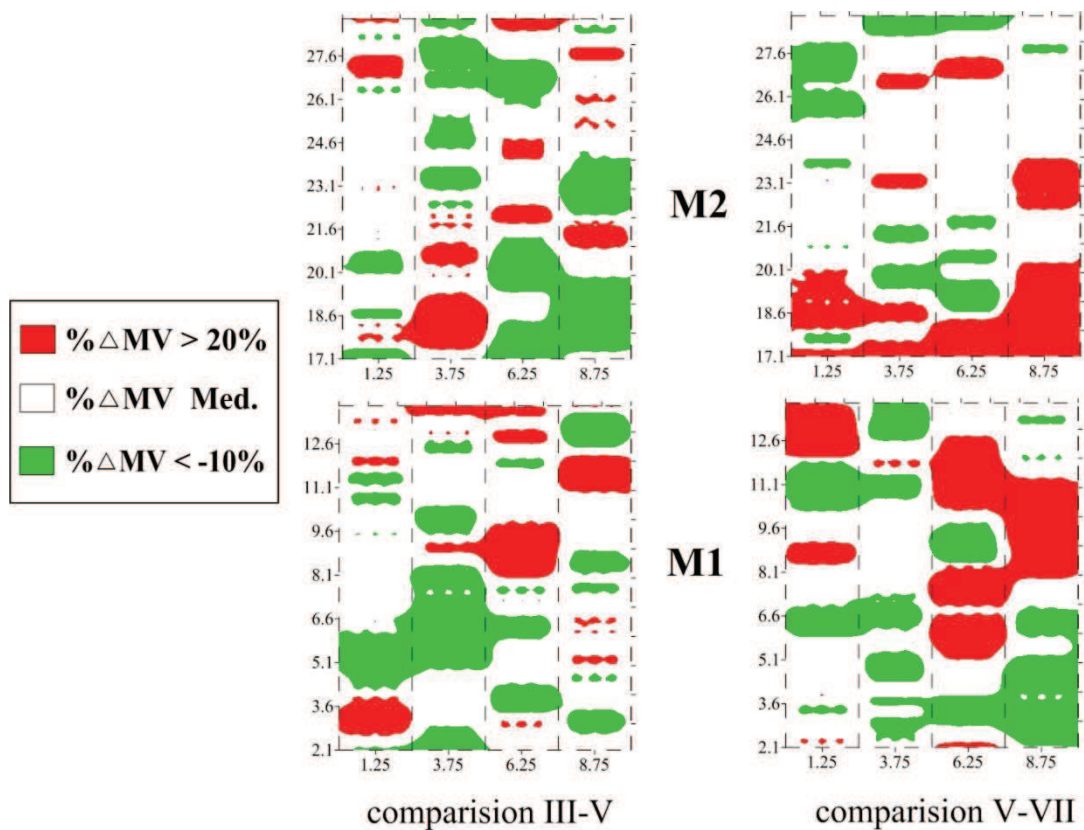
Consider also the graphs above show average results over half of the area:

the mapping of $\% \Delta MV_i$ data in figure 6.19 shows a more extensive distribution of values outside the range considered (between -10% and 20%) acceptable compared to the figure 6.16 reporting the layer 2;

in several cases, red coloured areas (negative spots) on every single lane are countered by green colored ones (positive spots) on the same progression, reason for which the graphs show then acceptable $\% \Delta MV_i$ values.

Therefore not always Acceptance is met separately analyzing each single lane as the figures 6.20 shown

Comparing the single passes for each strip we can see how the Acceptance is met in particular for the center lanes while the outer lanes have more low $\% \Delta MV_i$;



6.19 - Mapping of $\% \Delta MV_i$ values for the layer L1 (Passes 3-5 and 5-7)

Chapter 7

Conclusions

This dissertation deals with an experimental investigation and analysis on the use of CCC systems to characterize Construction and Demolition (C&D) waste to be used in pavement foundation layers. The research has been carried out both in laboratory, in order to determine the most suitable mixtures, and in situ to evaluate their bearing capacity and durability. C&D materials have been physically, chemically and mechanically characterized to evaluate their use in the production of mixtures for embankments, foundations and bases. Relying on the results, different bound and unbound mixtures have been manufactured.

A first analysis of the results shows that the several mixtures meet the requirements of the specifications in terms of mechanical performance.

To evaluate the elastic modulus/stiffness from currently available CCC data of these materials a full-scale experimental field was built on an area of suitable characteristics.

The three-lift embankment is constituted by a first layer of unbound C&D waste materials and a second layer of cement stabilized C&D waste materials. The field test was designed to allow the analysis of bound and unbound mixtures, in order to subsequently explaining the relative influence of layer properties (layer modulus and layer thickness) on roller-measured composite soil stiffness.

Roller-integrated Evib was used with limited fixed amplitude (0,7 mm) and frequency (28 Hz) to perform stability and uniformity tests of the subgrade compaction in situ (proof rolling).

In the light of laboratory investigations and mechanistic measurements from experimental tests it can be argued that:

- CCC system can be very useful in particular for the relative data analysis if no other strength-based instruments are used.
- The Evib values available in real-time have allowed the instantaneous stiffness data analysis of lifts and was possible to estimate how compaction evolves during

compaction in such a way to evaluate when optimum compaction degree has been achieved.

- CCC data comparison between internal and external trips demonstrates the importance of the boundary condition for the embankment to be compacted.
- Use the proof roller analysis with different fixed amplitude and frequency and the presence of the concrete curb has permitted to evaluate the importance of roller parameter settings and the thickness of influence achieved.
- An excessive number of passes and/or roller setting can be needless or even counterproductive.
- An excessive amplitude is pointless for thin lifts overlaid on soft soils.
- Acceptance for Options have confirmed a discrete homogeneity over the experimental pad, in particular for middle lanes.
- The roller measurement values (Evib) were able to identify the weak or stiff areas of the pavement layers.
- The construction aggregates applied, arising from a targeted recycling process, are able to provide performance comparable to those one obtainable from virgin aggregates in the formation of subbase and foundations of roadway paving, if properly selected and mixed, ;
- The laboratory mechanical tests show that mixtures meet the main specifications requirements and that hydraulic binders from recycling process may be conveniently employed.
- The unbound mixtures used on site, show a predisposition to compaction, reaching maximum elastic modulus/stiffness from currently available CCC data after a few vibratory passes;
- On site, the bound mixtures record significantly bearing capacity values; Soil stiffness continuously increases and vouches a final Evib values on average above 70 MPa.;
- Regarding the several composite soils ,by using CCC measurements, we can see that the embankment section containing predominantly concrete (M1 and M3) provides higher bearing capacity values compared to the remaining sections; The section M2-M4 is the least stiff.

- With reference to compaction and control of earthwork construction process, it can be stated that CCC systems can significantly contribute in verification processes both in terms of time consuming and data representation, allowing currently-available densification, homogeneity and stiffness monitoring of compaction.

It has been demonstrated, therefore, as the recycled materials can be seriously considered for embankment and road foundation construction if well designed and performed with the application of innovative compaction technologies

In conclusion, for future utilization measures of ground stiffness from vibratory rollers will allow all transportation stakeholders (owners, consultants, contractors) to directly evaluate the elastic modulus of individual lifts or layers using vibratory CCC roller data.

References

- Adam ,D.“*Roller-integrated Continuous Compaction Control (CCC) Technical Contractual Provisions & Recommendations*”.University of Technology & Consulting Engineer,Vienna.
- Ammann (2003). “*ACE-Soil Compaction and Compaction Control,*” CD, AMMAN Verdichtung AG, Langenthal, Swiss.
- Briaud,J.L. and Seo,J. (2003,December). “*Intelligent Compaction:Overview And Research Needs*”.Texas A&M University.
- European Commission (DG ENV), (2011). “*Service Contract management of Construction and demolition*”.
- Kalofotias,A.,Mavridou,S., Oikonomou, N. ,(2011). “*Report on characteristics of natural aggregates*”.Intl. Foundation Congress and Equipment Expo (IFCEE) Orlando, Florida.
- Meehan,C.,Tehrani,F.S. (2009). “*An Investigation of Continuous Compaction Control Systems*”. Duffield Associates, Inc., Wilmington, DE
- Mooney,M.,Facas,W. (2013).”*Extraction of Layer Properties from Intelligent Compaction Data*”.Colorado School of Mines (CSM), Golden, CO.
- Mooney,M.,Dietmar,A.(2007). “*Vibratory Roller Integrated Measurement of Earthwork Compaction*”.Vienna University of Technology, Vienna.
- NCHRP Report 676, (2010). “*Intelligent Soil Compaction System*”.
- NCHRP 10-65, (2008):“*Nondestructive testing technology for quality control and acceptance of flexible pavement construction*”.
- Petersen,D.L., (2004) “*Continuous Compaction Control, MnRoad Demonstration*”. Mn/DOT Report MN/RC - 2005-07, CNA Consulting Engineers, Minneapolis,
- Mn.Rinehart,R.,Mooney,M.,Facas,N. F.,Musimbi,O. (2009) .”*Examination Of Roller-Integrate Continuous Compaction Control On a Colorado Testsite*”. TRB 2012 Annual Meeting.
- Sáez,V.P. , Merino,M., Porrás-Amores, C. (2011).”*Managing construction and demolition (C&D) waste – a European perspective*”.Technical University of

Madrid, Spain.

Saki, O. (2010). "Overall trends in waste generation and management in Europe". European Environment Agency.

Sangiorgi, C., Lantieri C., Marradi A., Betti G. (2013). "Quality assessment of recycled C&Ds' materials compacted using Continuous Compaction Control".

Sangiorgi, C., Marradi A., Kloubert H.J. & Wallrath W. (March 2012): "A CCC experimental site for studying the compaction evolution of C&D materials", 3rd International Seminar on Earthworks in Europe, Berlin, Germany.

Sangiorgi, C., Marradi, A., Lantieri, C. and Pinori, U., (2009). "Dynamic field assessment of bearing capacity for pavement subgrades and foundations". 6^o International Conference on maintenance and rehabilitation of pavements and technological control, Torino.

Sangiorgi, C., Bignozzi, M. C., Bonoli, A., (2013). "La valorizzazione di scarti per la produzione di materiali da costruzione sostenibili e ad alta efficienza ambientale ed energetica". Department of Civil, Chemical, Environmental, and Materials Engineering – DICAM– Bologna University.

Susante, P.J., Mooney, M. (2008). "Capturing Nonlinear Vibratory Roller Compactor Behavior through Lumped Parameter Modeling". Journal of engineering mechanics.

Turner, H.F., Sandstrom, Å. (2000). "Continuous Compaction Control, CC" European Workshop Compaction Of Soils And Granular Materials".

Vennapusa, J.P. (2008). "Investigation of roller-integrated compaction monitoring and in-situ testing technologies for characterization of pavement foundation layers". Iowa State University.

Vennapusa, J. P., White, D.J., Gieselman, H. (2009). "Influence of support conditions on roller integrated machine drive power measurements for granular base.

, Vennapusa, J.P., White, D., (2010). "A Review Of Roller-Integrated Compaction Monitoring Technologies for Earthworks". Iowa State University.

Sitography:

- [1] www.ec.europa.eu/environment/waste/construction_demolition.htm or <http://ec.europa.eu/>
- [2] www.bomag.com/
- [3] www.dot.state.mn.us/materials/researchic.html or www.dot.state.mn.us/
- [4] http://www.fhwa.dot.gov/pavement/ic/techbriefs/ic_soils.cfm or www.fhwa.dot.gov/

Standards:

- CNR UNI 10014: 1964

“Soil tests. Determination of the consistency (attemberg) of a soil”.

-EN 933-1:1997

“Tests for geometrical properties of aggregates - Determination of particle size distribution - Sieving method”.

-EN 933-03:1997

“Tests for geometrical properties of aggregates -Determination of particle shape - Flakiness index”.

-EN 933-04:1999

“Tests for geometrical properties of aggregates - Determination of particle shape - Shape index”.

-EN 933-8:1999

Tests for geometrical properties of aggregates - Assessment of fines– Sand equivalent test”.

-EN 933-11: 2009

“Tests for geometrical properties of aggregates - Classification test for the constituents of coarse recycled aggregate”.

-EN 1097-2:1998

“Tests for mechanical and physical properties of aggregates - Methods for the determination of resistance to fragmentation, through the Los Angeles method”.

-EN 1097-3: 1998

“ Tests for mechanical and physical properties of aggregates -Determination of loose bulk density and voids”.

EN 1097-7:1998

“Tests for mechanical and physical properties of aggregates - Determination of the particle density of filler - Pyknometer method”.

EN 1097-6:2013

“Tests for mechanical and physical properties of aggregates - Determination of particle density and water absorption”.